Doctoral theses at NTNU, 2024:331

Sondre Bergtun Auganæs

# Laboratory Friction Testing of Cross-Country Skis

## Experimental Investigation of Ski Design Parameters' Effect on Friction

Doctoral thesis

NTNU
Norwegian University of Science and Technology
Thesis for the Degree of Philosophiae Doctor
Faculty of Engineering
Department of Civil and Environmental Engineering

NTNU
Norwegian University of Science and Technology

Sondre Bergtun Auganæs

# Laboratory Friction Testing of Cross-Country Skis

## Experimental Investigation of Ski Design Parameters' Effect on Friction

Thesis for the Degree of Philosophiae Doctor

Trondheim, August 2024

Norwegian University of Science and Technology
Faculty of Engineering
Department of Civil and Environmental Engineering

NTNU
Norwegian University of
Science and Technology

**NTNU**
Norwegian University of Science and Technology

Thesis for the Degree of Philosophiae Doctor

Faculty of Engineering
Department of Civil and Environmental Engineering



ISBN 978-82-326-8254-6 (printed ver.)
ISBN 978-82-326-8253-9 (electronic ver.)
ISSN 1503-8181 (printed ver.)
ISSN 2703-8084 (online ver.)

Doctoral theses at NTNU, 2024:331

Printed by NTNU Grafisk senter

# Abstract

Cross-country skiing holds a significant place in Norway's cultural history as the national sport. It plays a crucial role both in public health as a recreational activity and as a highly competitive sport. A decisive factor for performance in cross-country skiing is the friction between the ski and snow. As a consequence, a lot of effort is put into developing fast skis and glide products. In this development process, glide testing is essential to distinguish small differences between the products. However, a significant influence of changing weather, snow conditions and skier position make this task challenging in the field. This has made researchers develop laboratory setups to better control external factors. However, to obtain stable measurements, simplifications have been made by substituting snow with ice, and reducing both the sample size and speed. Therefore, the primary objective of this thesis has been to examine the friction between skis and snow within a controlled environment, under conditions that apply to cross-country skiing.

The first part of this work consisted of the development of a ski-snow tribometer (an instrument for measuring friction). This tribometer comprises a 6.5-meter-long snow track situated inside a freezing chamber. A ski is mounted to a carriage, which is driven across the track while the normal- and frictional forces are measured. Additionally, laboratory-grown dendritic snow has been produced by a custom-built snow machine as part of this setup. The results from the precision investigation showed that the setup could measure the friction coefficient of skis on new dendritic snow with a precision good enough to distinguish skis or glide products with very similar performance ($\Delta\mu \leq 0.001$).

Based on the insights from the first study a new method to test skis has been developed. This method reduces the impact of a constantly changing snow surface with repeated runs, on the measured coefficient of friction. By assuming a linear polishing/friction trend of the measured coefficients of friction, the data can be modified to remove the effect of a falling or rising trend. This approach has proven effective in mitigating the impact of a changing coefficient of friction on the average between the skis and has been used in subsequent experimental studies.

The second study investigated how loading conditions such as the normal load and placement of load (binding position) affected the macroscopic contact parameters and friction on a cross-country ski. To quantify the changes in macroscopic contact parameters we developed a rig for

measuring the pressure profiles of the contact zones on cross-country skis. This was achieved by pressing the ski onto loadcells to get the force measurement at every centimeter along the ski base. The results showed that increasing the normal load on the ski led to an increase in the contact length (apparent contact area), an increase in the average contact pressure, a larger load split towards the rear, and shorter spacing between the front and rear zones. The friction tests revealed that the coefficient of friction exhibited minimal variation with increased normal loads across three different snow conditions. Additionally, adjusting the ski binding to a more rearward position resulted in decreased friction levels under both cold (−10 °C) and warm (+5 °C) air temperatures. Due to the interconnected parameters of the modern cross-country ski, it was difficult to explain how the different contact parameters contributed to the measured change in the coefficient of friction.

Building on the knowledge from the second study, we developed an adjustable ski designed to isolate and manipulate the macroscopic contact parameters. This enabled the third study to focus on investigating the contact parameters isolated effect on the coefficient of friction. The adjustable ski decoupled the contact zones from the effect of the normal load, meaning that the apparent contact area was constant for different normal loads. In addition, the binding could be moved over the entire length of the ski, and the distance between the zones could be independently adjusted. These parameters were tested under settings relevant to cross-country skiing, meaning slider/contact zone configuration, speed, and snow conditions were in a range where the frictional trends have high validity to real-world skiing. The results showed that an increase in the average contact pressure was strongly connected to a reduction in the coefficient of friction at cold temperatures of -10 °C. At intermediate, (-2 °C) and warm (+5 °C) air temperatures the apparent contact area had a stronger effect on the friction than the normal load. The result of the load split between the contact zones at cold temperatures provided experimental evidence for the hypothesis that moving frictional power toward the front slider could create a thicker liquid-like layer earlier along the sliding ski, which consequently would result in a reduction in friction. Lastly, the effect of spacing showed a small, but consistent decreasing trend in friction for shorter spacing across the three temperatures tested.

# Sammendrag

Langrenn har en betydelig plass i Norges kulturelle historie som nasjonalsport. Skisport spiller en viktig rolle både som en fritidsaktivitet for folkehelsen og som en idrett med stor interesse og popularitet. En avgjørende faktor for prestasjon i langrenn er friksjonen mellom ski og snø. Som et resultat legges det mye arbeid i å utvikle raske ski og glidprodukter. I denne utviklingsprosessen er glidtesting avgjørende for å kunne skille mellom de små forskjellene i friksjon mellom de ulike produktene. Likevel er det utfordringer med å gjennomføre glidetesting i løyper utendørs på grunn av betydelig påvirkning fra skiftende værforhold, snøkvalitet og skiløperens posisjon. Dette har motivert forskere til å utvikle måleinstrumenter i laboratorium for å oppnå mer presis kontroll over eksterne faktorer. Imidlertid har forenklinger i form av å erstatte snøen med is, samt redusere størrelsen på prøvene (ski) og hastigheten blitt gjort for å sikre stabile målinger. Derfor har denne avhandlingen primært fokusert på å undersøke friksjonen mellom ski og snø i et kontrollert miljø, under betingelser som er typiske for langrenn.

Den første delen av dette arbeidet omhandler utviklingen av et tribometer for å kvantifisere friksjonen mellom ski og snø. Dette instrumentet omfatter en 6,5 meter lang snøbane som er plassert inni et kjølerom. Skiene monteres på en vogn som beveger seg over banen, og underveis måles friksjons- og normalkraften. For å komplettere oppsettet, blir naturlige snøkrystaller (dendritisk struktur) produsert ved hjelp av en spesialkonstruert snømaskin. Resultatene indikerte at oppsettet var i stand til å måle skiens friksjonskoeffisient på nyprodusert dendritisk snø med tilstrekkelig nøyaktighet for å differensiere mellom ski eller glidprodukter med svært lik ytelse ($\Delta\mu \leq 0{,}001$).

Basert på innsiktene fra den første studien, har det blitt utviklet en ny metode for skitesting. Denne metoden reduserer påvirkningen fra kontinuerlige endringer i snøoverflaten under gjentatte målinger av skiene. Ved å utnytte den lineære trenden i polering og slitasje observert i friksjonsmålingene for de forskjellige skiene, kan den gjennomsnittlige friksjonskoeffisienten for hver ski justeres. Dette reduserer effekten av en avtagende friksjonskoeffisient (raskere spor), noe som gjør sammenligningen mellom ski mer pålitelig. Denne metoden har blitt anvendt i de etterfølgende eksperimentelle studiene.

Den andre studien undersøkte hvordan normalkraft (løpervekt) og plassering av kraft (bindingsposisjon) påvirket de makroskopiske kontaktparameterne (kontaktareal, kontakttrykk, lastfordeling og avstand mellom kontaktsonene) og friksjonen på en langrennsski. For å kvantifisere endringene i de makroskopiske kontaktparameterne ble det utviklet en rigg for å måle trykkprofiler i kontaktsonene på langrennsski. Dette ble utført ved å trykke en ski ned på lastceller for å få kraftmålinger for hver centimeter langs skisålen. Resultatene viste at økende normalkraft på skien førte til en lengre kontaktsoner (større kontaktareal), en økning i gjennomsnittlig kontakttrykk, en større lastfordeling mot bakre kontaktsone, og kortere avstand mellom for- og bakre kontaktsone. Friksjonmålingene av skien viste at friksjonskoeffisienten ble lite påvirket av en økning i normalkraften på tvers av tre forskjellige snøforhold. Videre førte justering av skibindingen bakover til reduserte friksjonsnivåer under både kalde (-10 °C) og varme (+5 °C) lufttemperaturer. Fordi de sammenkoblede parameterne til den moderne langrennsskien endret seg uavhengig av hverandre, var det vanskelig å forklare hvordan de forskjellige kontaktparameterne påvirket den observerte endringen i friksjonskoeffisienten.

Ut fra innsikten oppnådd i den andre studien, ble det utviklet en justerbar ski spesilet designet for å isolere og manipulere de makroskopiske kontaktparameterne. Dette gjorde det mulig å undersøke deres isolerte effekt på friksjonskoeffisienten. Den justerbare skien isolerte kontaktsonene fra effekten av normalkraften, noe som betyr at det synlige kontaktarealet var konstant for forskjellige normalkrafter. I tillegg kunne bindingen flyttes over hele skiens lengde, og avstanden mellom sonene kunne justeres uavhengig. Disse parameterne ble testet under forhold relevante for langrenn, noe som betyr at modelskien/kontaktsonens konfigurasjon, hastighet og snøforhold var i et spekter der friksjonstrendene har overførbarhet for langrenn ute i løypen. Resultatene viste at en økning i gjennomsnittlig kontakttrykk var sterkt koblet til en reduksjon i friksjonskoeffisienten ved kalde temperaturer på -10 °C. Ved mellomliggende (-2 °C) og varme (+5 °C) lufttemperaturer hadde det synlige kontaktarealet en sterkere effekt på friksjonen enn normalkraften. Resultatet av lastfordelingen mellom kontaktsonene ved kalde temperaturer ga eksperimentelt bevis for hypotesen om at flytting av kraftpunktet (bindingen) mot den fremre kontaktsonen kunne skape større friksjonsvarme lengre frem på skien. Dette ville igjen fremme tidligere dannelse av en vannfilm for smøring langs skien under glid, noe som igjen ville lede til en nedgang i friksjon. Til slutt viste resultatene at avstanden mellom kontaktsonene hadde en liten, men konsistent synkende trend i friksjon for kortere avstand mellom kontaktsonene over de tre temperaturene som ble testet.

# Preface

This thesis is submitted to the Norwegian University of Science and Technology (NTNU) for the fulfillment of the degree of philosophiae doctor (PhD). This doctoral work has been performed at the Department of Civil and Environmental Engineering, NTNU, Trondheim, with Professor Alex Klein-Paste as the main supervisor and Associate Professor Audun Formo Buene as co-supervisor. This work was funded by the Norwegian Research Council (NFR) through the Nano2glide project, project number 296540.

Throughout this research, I have delved into the intricate relationship between snow and skis, discussing its complexity. During a particularly engaging discussion about the mechanisms of friction in one of our supervision meetings, Alex remarked, "I wish I could be a snowflake to see what is really happening when the ski slides over me." This whimsical comment stayed with me, inspiring the creation of the following poem, which seeks to capture the wonder and mystery of this phenomenon.

***Whispers of Snowflakes: A Journey Beneath the Skis***

*Do you wanna be a snowflake, lying 'neath a sliding ski, To understand the secrets there, it's such a mystery? I wish you'd share your hidden truths, reveal what's really so, Is there a lubrication film of water, or is there more to know?*

*Do you wanna be a snowflake, tell me what you see, The science of the icy glide, beneath the wintry spree. I thought it was a water film, slick and clear and bright, But now I hear it's changing along the ski, and I'm puzzled in the night.*

*Do you wanna be a snowflake, whispering your tale, Of friction, force, and icy dance beneath the winter's veil? Why do the skis slide fast at times, and sometimes slow, I ask, What's the hidden magic there, behind the skier's task?*

*Do you wanna be a snowflake, tell me what's begun, Why does the ski glide faster with every single run? Is it friction's warming touch, or the base that's getting fine, Or is the snow compacting with every curve and line?*

*Do you wanna be a snowflake, lying 'neath a sliding ski, To grasp the wonders happening, and solve this mystery? I thought it was a water film, but now I'm left in doubt, Oh, tell me little snowflake, what is it all about?*

# Acknowledgments

First and foremost, I must extend my gratitude to my supervisor, Alex Klein-Paste, for his unwavering belief in me and for persuading me to embark on this PhD journey. Despite my initial skepticism about pursuing a PhD, you triggered a curiosity in me, and you still do. Your enthusiasm when looking at experimental results is contagious, in a good way. The way your face lights up during discussions of new ideas has consistently made our supervision meetings enjoyable.

Special thanks are due to my co-supervisor, Audun Formo Buene, whose guidance has been indispensable in my PhD journey. Audun has relentlessly pushed me to hone my skills as a scientist, setting high standards in experimental work and academic writing. His role as a discussion partner in our daily office interactions has been invaluable. Even though we did not always agree, these discussions usually brought some new insights when I needed help or other perspectives.

I would like to acknowledge the Nano2glide consortium for their collaboration, particularly Christian Gløgård, Bjørn Ivar Austrem, Svein Ivar Moen, Felix Breitschädel, and Svein Iversbakken. Their practical insights into ski-related issues and the provision of essential ski and wax equipment have been crucial.

I would also like to thank colleagues at the Road, Railway and Transport group at NTNU for all the coffee breaks and stimulating discussion around the lunch table. The technical staff and workshop at the department of Civil and Environmental Engineering, especially Bent, Frank, Tage, and Per, deserve special mention for their assistance in constructing the tribometer and other experimental equipment. I also wish to acknowledge the Center for Sport Facilities and Technology for financial support for my duty work, and my colleagues here for interesting project discussions within the topic of sports technology.

I owe a big thanks to my training buddies Terje, André, Simon and Erik, who have been a source of mental support, sharing many of the total 35.000 km of skiing, biking, running and swimming the last four years. This has helped me stay sane in stressful periods. Additionally, I extend heartfelt thanks to my friends who have been a constant source of support and encouragement throughout my academic journey.

Lastly, but most certainly not least, my profound gratitude goes to my family, whose unwavering encouragement and support have been my bedrock throughout this journey. Their belief in my abilities and aspirations, even during moments of doubt and challenge, has been a source of strength and motivation. It is their constant love, understanding, and patience that have made the demanding and often solitary pursuit of a PhD not just bearable, but fulfilling. Their enthusiasm for my work has been vital in keeping me focused and resilient. The collective impact of their support has been a cornerstone in my achievements, and for that, I am eternally grateful.

Trondheim, March 9, 2024

Sondre Bergtun Auganæs

# Table of Contents

# Nomenclature

| | | |
|---|---|---|
| $A_{app}$ | Apparent contact area between ski and snow | [$mm^2$] |
| $A_r$ | Real contact area between ski and snow | [$mm^2$] |
| $\Delta d$ | Compression depth of ski | [µm] |
| $F_F$ | Friction force | [N] |
| $F_N$ | Normal force | [N] |
| $F_{shear}$ | Shear force | [N] |
| $F_{plow}$ | Compaction and plowing force | [N] |
| g | Gravitational force | [$m/s^2$] |
| H | Snow harness | [MPa] |
| h | Film thickness of lubrication layer | [µm] |
| m | mass | [g] |
| $P_{friction}$ | The friction power of a ski | [W] |
| PR | Penetration resistance | [N] |
| $R_a$ | Arithmetic mean roughness of a profile | [µm] |
| $S_a$ | Arithmetic mean roughness of a surface | [µm] |
| $S_{dyn}$ | Penetration depth into snow | [mm] |
| $S_z$ | Maximum pit to peak height of a surface | [µm] |
| SPC | Arithmetic mean peak curvature of a surface | [$mm^{-1}$] |
| SPD | The density of peaks of a surface | [$mm^{-2}$] |
| $S_{pk}$ | Reduced peak height of a surface | [µm] |
| *v* | Speed of ski | [m/s] |
| *w* | Width of the ski | [mm] |
| µ | Kinetic coefficient of friction | [-] |
| $\Delta$ µ | Difference in the coefficient of friction | [-] |
| $\tau_c$ | Shear stress | [MPa] |
| η | Viscosity of water | [Pas] |
| $\rho_s$ | Density of snow | [$kg/m^3$] |

# Abbrevations

| | |
|---|---|
| CI | Confidence interval |
| IMU | Inertial measurement unit |
| LWC | Liquid water content |
| NTNU | The Norwegian University of Science and Technology |
| relRCA | Relative real contact area |
| RQ | Research questions |
| RSD | Relative standard deviation |
| UHMWPE | Ultra-high molecular weight polyethylene |

# 1 Introduction

## 1.1 Background

Cross-country skiing has evolved from being a means of winter transportation to becoming a recreational activity and a highly competitive sport. Its evolution has been defined by advancements in equipment, technique, snow track preparation, and an improved understanding of the physical principles governing the interaction between skis and snow (Pellegrini et al., 2018). The pursuit of minimizing friction between skis and snow remains an active area of research, recently driven by a global ban on the use of fluorine-containing waxes and ski bases (International ski federation, 2021). With the ski industry seeking fluorine-free alternatives, there arises a demand for testing facilities capable of providing representative data across a spectrum of snow conditions. However, achieving precise and representative measurements of the friction between skis and snow remains a challenge (Nachbauer et al., 2016).

Today skis and glide wax products are mainly tested in the field. This provides the benefit of conducting product testing directly within the end-user environment, leading to a high level of validity. However, the methods used by the industry have low precision due to variations in the skier's position, constantly changing snow surface and other environmental factors (Hasler et al., 2016). To reproduce the testing conditions outside from test to test is also difficult. Because the testing is mainly based on comparing the relative difference between two ski pairs, it is difficult to know which characteristics of the ski, snow or wax, or a combination makes the ski glide faster. This has led researchers to develop laboratory set-ups to be able to measure friction in a controlled environment (Buhl et al., 2001; Bäurle et al., 2006; Nachbauer et al., 2016). However, simplifications in the form of substituting the snow with ice, and reducing the sample size and speed have been made to get more stable measurements. This made the review by Colbeck (1992) highlight the need for more experimental data with full-size skis, at high speeds and on realistic snow surfaces.

The importance of precise measurements of the friction coefficient ($\mu$) was highlighted in a study by Breitschädel et al. (2012), who emphasized that achieving a resolution of $\Delta\mu \approx 0.001$ is imperative to distinguish between race-prepared skis. According to the power balance model of Moxnes et al. (2014), a reduction in the coefficient of friction by 0.001 resulted in a 7.1-

second reduction in finishing time for a skier during a simulated 4 km race. It is important to distinguish such small differences in the friction, especially when one considers that in biathlon World Cup races, the time separating the first and tenth positions often falls within a narrow margin of 3-5%, while in Nordic skiing, the time gap between the first and fourth place is often less than 1% of the overall finishing time (Breitschädel, 2014; Luchsinger et al., 2017). Experimental investigations into the friction between cross-country skis and snow have the potential to yield new insights and knowledge regarding ski properties. This knowledge can serve as the foundation for developing innovative solutions to reduce ski-snow friction, which, in turn, can facilitate the transition to a fluorine-free winter sport and further developments in cross-country skiing.

A cross-country ski has an arched design which makes the load response very different compared to a model slider with a fixed contact area. As a modern ski is essentially two sequential sliders, there is a complex interplay between the partitioning of load and friction between the front and rear contact zones. The magnitude and placement of the load control the compression of the ski, and thus how the reaction pressure from the snow along the ski base is distributed. The fact that the load response results in several changes on the macro level at the same time makes testing of cross-country skis more complex (Kalliorinne et al., 2023b; Mössner et al., 2023).

Due to the complexity of full-scale skis, research efforts have often utilized model sliders to understand the effect of various factors on friction, including load, apparent contact area, speed, and base structure (Bowden & Hughes, 1939; Buhl et al., 2001; Bäurle et al., 2006; Giesbrecht et al., 2010). In such studies, the normal load on model sliders is adjusted to replicate the average contact pressure experienced by real skis, with the assumption that this triggers similar friction mechanisms. Because of the reduced normal load, the total frictional work generated by model sliders is lower than that of a cross-country ski, assuming a similar coefficient of friction. This reduction might also affect the amount of frictional heating of the snow. Nevertheless, Bäurle (2006) argued that the primary determinant in the formation of a lubrication layer through heating was the frictional power per unit area, a factor that remained consistent between model sliders and real skis.

However, there still exists a gap in the understanding between the experimental results obtained from small-scale sliders and the more intricate response observed on cross-country skis. Particularly in terms of how mechanical ski properties impact the coefficient of friction, we

lack the understanding to confidently translate results from model sliders to full-scale skis. Therefore, there is a need for more knowledge about how the macroscopic ski contact characteristics, such as apparent contact area, normal load, and load split, differ from a model slider. To address this gap, it is essential to isolate ski parameters and conduct experiments at full-scale and high speeds on snow surfaces, to provide a more accurate representation of real-world skiing conditions.

## 1.2 Research objectives

The overall objective of this thesis is to better understand friction testing of cross-country skis, and how the loading of modern skis impacts both the macroscopic contact parameters and the resulting ski-snow friction forces. This includes the following objectives with their associated research questions (RQ):

- Develop a laboratory method for testing the friction of full-scale cross-country skis at high speeds on realistic snow surfaces.
  - RQ 1 – What is the measurement precision obtainable with this method?
  - RQ 2 – How does the snow surface change with repeated sliding of a ski?
  - RQ 3 – How should skis be tested to facilitate the best comparison?

- Examine how macroscopic contact parameters change with different loading conditions on a skating cross-country ski.
  - RQ 4 – How does the load and load application point impact the macroscopic contact characteristics on a cross-country ski?
  - RQ 5 - How does the load and load application point impact the coefficient of friction on a cross-country ski?

- Examine the effect of isolated macroscopic contact parameters on gliding friction.
  - RQ 6 – How do average contact pressure, load distribution between front and rear contact zones, and the spacing between these zones influence the ski-snow friction?

## 1.3 Research approach

This thesis is mainly based on experimental work. An experimental ski-snow tribometer was designed, built, and tested in the NTNU Snowlab. This work resulted in Paper I. Based on these results a method was developed and used to quantify the effect of normal load and load application point on friction for a modern cross-country ski in Paper II. The second paper focuses on understanding how the macroscopic contact parameters change with loading. To understand this a force measurement rig was built to quantify these changes. Paper III focuses on the effect of different macroscopic contact parameters on the coefficient of friction. On a modern ski, several of these characteristics changed at the same time, therefore an adjustable test ski was built to isolate these variables. This enabled the quantification of the influence of each parameter on friction, while also enhancing our understanding of the differences between testing model sliders and full-size skis.

## 1.4 Thesis structure

This thesis is composed of six chapters, followed by a section that presents the three papers, and an Appendix. Chapter 1 introduces the problem, including research questions, approach and overview of published papers. Chapter 2 provides relevant theory on ski-snow friction and testing methods. Chapter 3 describes the research methods used to solve the problems. This includes the development of the ski-snow tribometer, contact pressure profile measurement rig and a tunable test ski. Chapter 4 presents the main results, separated into the results of the three different papers. In Chapter 5 the results are discussed. The discussion is divided into four parts: 1) methodological development and considerations around the laboratory test method, 2) measurements of contact parameters on skis, 3) the effect of isolated parameters on friction, 4) how the findings from this thesis contribute to knowledge for better evaluation of ski-snow friction. Lastly, Chapter 6 presents the main conclusion of the thesis together with suggestions for future work.

## 1.5 Papers

This thesis is presented in the form of a collection of three papers. The papers are briefly described in the following section.

**Paper I - Laboratory testing of cross-country skis – Investigating tribometer precision on laboratory-grown dendritic snow**

Auganæs, S. B., Buene, A. F., & Klein-Paste, A. (2022). Tribology International, 168, 107451. https://doi.org/10.1016/j.triboint.2022.107451

This article describes the development of a linear tribometer and its precision. The setup was able to measure the coefficient of friction with a precision to distinguish skis with $\Delta\mu \leq 0.001$. Furthermore, the precision was examined on three different levels; within one single track, between parallel tracks and between preparation of a snow testbed. Lastly, the polishing on the snow surface with repeated runs of a ski was investigated by 3D surface imaging and the development of the measured coefficients of friction.

My contribution to this work was to perform all experimental tests, data analysis and writing of the paper. Audun Formo Buene contributed to the data analysis and writing of the paper. Alex Klein-Paste contributed with the idea of the study, discussions on the experimental setup and reviewing the manuscript.

**Paper II - The Effect of Load and Binding Position on the Friction of Cross-Country Skis**

Auganæs, S. B., Buene, A. F., & Klein-Paste, A. (2023). Cold Regions Science and Technology, 212, 103884. https://doi.org/10.1016/j.coldregions.2023.103884

This article describes how measured ski-snow pressure profiles change with different loading conditions, and how this affects the coefficient of friction. Four different parameters believed to affect the friction were identified and measured to change independently of each other when the loading conditions changed. The ski-snow friction was measured in the tribometer at three different snow temperatures, with the same loading conditions on the ski.

My contribution to this work has been to design the research idea, perform all experimental tests, data analysis and write the paper. Audun Formo Buene contributed to the development of the ski pressure rig, data analyses and writing of the paper. Alex Klein-Paste contributed with discussions during the measurements and analysis, and reviewing the manuscript.

**Paper III – Experimental Investigation into the Effect of Macroscopic Cross-Country Ski Parameters on Gliding Friction**

Auganæs, S. B., Buene, A. F., & Klein-Paste, A. (2024). Cold Regions Science and Technology, 225, 104264. https://doi.org/10.1016/j.coldregions.2024.104264

In this study, a custom adjustable ski was developed to isolate the effect of normal force, apparent contact area, spacing, and load split on the coefficient of friction. The effect of these parameters on friction was then tested in the tribometer at three different air temperatures, respectively -10 °C, -2 °C and +5 °C.

My contribution to this work was to design the research idea, perform all experimental tests, and data analysis and write the paper. Audun Formo Buene contributed to the development of the adjustable test ski, data analyses and writing of the paper. Alex Klein-Paste contributed with discussions during the measurements and analysis, and reviewing the manuscript.

## 1.6 Other scientific contributions

These contributions, though relevant to the thematic core of the thesis centered on friction measurement utilizing the tribometer, lie outside the research scope and, as such, will not be integrated into the thesis's results and discussion.

**Paper IV - Dynamic and Static Friction Measurements of Elastomer Footwear Blocks on Ice Surface**

Jakobsen, L., Auganaes, S. B., Buene, A. F., Sivebaek, I. M., & Klein-Paste, A. (2023). Tribology International, 178, 108064. doi:https://doi.org/10.1016/j.triboint.2022.108064

Together with a Danish PhD student, we performed experiments in the tribometer with elastomer footwear blocks on ice surfaces. Some modifications were made to the tribometer motor program to be able to test the static friction. The testing on ice also showed much better precision due to ice being a more stable material than snow.

My contribution to this study was helping with designing and performing the experiments and doing the data analysis from the friction track, as well as reviewing the manuscript.

**Paper V - Effect of Polydimethylsiloxane Oil Lubrication on the Friction of Cross-Country UHMWPE Ski Bases on Snow**

Buene, A. F., Auganæs, S. B., & Klein-Paste, A. (2022). Frontiers in Sports and Active Living, 4. doi:10.3389/fspor.2022.894250

This article investigated the effect of silicon oil as a lubricant between ski and snow. The high hydrophobicity of silicon oil showed friction-reducing effects under very wet conditions. However, it did not outperform the commercial wax products. In addition, the range where it might benefit was very small, since the performance was very poor on dry snow.

My contribution to this study was helping the main author with discussions around the experimental set-up and results, as well as reviewing the manuscript.

# 2 Ski-snow friction state of the art

When a ski slides over snow, the two surfaces interact in relative motion with each other. The force that resists the motion of sliding is referred to as the friction. The equation for the friction force was first formulated in 1785 by Charles Augustin Coulomb (1736-1806) as:

$$F_F = \mu F_N \qquad (2.1)$$

where $F_F$ is the frictional force, $F_N$ is the normal force, and $\mu$ is the coefficient of friction.

The coefficient of friction is often used as an empirical value that describes the ratio between the friction force and the normal force. Sometimes it is used as a material parameter, but it is more of a system parameter depending on several factors of the two surfaces and the environment where it operates (Stachowiak & Batchelor, 2006). The ski-snow tribosystem consists of three main components, the ski base of ultra-high molecular weight polyethylene (UHMWPE), the snow surface and a lubricating liquid-like layer, as depicted in Figure 2.1 (Kietzig et al., 2010).

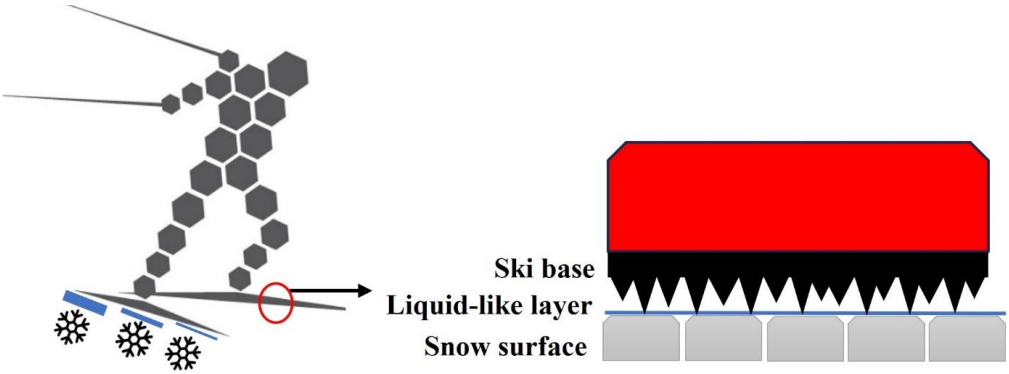


Figure 2.1 Schematic representation of cross-country ski interaction with snow. The left panel illustrates the liquid-like layer formed along the ski sole and the snow surface during sliding. The right panel represents a cross-section view of the ski-snow tribosystem, illustrating the liquid-like layer as lubrication between the ski and snow.

The liquid-like layer, often referred to as the quasi-liquid layer, is a film of water molecules that exist on the surface of ice or snow, even at temperatures below the freezing point (Dash et al., 2006). This layer acts as a lubricant between the ice/snow and any object in contact with it.

The thickness of this liquid-like layer depends on the temperature and the specific characteristics of the ice or snow surface. For the snow surface, factors like temperature and humidity, strength/hardness, and surface topography are important for friction. For the ski, parameters like the load, speed, bending stiffness, camber height, surface chemistry and wax treatment, and surface topography of the sole are important (Almqvist et al., 2022; Colbeck, 1992; Moldestad, 1999).

The research field of ice and snow friction has intrigued scientists for decades with numerous publications. A bibliography on snow and ice friction by Colbeck (1993) counts around 500 publications. Understanding the complex interplay between solids in contact with ice or snow is essential for designing efficient winter tires, enhancing ice skate or ski performance, and ensuring safe walking on icy surfaces. For many years it was believed that pressure melting was the reason for the low friction coefficient on ice (Reynolds, 1901). Later, Bowden and Hughes (1939) introduced the theory of self-lubrication by frictional heating based on their experiments showing that the friction coefficient was dependent on temperature, load and velocity. However, there are, still to this day, discussions of the frictional mechanisms thought to govern the low friction observed on skis (Lever et al., 2019).

The rest of this chapter aims to give the reader a better understanding of the properties of skis and snow, and their interaction through friction theory relevant to this thesis.

## 2.1 Snow and ice friction

The low sliding friction of skis has been explained with a thin lubricating film created from frictional heating between the ski and snow. This theory by Bowden and Hughes (1939) has further been supported by other studies estimating the thickness of meltwater film between the ski and snow. Ambach and Mayr (1981) estimated the film thickness based on a capacitor sensor placed on the ski base to measure the dielectric constant when the ski was gliding on snow. Their findings indicated a rise in film thickness corresponding with an increase in snow temperature. This suggests the significance and impact of snow temperature, frictional heating, and heat loss on the formation of water films.

Colbeck and Warren (1991) measured the thermal response along an alpine ski base with thermocouples as evidence that frictional heating could provide meltwater for lubrication. They noted that the temperature increase of the moving ski base was greater at lower snow

temperatures. This was attributed to increased heat production, stemming from reduced development of the water film and thus a higher coefficient of friction. Additionally, the temperature rise was more pronounced under larger normal loads. Colbeck (1994) and Schindelwig et al. (2014) used a similar approach on a cross-country skating ski. They found an increasing temperature rise along the ski, with the largest temperature just behind the foot, where the peak pressure is located. Other studies on ice friction, where a decrease in the coefficient of friction by speed or load has been connected to lubrication by heating, include (Bowden, 1953; Buhl et al., 2001; Bäurle et al., 2006; Kuroiwa, 1977; Oksanen & Keinonen, 1982).

### 2.1.1 Overview of the different friction mechanisms

Reviews on snow and ice friction mechanism related to sliding have been given by Glenne (1987), Colbeck (1992), Kietzig et al. (2010), Nachbauer et al. (2016), Lever et al. (2021) and Almqvist et al. (2022). Various friction mechanisms contribute to the resistance encountered when a ski slides on snow. A general agreement is that there are several mechanisms working simultaneously. These include adhesion, plowing, compaction, viscous shearing, and water bridging/capillary attraction. The dominant mechanism among these depends on the specific friction regime in which the system operates. The friction regime varies based on factors such as the thickness of the liquid-like layer and can be divided into dry, boundary, mixed, or hydrodynamic (Kietzig et al., 2010).

In the dry friction regime, interactions occur primarily between solid surfaces. Friction in this regime originates from the shearing of adhesive bonds formed between the tips of snow asperities and the ski base, either chemically and/or as mechanical interlocking by irregularities between the surfaces. The force required to overcome these adhesive bonds can be described as:

$$F_{shear} = \tau_c A_r \tag{2.2}$$

where $\tau_c$ is the shear strength, and $A_r$ is the area of real contact between the asperities. However, real dry friction on ice does not exist at temperatures relevant for skiing because a molecular thin liquid-like layer is still present at the sliding interface at very low temperatures (Petrenko & Whitworth, 1999). When studies refer to dry friction in skiing, they are essentially discussing boundary lubrication. This friction regime is characterized by a liquid-like layer with a thickness of just a few molecules. In this regime, the temperature of the snow asperities in contact with the ski remains below the melting point (Kietzig et al., 2010).

In most cases, a combination of lubricated contacts and boundary friction occurs during sliding. The boundary friction regime is believed to dominate the front portion of the ski where it initially comes in contact with the snow (Colbeck, 1992). As more of the ski travels over the same snow asperities a gradual transition to mixed lubrication will occur due to frictional heating. The mixed friction regime is characterized by some points within the contact zone reaching the melting temperature. In this regime, the load of the ski base asperities is partly supported by some contacts through a lubrication film and some points as boundary contacts. This thin film reduces the shear force due to lower solid-solid adhesion. However, the lubrication layer also introduces capillary water bridges between the asperities, which can add frictional resistance (Colbeck, 1988).

In situations where there is a full lubrication film separating the two surfaces, the regime is called hydrodynamic. In this regime, the lubricating layer carries all the load, and the friction force is equal to the shearing of thin water film (Oksanen & Keinonen, 1982). The friction force can be expressed as:

$$F_{viscous\ shear} = \frac{A_r \eta v}{h} \tag{2.3}$$

where $A_r$ is the real area in contact with the water film, η is the water viscosity, $h$ is the film thickness and $v$ is the speed of the ski.

A difference between friction mechanisms of a ski gliding on ice compared to snow is the added resistance due to compaction and plowing. The compaction of snow in front or under the ski is a process that dissipates energy due to plastic deformation in the snow matrix. The process thus depends on the compaction strength of the snow and the pressure exerted by the ski. Glenne (1987) formulated the force due to compaction and plowing as:

$$F_{plow} = \rho_{snow} w v^2 \Delta d \tag{2.4}$$

where $\rho_{snow}$ is the snow density, $w$ is the ski width, $v$ is the speed, and $\Delta d$ is the compression depth.

### 2.1.2 Real contact area and lubrication film thickness

Important factors for determining friction on snow and ice are the real contact area and the shear stress at the contact points (Bäurle et al., 2007). The real contact area is only a fraction of the total area of the ski that appears to be in contact ($A_{app}$). In studies related to skiing the real contact area is often reported as the relative real contact area (relRCA). This is the real contact

area divided by the apparent contact area. By reporting the relRCA, the influence of the sample size is removed. Theile et al. (2009) calculated the relative real contact area under static loading to be 0.4%. Another study modeled the relRCA of a single snow grain and ski sole to vary from 0.04% to 6% depending on the normal load and radius of the snow grain (Mössner et al., 2021). However, it is believed that the real contact area increases during sliding due to the presence of a meltwater film (Colbeck, 1992).

Bäurle et al. (2007) calculated the water film thickness along a polyethylene slider on ice to be below 100 nm at low temperatures of -15 °C and up to 1 µm at temperatures close to 0 °C. The relRCA increased from a few percent in cold conditions to almost 100% under warm conditions. Figure 2.2 illustrates how the friction force depends on the water film thickness and the relative real contact area. The equation used to derive the friction curve is based on viscous shear. It's important to use such graphs cautiously for absolute values since they are based on a set of assumptions. However, they provide a useful visualization of how the friction force depends on parameters like temperature, load, and sliding speed.

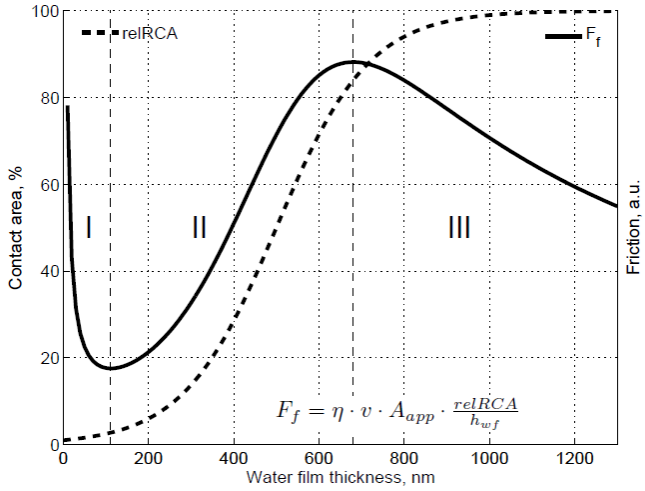


Figure 2.2 Relative real contact area (dashed line, left axis) and friction force (solid line, right axis) as a function of water film thickness. The friction force is a qualitative curve based on the equation in the graph (from Bäurle (2006)).

Temperature measurements of the ski sole has shown temperature increases ΔT from 1 °C to 5 °C depending on skiing speed (Ambach & Mayr, 1981; Colbeck & Warren, 1991; Schindelwig

et al., 2014). Bäurle et al. (2006) used an infrared camera to measure a temperature increase of approximately 2 °C at the ice surface after the slider had passed. Lever et al. (2019) used the same approach but reported very small temperature increases. Their calculations indicated that the contact spot temperatures never approached the melting point. They argued that abrasion was the primary mechanism responsible for the low friction observed on skis. However, it's important to note that they conducted their experiments at speeds ranging from 0.36 to 1.4 m/s and with average contact pressures in the range of 0.8 to 4.5 kPa, which is ten times lower than typical speeds and contact pressures.

More recently Hasler et al. (2021) employed a similar approach, measuring temperature behind a full-scale cross-country ski at high speeds (5-25 m/s) with an IR camera. They calculated the snow contact spot temperature from the average pixel temperature (with each pixel measuring 0.5 × 0.4 mm). The relative contact area was estimated based on the difference between the measured average snow temperature and the bulk temperature, divided by the difference of snow contact spot temperature limited to 0 °C and the bulk temperature. This means that if the measured average temperature of all the pixels reached 0 °C, the relative contact area would be 100%. They reported the relative contact area to vary from 21-98% depending on the speed.[1]

## 2.2 Snow properties

Snow can be described as ice crystals with varying shapes depending on temperature and humidity. Snow originates in the clouds where individual crystals nucleate, grow, and eventually fall to the ground. Naturally, it exhibits a wide range of grain sizes and shapes, impacting the density and sintering of snow on the ground (Fierz et al., 2009). It is important to differentiate between natural snow and machine-made snow. Unlike natural snow, machine-made snow is produced from small water droplets that freeze from the outside and inwards, resulting in rounded grains and a close-packed, high-density structure (Lintzén, 2013). This higher density makes it more durable and weather-resistant compared to natural snow. Kuroiwa and LaChapelle (1973) pointed out that processing machine-made snow into a racetrack is easier than working with the natural product because it is already in an advanced state of metamorphosis. Snow metamorphosis refers to the process by which snow undergoes physical

[1] It should be noted that they did not measure the relative real contact area but estimated a relative contact area from temperature measurements. This might be better the described as how much of the snow surface has been touched after a sliding ski and should not be compared to the relative real contact area of the ski at a given time.

and structural changes after it has fallen. These changes are primarily driven by variations in temperature, humidity, and other environmental factors.

Snow is an ever-changing material due to its proximity to its melting point. Even minor temperature fluctuations can significantly alter its mechanical properties. The mechanical characteristics of snow are influenced by its microstructure (grain shape, size and bonds), density, temperature, moisture content, and loading rate (Johnson & Schneebeli, 1999). Table 2.1 displays how the snow strength is affected by the different properties in a generalized way, meaning that the snow strength does not always follow these rules. For example, when the snow is soaked with water the density is high, but the strength is still low. The strength of snow primarily relies on the bonding between its grains, with a higher density of bonds per unit volume contributing to greater strength (Shapiro et al., 1997).

For many materials, density is often closely related to strength. Snow however can experience large differences in strength with the same density (Shapiro et al., 1997). The compression strength also depends on the rate of loading. At slow deformation rates, snow behaves plastically, similarly to a viscous fluid. At fast deformations, it becomes elastically brittle (Wolfsberger et al., 2019). This means it can return to its original state if the load does not exceed the elastic limit. If this limit is exceeded the bonds in the snow matrix will start to break.

Cold snow is typically harder than warm snow, as its compressive strength tends to increase with lower temperatures (Wolfsberger et al., 2019). Consequently, cold snow is more resistant to deformation and preparation. The liquid water content (LWC) of snow is closely tied to temperature, but close to 0 °C LWC can vary widely. High LWC indicates the presence of water between snow grains, which significantly reduces its strength.

Table 2.1 Overview of how snow strength is affected by the snow's structural properties. (Adapted from (Wolfsberger et al., 2019))

| **Properties** | **Snow strength is:** | |
|---|---|---|
| | **Low** | **High** |
| **Density** | Low | High |
| **Grain shape** | New snow-faceted | Rounded |
| **Grain size** | Large | Small |
| **Bonds** | Few | Many |
| **Temperature** | Warm | Cold |
| **Liquid water content** | Soaked | Dry |

### 2.2.1 Snow track requirements

The requirement for a cross-country skiing track is that it should be firm enough to support a push of without collapsing (soft), but not too firm (icy) to cause the ski to slip (Wolfsberger et al., 2019). The snow in a racetrack undergoes several processes before it becomes ready for skiing, as depicted in Figure 2.3. Initially, an assessment of the quality of the current snow track conditions is essential before any preparation work can start. Based on this assessment, decisions are made regarding the choice of equipment and the preparation process carried out by the grooming machine. The preparation process involves mechanical treatment of the snow, primarily through compaction and occasionally by breaking down snow crystals into smaller particles using a tiller (rotating blades that churn and mix the snow).

After track preparation, some time is required for the track to sinter. This is a process in which ice particles bond together at temperatures below the melting point. Most mechanisms that contribute to ice sintering are slow, but the rate depends on the temperature gradient within the snowpack, and thus the weather after preparation influences the sintering. However, Szabo and Schneebeli (2007) showed that the freezing of a liquid-like layer present at the surface of the ice can contribute to ice bonding in less than 1 second.

The final snow surface depends on the history of the snow, the last preparation, and the time and weather during the sintering process. When the tracks are used by skiers during the day, the quality will often deteriorate. In such cases, the entire process must be repeated in the evening or the following day.

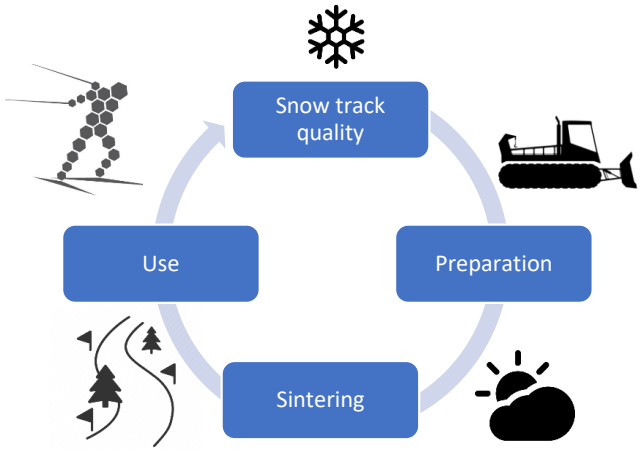


Figure 2.3 Illustrates the process a snow track undergoes, from initial snow conditions to the finished surface used by the skiers.

Measurements of snow properties in friction studies usually include the snow temperature, LWC or humidity, and density. In addition to these parameters, the study by Wolfsperger et al. (2021) measured the specific surface area and penetration resistance. They showed that a multivariate regression model with these snow parameters could, to some degree ($R^2 = 0.75$), explain the measured differences in the glide times of skiers.

The snow resistance to deformation is important for predicting the depth to which the ski will penetrate the snow, which in turn influences the apparent contact area. This resistance also affects how much of the frictional work is going to compaction and plowing. Due to the snow's proximity to the melting point, the hardness can vary a lot. Moldestad (1999) calculated the snow hardness to vary from 4.3 kPa to 2800 kPa, with an average of 150 kPa, from dropping a steel ball onto cross-country ski race tracks. Wolfsperger et al. (2021) calculated the penetration resistance using a Swiss Rammsonde with an adapted penetration body (d = 15 mm; cone angle = 60°) for groomed snow. The measurements varied from 67 N to 146 N. Mössner et al. (2013) argued that the best way to report snow hardness was as reaction force per volume displacement to make the measurement independent of the applied load. They found the snow hardness to vary from 0.04 $N/mm^3$ on fresh new snow on ski slopes to 90 $N/mm^3$ for late summer ski slopes on glaciers. This highlights the significant variations and underscores the difficulty in comparing measurements due to the diverse methods of reporting them.

Another significant aspect to consider is the deformation caused by repeated sliding. The extent to which a ski slides on a fresh track during a race can be discussed, but it remains crucial to

acknowledge this distinction. Differentiating between the effects of a ski on untouched snow versus its impact on a path that has undergone multiple passes is essential for a comprehensive understanding of snow deformation and ski performance.

The snow surface experience plastic deformation during the first run when it is compressed by a ski (Hasler et al., 2022; Theile et al., 2009). With repeated loading less permanent deformation was observed. Instead, the snow matrix demonstrates elastic deformation, more specifically, a delayed elastic deformation. This indicates that the compressed snow needs time to revert to its original shape after being compressed, leading to energy loss in a hysteresis loop. Theile et al. (2009) observed an irreversible deformation of 200 µm during the first loading, while only 20 µm delayed elastic deformation was observed with repeated loading. A study conducted by Hasler et al. (2022) found the snow to compact around 0.5 to 1 mm during the first pass of a ski. This initial compression is significant, indicating a notable alteration in the snow's structure due to the pressure exerted by the ski. In subsequent runs over the same track, the study observed a decrease in the degree of permanent deformation.

## 2.3 Cross-country ski properties

Cross-country skis are constructed from several components, including the base material, core, modular carbon fibers and top sheet (Kuzmin & Fuss, 2013). The most used base material is press-sintered UHMWPE. The core is typically made from lightweight materials like foam, wood, or composites, often reinforced with layers of carbon fiber to enhance bending stiffness. A thin layer of thermoplastic or fiberglass typically serves as the top sheet. These various layers are then securely bonded together using an adhesive, such as epoxy, within a mold to create the ski's characteristic arched shape. The final manufacturing step involves structuring the ski's sole through stone grinding, which imparts the distinctive "grooves" aligned along the sliding direction.

### 2.3.1 Mechanical properties and pressure distribution

A common approach for assessing the mechanical properties of cross-country skis involves compressing the ski onto a hard flat surface while progressively increasing the normal load. The distance between the ski sole and the rigid surface is measured during this process, resulting in camber curves as illustrated in Figure 2.4. Typically, any reading below a defined threshold value of 0.1 mm is considered as contact (Breitschädel et al., 2010). By using this threshold,

the length of the contact zones in both the front and rear parts of the ski can be determined. Additionally, various parameters, including camber height at the balance point, peak camber height, and characteristics related to tip and tail openings, can be derived from the camber curve data.

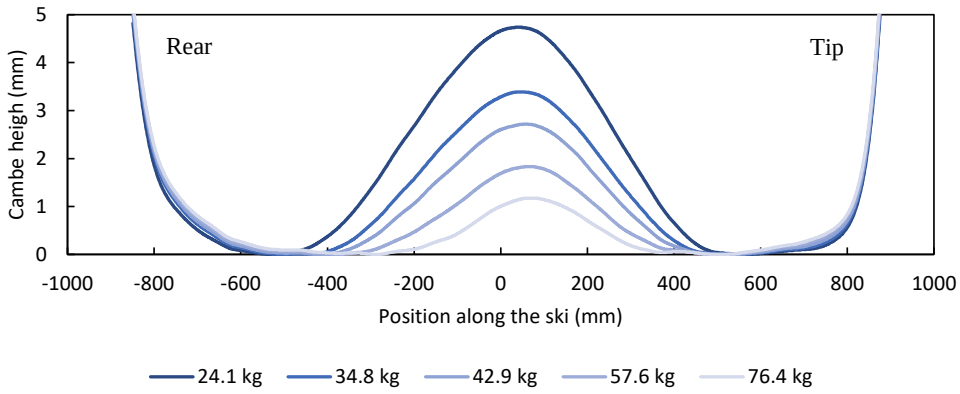


Figure 2.4 Example of camber curves for a Madshus skating ski with normal loading from 24.1 kg to 76.4 kg.

Breitschädel et al. (2010) applied the method mentioned above to investigate the temperature dependence of ski characteristics. They observed an average reduction of 125 mm in the apparent contact length when comparing measurements at 20 °C to -15 °C. Kalliorinne et al. (2022) employed a boundary element method to compute the reaction force along the camber profile, enabling them to determine the distribution of reaction pressures along the ski. Through the manipulation of Young's modulus of the counter surface (snow), they were able to examine the variations in the ski's apparent contact area with changes in snow strength.

Mössner et al. (2023) used a new method to determine ski characteristics when they pressed a ski onto an elastomer pad with hardness resembling that of snow. Figure 2.5 illustrates the camber curve (c+h) as the ski compresses against the elastomer, alongside the penetration depth (-e) and the corresponding reaction pressure (p). This approach was employed to validate a ski-snow contact model, with the pressure distribution being determined from the ski's penetration depth using a hypoplastic force-penetration relationship for the snow. Using this model, they investigated the effect of load and snow hardness on the contact lengths in the front and rear

zone, relative apparent contact area, maximum pressure, and the distance from the load application point to the center of pressure.

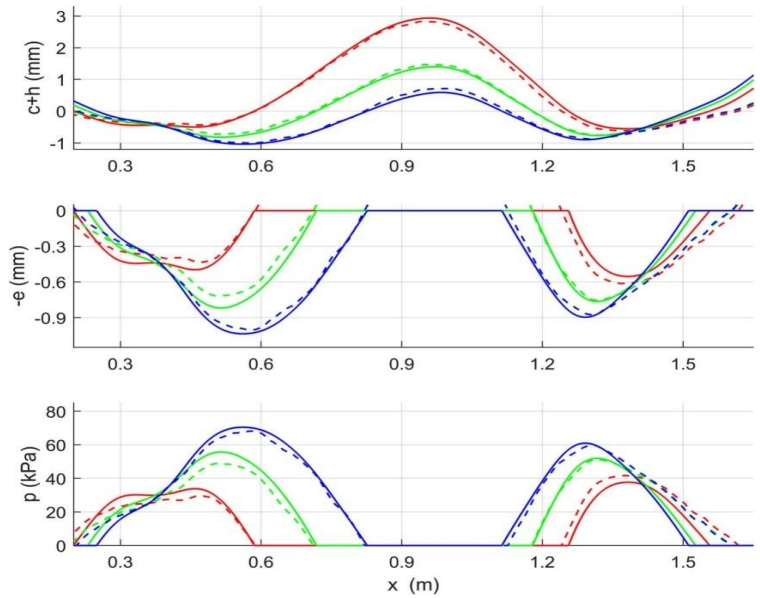


Figure 2.5 Position of the ski base when pressed against the elastomer (c+h), penetration depth into the elastomer (e), and pressure distribution along the ski. The red, green and blue lines represent a load of 290, 490 and 690 N respectively. Dashed lines represent measured data while solid lines represent modeled data (from Mössner et al. (2023)).

Another method used to measure the pressure distribution involves dragging a load cell underneath the ski measuring the reaction force in a single point while it lifts the ski (Bäckström et al., 2009). In another study, a strip of plastic was pulled under a loaded ski while measuring the pulling force. By assuming a constant friction coefficient, they derived the normal force along the ski (Schindelwig et al., 2014). Nilsson et al. (2013) utilized Tekscan$^{TM}$ pressure mats placed between Teflon and rubber sheets to measure pressure on a surface resembling snow. The measurements of the contact zones resulted in relatively long contact lengths of 60 and 80 cm (front/rear) at a normal load of 800 N and a relatively low peak pressure of around 25 kPa.

### 2.3.2 Ski base surface topography

The material of the ski sole is stone-ground to create specific patterns and roughness. This is done by pressing the ski against a rotating stone, which cuts longitudinal grooves along the ski's

sliding direction, as seen in Figure 2.6 . Depending on the snow conditions different roughness is chosen on the skis. Moldestad (1999) divided the arithmetic mean roughness ($R_a$) of skis into four categories: fine ($R_a$ = 1-4 µm), medium ($R_a$ = 4-7 µm), coarse ($R_a$ = 7-10 µm) and very coarse ($R_a$ > 10 µm). Typically, fine structures are used in cold snow or in new snow conditions. This helps to reduce micro-plowing by having shorter and/or rounder peaks, which in turn reduce the plastic deformations or fractures of snow grains (Almqvist et al., 2022; Rohm et al., 2016). Conversely, coarse roughness is preferred in conditions with high liquid water content in the snow. This helps to minimize viscous friction by reducing the contact area with the water film, thus accommodating excess water more effectively (Moldestad, 1999).

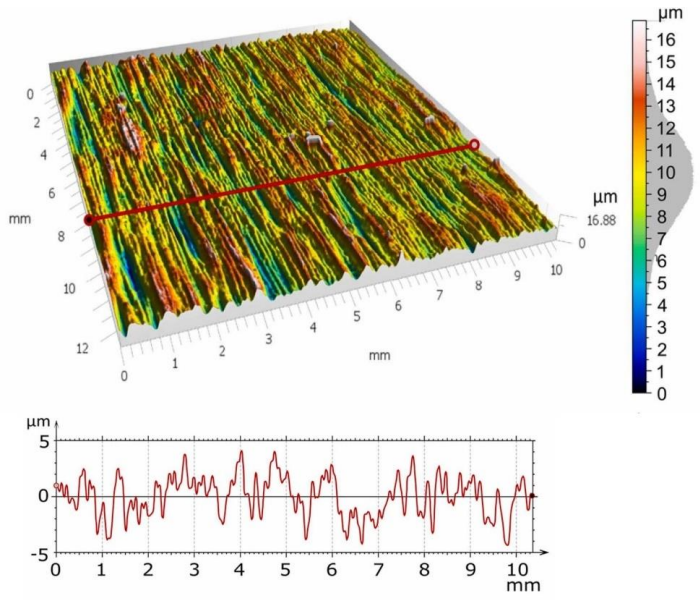


Figure 2.6 Illustration of the ski surface topography, with corresponding height distributions. To enhance visualization, the z-axis is enlarged by 5%. The red line depicts the profile extracted below (Auganæs et al., 2022).

Because the roughness of the ski or slider affects friction, most experimental studies have started reporting the $R_a$ value. Giesbrecht et al. (2010) found an optimum $R_a$ value in the range of 0.5-1 µm when testing different roughness on model skis at a temperature of around -4 °C. However, Rohm et al. (2016) pointed out that the mean roughness of the surface ($S_a$) only gives information about the variation in height, and not about the slope, shape or size of the asperities. They demonstrated that two skis, despite having similar $S_a$ and maximum pit-to-peak height

($S_z$) values, exhibited different friction characteristics due to their distinct bearing ratios. The bearing ratio, which provides information about the size and proportion of valleys and plateaus on a surface, played a crucial role. Specifically, the ski designed with a bearing base structure featured wide plateaus and narrow grooves, while the other ski had the opposite configuration. Under extremely cold conditions (-19 °C) and at low velocities (5 m/s), the ski with the bearing base structure exhibited the lowest coefficient of friction. In contrast, at warmer temperatures (-2.6 °C) and higher velocities (15-20 m/s), the ski with the non-bearing structure displayed the lowest friction on snow.

More recently Kalliorinne et al. (2023a) showed that the texture of the ski base plays a critical role in determining the average real contact pressure, real contact area, and the minimal average interfacial separation (volume of void space) between the ski and snow. The results showed that surfaces with higher $S_{pk}$-values (reduced peak height), which represents the mean height of peaks above the core surface, had less real contact area. This parameter is related to the load-bearing capacity of the surface, and a surface with higher $S_{pk}$ can be seen as a surface with broad grooves and narrow plateaus. The average roughness $S_a$ was correlated to the average interfacial separation which is connected to viscous friction.

### 2.3.3 Wax

One of the reasons for applying wax to the base of skis is to provide a softer "sacrificial" layer that reduces the shear force between base and snow asperities. This layer should ideally be very thin to avoid an increase in the real contact area. The layer should also have a strong bond to the ski sole and be hard to avoid wearing off quickly (Rohm et al., 2017). Among ski waxing professionals there also exists a belief that wax can reduce wear on the ski base structure and fill micro irregularities. Commercial waxes are usually characterized by their hardness and fluorine-based additive content. Fluorine-based waxes have been shown to increase the hydrophobicity with water and are thus believed to reduce the adhesion between the ski and the liquid-like layer (Colbeck, 1997; Rogowski et al., 2007).

Since the wax is softer than ice particles, it wears down as the ski is used. After the waxing and brushing process, a thin wax layer covers the base structure. As the ski is used, the wax on the peaks carrying the majority of the load will wear down first. Gradually, additional wax is removed, as depicted in Figure 2.7. Wax wear is one of the reasons skiers experience an increase in friction throughout a race. Rohm et al. (2017) measured the wax wear with accumulated kilometers of skiing inside a tribometer. They found higher wax wear in the front contact zone

compared to the rear, and higher wear at colder snow temperatures. They also demonstrated that skis treated with fluorinated waxes exhibited a smaller increase in friction compared to skis coated with paraffin wax over accumulated skiing distances. However, Kuzmin (2010) argued that the increase in friction with skiing was due to dirt absorption in the softer wax. He observed larger increases in glide times for the waxed ski after skiing, compared to the unwaxed ski.

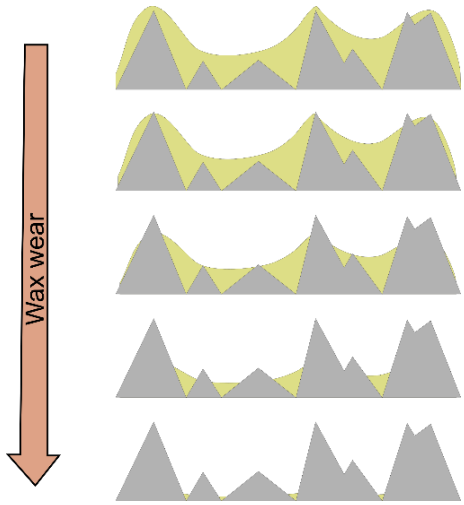


Figure 2.7 Illustration of the ski wax wear process.

## 2.4 Ski-snow friction testing

Today, ski manufacturers primarily rely on full-scale field testing for the evaluation of new skis, products, or preparation techniques. While these tests can provide valuable insights into friction optimization, they are often hindered by fluctuating environmental conditions and variations in the skier's position. Determining the coefficient of friction from field tests also necessitates the separation of air drag and gliding resistance, making it challenging to achieve high-precision friction coefficients from field measurements (Hasler et al., 2016). This has led researchers to develop laboratory set-ups to reduce these variations. In the investigation of ski-snow friction, various test methods have been explored, each yielding different outcomes in the literature. For simplicity, we can categorize these methods into field and laboratory approaches.

### 2.4.1 Field testing

When ski technicians assess skis before a competition, they primarily rely on methods such as parallel tests, timed trials, and subjective assessments based on feel (Breitschädel et al., 2012).

Even though the feeling is an important part of choosing the best skis for an athlete, it is not possible to measure quantitatively and is therefore not given much attention in scientific studies. However, Federolf et al. (2006) found a strong difference in the subjective assessment of ski performance in alpine skiing and highlighted that whether a ski exhibits a good performance depends on the system of the athlete, binding, ski, and snow. In cross-country skiing the feeling is usually evaluated based on a combination of ease of movement (float), stability, and glide[2].

Both glide-out tests and timed tests can be performed individually and give valuable information on the friction performance under the given test conditions. Parallel tests are performed with two athletes gliding side by side to evaluate the relative performance of each ski pair. This is a method suited to rank the different ski pairs on the given snow conditions before a race. However, tests reporting only relative differences like time or distance make it difficult to compare data, since the test slope and snow conditions vary from place to place (Budde & Himes, 2017).

While timed glide tests have been employed to assess friction performance in several studies (Breitschädel et al., 2014; Federolf et al., 2008; Nilsson et al., 2013), they have faced difficulties associated with significant measurement uncertainties. These uncertainties have made it challenging to obtain statistically significant and reliable results when quantifying skiing friction. Breitschädel et al. (2012) utilized inertial measurement unit (IMU) sensors attached to the skis in combination with photocells to calculate the friction coefficient during gliding experiments. Their methodology provided a resolution of $\mu \pm 0.01$. However, they underscored the importance of attaining a higher resolution of $\pm 0.001$ to precisely distinguish between high-performance race skis.

To mitigate uncertainties arising from variations in athlete position and air drag, Budde and Himes (2017) conducted experiments involving a weighted sled equipped with skis traversing a flat test track. In this setup, eight optical sensors spaced 30 cm apart measured the time and position of the sled along the track. Based on the reduction in speed due to friction, the coefficient of friction was calculated. They conducted six runs at different speeds and reported the mean run-to-run variability as a 95% confidence interval (CI) of $\mu \pm 0.00063$ at a speed of 5 km/h. Consequently, they concluded that the measurement uncertainty of the apparatus was lower than the overall ski-snow friction variation.

[2] Personal communication with ski technicians at Madshus AS, a company known for its expertise in cross-country ski manufacturing.

The development of smaller and more accurate differential Global Navigation Satellite Systems has made it possible to equip athletes with a small receiver to track their position. In a study conducted by Wolfsperger et al. (2021), this technology was used to estimate the friction coefficient of skiers and snowboarders sliding down a test section. The estimate of $\mu$ was calculated from the force balance model of the kinetic energy of the skiers. The lowest standard deviations of around $\mu \pm 0.001$-$0.006$ were found for old snow while a standard deviation of $\mu \pm 0.007$-$0.015$ was found for new snow.

In more recent research, Sandberg et al. (2023) used a more advanced sled equipped with an optical correlation sensor recording the velocity at a rate of 500 Hz. To achieve the desired test speeds of up to 21 km/h, a winch was utilized to accelerate the sled. During the subsequent deceleration phase of the sled, the researchers calculated the average coefficient of friction at speeds of 5, 3.89, 2.78, and 1.67 m/s based on a velocity interval of $\Delta v = 1.1$ m/s. The precision of their measurements was quantified as the relative standard deviation (RSD) across 25 runs, which ranged from 0.5% to 2% (equivalent to a standard deviation of $\mu \pm 0.0001$ to 0.0004). Notably, this setup offers the advantage of assessing friction at different speeds within a single run, and it can be easily transported to various testing locations, including both outdoor and indoor snow facilities.

### 2.4.2 Laboratory testing

The main advantage of friction testing in the laboratory is the controlled environment. This controlled setting helps to reduce variations during testing and enhances the reproducibility of snow or ice conditions between different experiments. In laboratory settings, two primary setups are commonly employed. The most common is the “pin on disc”, where a disc of snow or ice is rotated, and a pin with the sample material is pressed on the disc while the friction force is measured (Bowden & Hughes, 1939; Buhl et al., 2001; Bäurle et al., 2006; Takeda et al., 2010). The testing of small slider samples gives the benefit of controlling one variable like load without changing the contact area. As modern skis are essentially two sequential sliders, there is a complex interplay between the partitioning of load, apparent contact area, and friction between the two contact zones. However, the pin-on-disc set-up uses a single slider with a limited sample size, which might not capture the complex friction effects along the full length of a ski (Colbeck, 1992). There are also concerns about temperature and water film development with the repeated contact of the sample with each rotation (Hasler et al., 2016).

Another point is the difference in the scaling of frictional power between full-size skis and scaled-down model sliders. The frictional power generated by the ski, measured in joules per second (W), is calculated as:

$$P_{friction} = \mu v F_N \tag{2.5}$$

Where μ is the coefficient of friction, $v$ is the speed and $F_N$ is the normal load. In practice, experiments with model sliders often aim to replicate the average contact pressure observed on full-size skis and assume that the frictional mechanisms will be identical. However, as shown in Table 2.1, studies involving model sliders have consistently lower frictional power than those observed in linear tribometer tests utilizing full-size skis. This implies that during the slider's pass, less heat is transferred to the snow, potentially resulting in a thinner average lubrication film along the slider. Since the friction coefficient often is linked to the average film thickness, a full-size ski might thus experience some difference in the frictional mechanisms compared to a small-scale slider. Nonetheless, the broad array of parameters employed across studies complicates direct comparisons, underscoring the complexity of accurately scaling frictional behavior from model sliders to full-size skis.

Table 2.1 Overview of the difference in frictional power for experimental set-ups used to measure friction between ski base and snow/ice. The frictional power range is calculated based on speed, normal force, and μ.

| **Study** | **Surface** | **Temp (°C)** | **$F_N$ (N)** | **$A_{app}$ ($cm^2$)** | **Pressure (kPa)** | ***v*** **(m/s)** | **μ range** | **Power (W)** |
|---|---|---|---|---|---|---|---|---|
| **Pin on disc** | | | | | | | | |
| Buhl et al. (2001) | Snow | (-15 to -5) | 5 to 30 | 1 | 50-300 | 5 | 0.03-0.12 | 0.8-18 |
| Bäurle et al. (2006) | Ice | (-20 to +1) | 20-84 | 2 to 10 | 20-420 | 5 | 0.04-0.1 | 4-50 |
| Takeda et al. (2010) | Snow | (-15 to -1) | 280 | 55 | 0.5 | 1 | 0.05-0.1 | 14-28 |
| Lever et al. (2018) | Snow | (-8 to -5) | 30-135 | 380 | 0.8-3.6 | 0.3-1.3 | 0.025-0.05 | 0.2-8.8 |
| **Linear** | | | | | | | | |
| Böttcher et al. (2017) | Ice | (-10 to -2) | 40-80 | 26 | 15-30 | 1 | 0.02-0.05 | 0.8-4 |
| Hasler et al. (2016) | Snow | -5 | 400 | CC ski ≈ 250 | 16 | 2-10 | 0.03-0.06 | 24-240 |
| Lemmettylä et al. (2021) | Snow | (-12 to -1) | 600-1200 | CC ski ≈ 250 | 24-48 | 2-6 | 0.01-0.025 | 24-180 |

The limitations mentioned above led to the development a of linear tribometer capable of testing full-size skis at high speeds (Hasler et al., 2016). The track is placed inside a cold room that is 24 m long. This gives the possibility to reach testing speeds up to 30 m/s. Artificial snow from a snow cannon is produced in a separate room. To test the precision of the system a ski was repeatedly run 50 times in the same track, and the standard deviation to a decreasing linear trend line was used as the precision. The relative standard deviation was found to be speed-dependent and varied from 0.35% to 1.24% for 4 m/s to 10 m/s. The difference in precision by changing to another snow track and/or waxing the ski had a relative standard deviation of 1.7%.

Another full-scale linear tribometer incorporated both static and kinetic friction measurements to simulate the kick-phase in classic skiing (Lemmettylä et al., 2021). Compared to the

tribometer of Hasler et al. (2016) which can utilize five snow tracks, this tribometer can only use one track. This made the precision due to changing track worse since the snow track needed to be prepared for each new test series. Another observation from the study was that the coefficient of friction level was almost the same for temperatures of -1 °C, -6 °C and -12 °C. Due to the low absolute friction level, the repeated measurements showed an increased friction trend in the 50-run series.

Challenges with these tribometers are the high acceleration needed to reach the testing speeds within a short snow track length. This acceleration introduced vibrations to the setup that might influence the friction force signal. A more obvious downside is their size, which results in high construction and operational costs (Lutz et al., 2023). Additionally, these devices predominantly utilize artificially produced snow from snow guns, which differs in structure from natural dendritic snow.

### 2.4.3 Comparison of skis on a constantly changing surface

As mentioned earlier, the snow surface changes with each pass of a ski. This phenomenon has been documented in several studies (Hasler et al., 2016; Lemmettylä et al., 2021; Sandberg et al., 2023), which have all observed an increasing or decreasing coefficient of friction correlating with the number of ski passes. Such a change in friction is a crucial factor that must be considered when planning the testing sequence for comparing different skis or ski-related products. However, the influence of the testing sequence has received relatively little attention in the literature.

A technical note by the wax manufacturer Swix$^{TM}$ suggests that testing different products should be conducted in consecutive order, for example, 1-5, and this process should be repeated six times (Karlöf et al., 2007). This approach ensures that the effect of polishing is evenly distributed across the samples. To determine any significant difference between the averages they used the standard error. However, since the coefficient of friction has a changing trend, the standard errors will be influenced.

Breitschädel et al. (2012) used three different ski pairs and tested them sequentially 1, 2, 3 and this sequence was repeated five times. The results showed increasing glide times through the series. They reported an average glide time for each ski pair with associated standard deviation, which was large and overlapping due to the increasing trend.

Budde and Himes (2017) implemented a different approach by testing one ski six times at varying velocities in the order of medium, low, high, medium, low, and high. Subsequently, a control ski was tested in the same sequence, followed by a comparison ski with a different wax or grind. The control ski was always tested second, while the order of the two test skis with varying waxes alternated between sessions. They normalized the data to obtain an average at a common velocity of 5 km/h using a linear regression fit.

In a study by Federolf et al. (2008), the impact of leaning forward and backward on alpine skis was examined. The testing sequence involved forward, neutral, and backward positions, repeated three times. A reference skier with the same position was used between each sequence. The reference skier demonstrated a standard deviation of 0.023 s or 0.11% of the glide times, indicating minimal fluctuations in external conditions and suggesting that differences in glide times could be attributed to the varied positions.

# 3 Research design

This thesis is primarily based on experimental work. The following chapter describes the process of developing an experimental setup to study the friction between snow and cross-country skis. It also covers the development of a rig for contact zone measurements and a tunable test ski for isolating different macroscopic ski parameters. The detailed specification and use are described in the papers and are therefore not repeated in detail here.

## 3.1 Design of a ski-snow tribometer

To study the process of ski-snow friction it is valuable to be able to perform experiments under controlled conditions. Laboratory experiments allow for the control of important parameters such as air and snow temperature, and relative humidity during testing. Another crucial aspect is having control over the snow production and preparation of the snow track.

As described in chapter 2.4.2 there have been some limitations to the tribometers developed for studying friction between ski and snow in the past. This led to the identification of the following requirements for the tribometer:

- Conduct measurements under conditions relevant for cross-country skiing in terms of normal loads, speed, full-size skis, and snow surfaces.
- Achieve a measurement precision of the coefficient of friction better than ± 0.001.
- Develop a method for preparing realistic snow test beds and quantify their main properties, such as density, surface topography, and liquid water content.

### 3.1.1 Experimental setup

When developing a method for measuring friction, there are many decisions involved in designing the setup. A cooling chamber containing the 8.8 m long track with linear motor drive was already developed (Giudici et al., 2017). As a result, it was more sensible to adapt this existing setup rather than beginning from scratch. The initial step involved establishing a connection between the ski and the fork while simultaneously measuring the horizontal and vertical forces, as depicted in Figure 3.1. This could have been accomplished using a triaxial load cell. However, a known issue with these load cells is the occurrence of cross-talk between

the various measurement axes. When dealing with a significantly higher vertical force in comparison to the horizontal force, this cross-talk could potentially introduce significant errors in the horizontal force signal.

To address this concern, we decided to incorporate a linear bearing that effectively decouples the force measurements in the horizontal and vertical directions. Ideally, this bearing should have a very low friction to not "interfere" with the force measurements. This means that if the linear bearing has a sliding friction higher than the ski all the force will be carried by the bearing and not measured with the load cell. According to existing literature, ski-snow friction can be as low as 0.015 (Budde & Himes, 2017). Consequently, the linear bearing should have a friction coefficient lower than this value. Rolling linear guides typically have a coefficient of friction ranging from 0.005 to 0.01, making them suitable for this use case. However, the resistance in the bearing must be considered when determining the coefficient of friction from the force signal. For instance, if the resistance in the bearing was $\mu = 0.005$ and the vertical force applied was 800 N, this would lead to a friction force of 4 N. Now, if we consider that the friction coefficient of the ski was 0.025 under the same applied downforce, the resulting friction force would be 24 N. However, the load cell would then only measure 20 N because 4 N is emitted in the bearing. This was the main reason why we decided to use a linear air bearing with a friction coefficient of approximately 0.001.

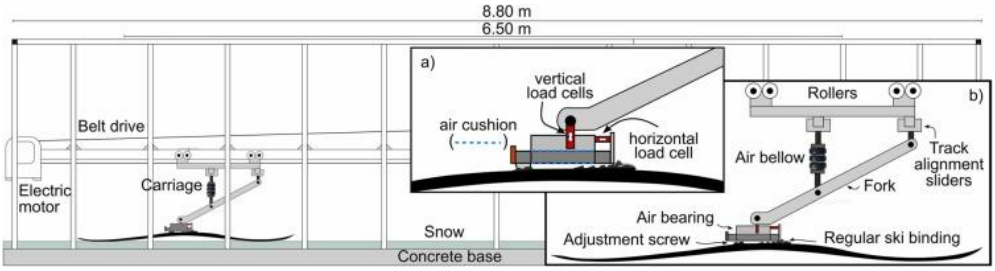


Figure 3.1 Illustration of the friction track featuring the carriage specially designed for cross-country skis. Insert (a) illustrates the linear air bearing and the placement of the load cells, whereas insert (b) provides a close-up view of the carriage (Auganæs et al., 2022).

A run in the tribometer consists of an acceleration phase, a constant speed phase, and a deceleration phase, as depicted in Figure 3.2a. The coefficient of friction is calculated from the average horizontal and vertical force during the constant speed phase highlighted in green. This corresponds to the position from 1.5 m to 5 m in the track. To be able to measure friction

coefficients up to 0.1 with a vertical load up to 1000 N, the horizontal load cell needed to be rated for 100 N. Additionally, the required precision was at least μ ± 0.001. When this is translated into the force resolution for the load cell at the lowest applied downforce of 200 N, we get a minimum resolution of the friction force to be ± 0.2 N.

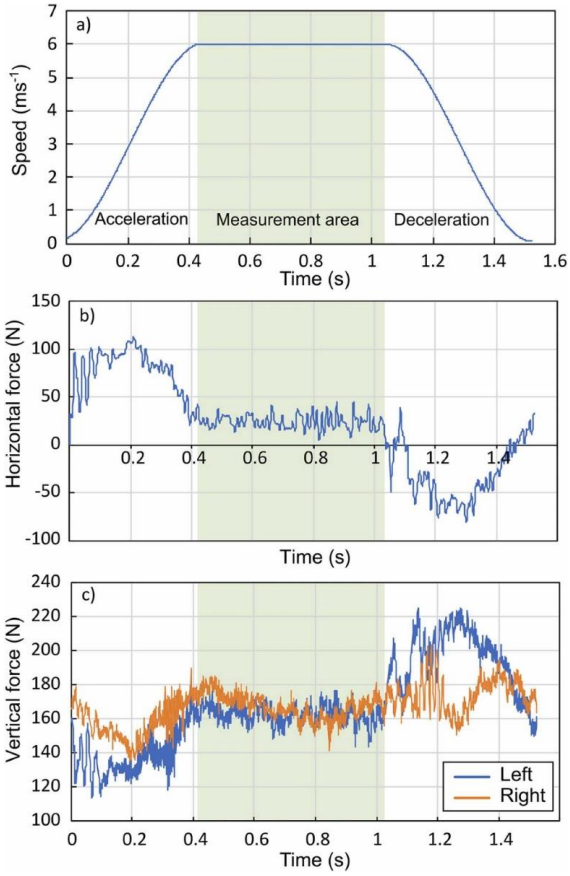


Figure 3.2 Illustration of the collected speed and force signal data a) Carriage speed, b) horizontal force, c) vertical force. The highlighted area is the measurement area (Auganæs et al., 2022).

Another critical aspect of the air bearing and load cell configuration was aligning the bearing horizontally on the ski. If any angle existed between the ski and the bearing, it would cause the vertical load to be decomposed into a horizontal force. For instance, a misalignment of 0.1 degrees could lead to a horizontal force of 0.7 N when decomposing a downforce of 400 N. The significance of alignment became even more apparent in Paper II when we began altering the load or the binding position of the cross-country ski. This was because the angle changed due

to the ski's compression. As explained in the paper, the angle had to be adjusted every time we made changes to the load.

Throughout the PhD project, there have been made several upgrades to the tribometer. Figure 3.3 provides an overview of the most significant upgrades and the data collection periods for the different papers. Initially, there were challenges with a low sampling rate (100 Hz), which made it difficult to capture signal peaks at speeds exceeding 4 m/s. Measurements of forces in dynamic systems always include vibrations, and due to the ski's spring-like behavior, transitioning from acceleration to a constant speed induced vibrations in the force signal.

To resolve this, we first tried to enhance the existing system by implementing data transfer through an Ethernet cable, allowing for a sampling rate of 1000 Hz. This was effective in capturing all peaks in the force signal up to a speed of 10 m/s. However, running an Ethernet cable at cold temperatures along the track proved to be unreliable. The cable was repeatedly stretched and bent, ultimately leading to failure after a limited time. As a result, we undertook a comprehensive upgrade of the data acquisition system in the fall of 2021. Additionally, we improved the tribometer by incorporating a high-precision magnetic ruler for accurately determining the position of the ski. The new wireless system had a sampling rate of 10,000 Hz, and additional details can be found in the article of Buene et al. (2022).

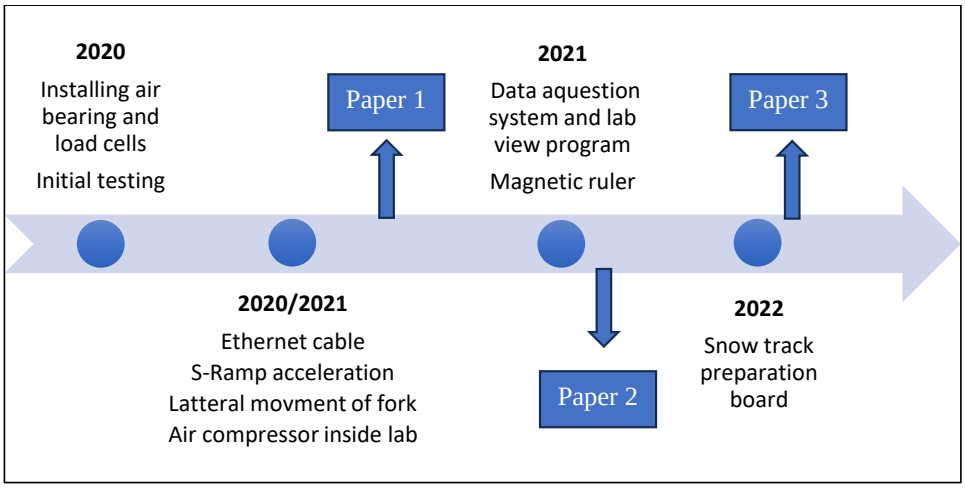


Figure 3.3 Timeline of upgrades to the tribometer, and when the data collection to each paper was performed.

### 3.1.2 Snow preparation

The snow used in the experiments was produced by a machine designed to replicate the growth process of natural snow. The snow machine produces water vapor from a heated bath, that is blown into a cold chamber of -20 °C, causing the supersaturated air to deposit on the strings, as illustrated in Figure 3.4. The size of the snow crystals can to a certain degree be altered by the interval time of the vibration motor (longer time between vibrations equals larger grains). The density of the produced snow is in the range of 50-80 kg/m$^3$, and the production capacity of the machine is around 0.1 m$^3$/day (Giudici et al., 2017).

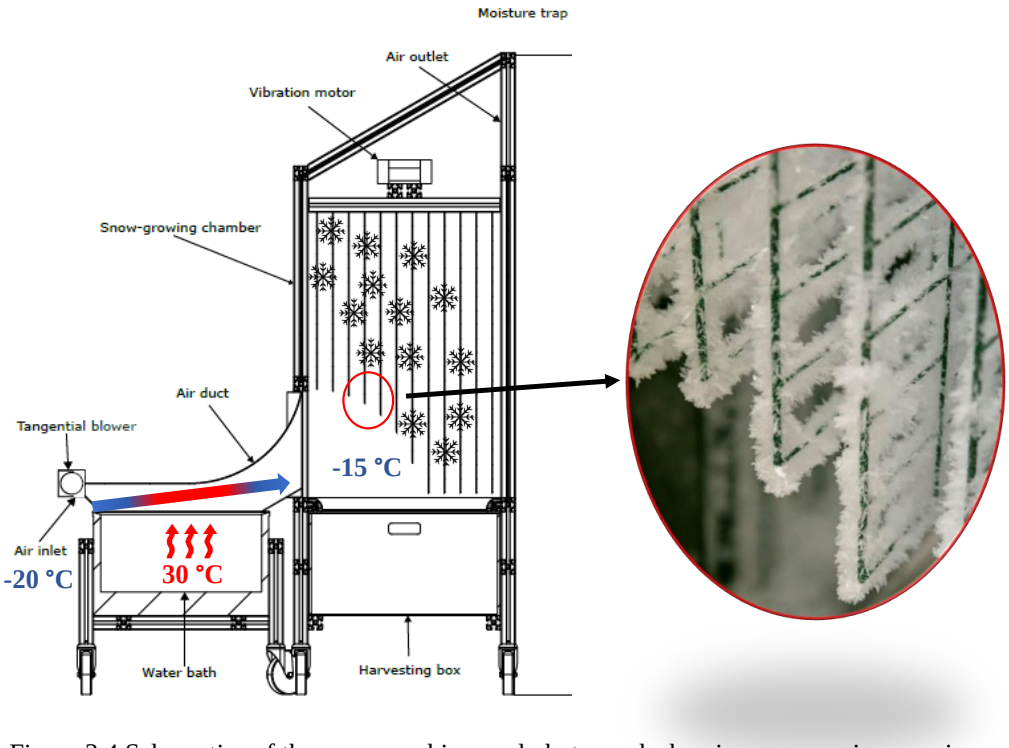


Figure 3.4 Schematics of the snow machine, and photograph showing snow grains growing on the strings.

The process of transforming dendritic snow into a compact and smooth track for our experiments presented several challenges. Our initial strategy involved filling the track, which measured 8.80 meters in length, 40 cm in width, and 5 cm in height, entirely with snow. However, this approach presented two problems. Firstly, it required a substantial amount of snow to fill the testbed. Secondly, the snow base tended to shift or slide along the supporting

wooden plates while we attempted to compact it evenly. This shift made achieving even compaction more difficult and time-consuming, which affected the reproducibility between preparations.

This not only made the process more labor-intensive but also less reproducible.

In response to these challenges, we devised a solution involving the creation of a solid snow or ice base, over which only a thin layer of snow needed to be prepared each time, as seen in Figure 3.5. This method significantly streamlined the process, as it allowed us to easily remove just the top layer of used snow after each testing session. To assist in this removal, we designed a custom adjustable steel blade. This blade could be smoothly dragged along the track, efficiently scraping off the top layer of snow and preparing the track for subsequent preparation.

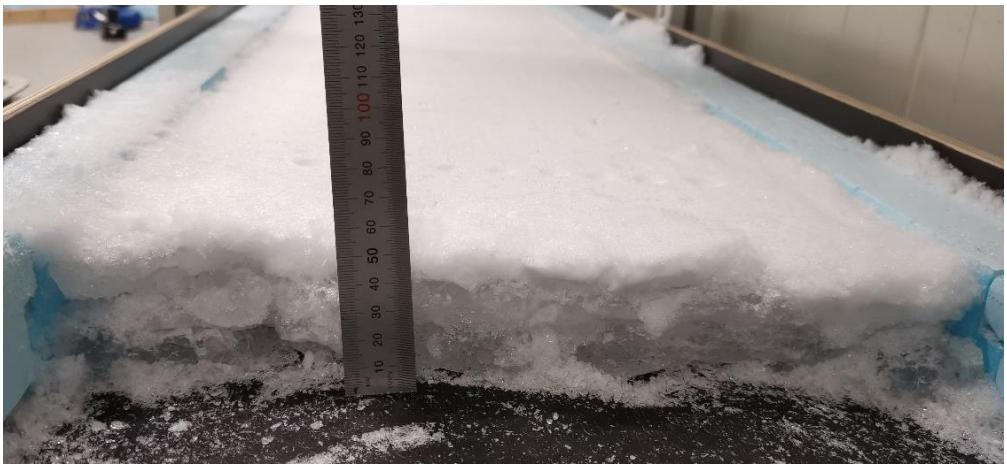


Figure 3.5 Cross-section view of the snow track. The bottom 4 cm shows an ice base that has built up over time. The top 1 cm shows a fresh compacted snow layer.

The different steps in the snow track preparation process are outlined in Table 3.1. The initial stage involved using a steel shovel to work the snow in the harvesting box, breaking up aggregated snow particles, and large snow crystals into smaller particles. To a certain extent, this process resembles what snow groomers do with the tiller. The subsequent step was to distribute the snow evenly inside a frame (dimensions 30 × 30 × 2 cm) which was moved along the track until a 2 cm layer of fluffy new snow covered the hard snow base. Following this, the snow layer was compacted by running a compaction board at a low speed of 0.5 m/s along the track. The dimensions of the compaction board were 30 cm wide and 60 cm long, with the base

plate covered with UHMWPE sole material. The applied normal load on the compaction board was ramped in steps from 100 N to 800 N. Subsequently, the track was left to sinter for 16 hours at the desired testing temperature the next day.

Table 3.1 Outlines the different steps in the snow preparation process and the tools used.

| Preparation process | Tools | Time use (h) |
|---|---|---|
| 1. Break large grains, by working the snow with a steel shovel | Shovel and box with snow | 0.1 |
| 2. Distribute the snow evenly inside a frame that is moved along the track (2.*) Sifted old snow is spread evenly on the track and leveled to the height of the Styrofoam plates | Frame, bucket, leveling tool Leveling tool | 1 |
| 3. Drive compaction board at 0.5 m/s with increasing normal load | Compaction board | 0.5 |
| 4. Sintering time | Cover lids | 16 |
| 5. Run-in protocol | Reference ski | 0.5 |
| 6. Measure snow parameters | Doser, thermometer, SLF density, Gel-sight | 0.1 |
| 7. Perform friction measurements | | 1-6 |
| 8. Scrape of used top layer | Adjustable steel blade | 0.5 |
| 9. Sieve used snow into a new box | Metal sieve 5 mm | 0.5 |

*When preparing old snow the distribution step varies slightly, or else the following steps are identical

A run-in protocol was performed before the testing series could start. This protocol involved gradually increasing the speed and normal force to match the levels used in the subsequent test series. First, the normal force was ramped in steps of 100 N before the speed was ramped in steps of 1 m/s. This initial phase used a reference ski, and its primary purpose was to stabilize the snow surface and minimize the degree of track compaction in the subsequent tests.

After running experiments in the four tracks the top snow layer was scraped off using an adjustable steel blade. This blade was affixed to a Rexroth profile, which rested on the

Styrofoam plates positioned on each side of the snow track. This setup allowed for precise control over the depth of the blade, ensuring effective and uniform removal of the snow layer.

The snow that was scraped off was then collected and sieved into a new box. For this process, a metal sieve with 7 mm holes was used. The initial step in the preparation of transformed snow involved evenly spreading the sifted, used snow over the hard base of the track. To achieve a uniform distribution along the track, a leveling tool was utilized. After this initial distribution, the subsequent steps in preparing the track mirrored those used in setting up a track with new dendritic snow. This process ensured the consistent quality and condition of the snow for each test, maintaining the reliability and accuracy of the experimental results.

### 3.1.3 Snow conditions for Study II and III

The snow conditions selected for the second and third study were chosen to represent various temperatures encountered during cross-country skiing competitions, where the air temperatures can span from -20 °C to as high as 10 °C (Sandbakk et al., 2021; Wagner & Horel, 2011). In this range, different friction regimes will be present, resulting in varying friction dependencies on ski parameters like load or apparent contact area. To obtain a more comprehensive picture of the dependence of snow friction on ski parameters, it is necessary to perform experiments at different temperatures (Buhl et al., 2001; Bäurle, 2006).

The selection of the coldest temperature, -10 °C, was chosen as it falls within the temperature range where load dependence on the coefficient of friction can be expected (Buhl et al., 2001). Moreover, it reflects a condition that is not so uncommon in ski racing. While it's feasible to go even colder in a laboratory setting, lower temperatures become less relevant for real-world skiing.

The selection of the intermediate temperature at -2 °C was made deliberately because this falls within the temperature range where the lowest friction between skis and snow typically occurs (Buhl et al., 2001; Bäurle, 2006). At this temperature, friction dependencies on ski parameters are usually not as clear because of the minimum point in the friction curve, as illustrated in Figure 3.6. At this point the liquid-like layer is believed to be around an optimum, balancing between the reduction in adhesion and the increase in hydrodynamic drag.

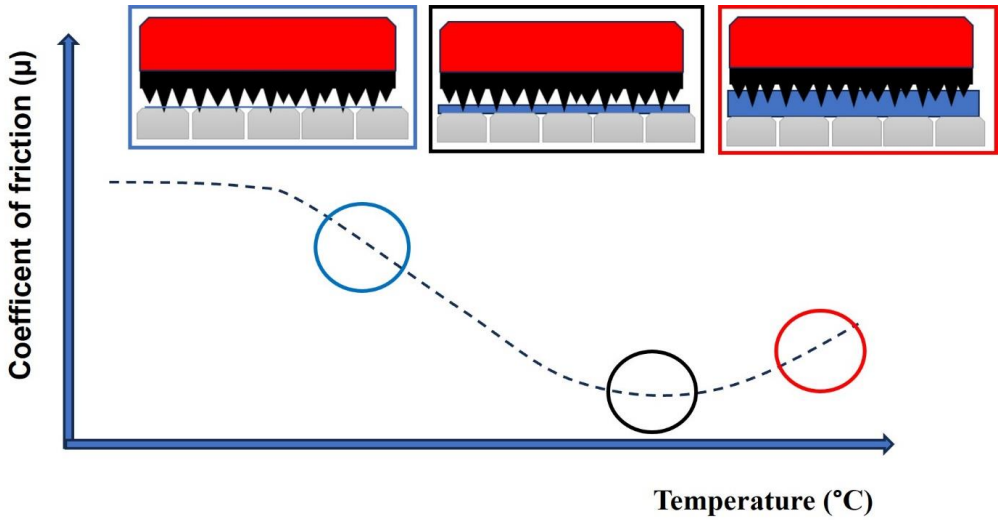


Figure 3.6 Generalized curve of the coefficient of friction vs snow temperature. The curve illustrates the changing trends in friction, which are largely dependent on the availability of a liquid-like layer present for lubrication. The graph features three distinct circles, each representing the temperature chosen for Paper II and III.

Under warm conditions, the air temperature was set to +5 °C to be able to induce melting and high moisture content on the surface. As described in Paper II the temperature was raised from -2 °C to +5 °C on the morning of the test day. This led to an increase in the water content in the top layer as the snow started to melt, as seen in Figure 3.7. Initially, we attempted to elevate the air temperature to +2 °C within the laboratory environment. However, it became apparent that this temperature gradient was insufficient to initiate surface melting within a few hours, as the snow received cooling from its base. It's worth noting that conditions characterized by temperature gradients spanning from sub-zero to several degrees above zero may not be the most representative of typical ski racing conditions. Still, such scenarios can occur when there are significant temperature fluctuations from nighttime to daytime, making them relevant for study and analysis.

Figure 3.7 Comparison of snow surface conditions at -2 °C (left) and +5 °C (right)

The snow surface characteristics were evaluated by measuring air and snow temperature, density, humidity and hardness before starting the tests. The characteristic values shown in Table 3.2 are taken from the Paper III. Snow temperature was recorded at the track's midpoint, alongside snow density and moisture at six locations spaced 0.5 meters apart, employing an SLF snow sensor (FPGA company GmbH, Switzerland) and a Doser snow moisture meter 011 (Doser Messtechnik GmbH & Co. KG, Germany). For assessing snow surface hardness, we utilized a 20 mm diameter 3D-printed hemisphere, dropped from a 48 mm height with a 76-gram weight. The penetration depth into the snow ($S_{dyn}$) was read from a pipe connected to the hemisphere, with markings for each millimeter. Based on these measurements, we calculated the penetration resistance (PR) using the following formula (Wolfsperger et al., 2021):

$$PR = \frac{m \times g \times h}{S_{dyn}} + m \times g \tag{3.1}$$

Where $m$ is the mass, $g$ is the acceleration due to gravity, $h$ is the height, and $S_{dyn}$ is the penetration depth. The hardness of a material can be defined as the reaction force per penetration depth, per contact area or volume displaced (Mössner et al., 2013). The hardness ($H$) was then calculated as:

$$H = \frac{PR}{A} \tag{3.2}$$

Where $A$ is the surface area of the 3D-printed hemisphere in contact with the snow.

Table 3.2 Measured snow parameters at the different temperatures. For each temperature, the average value is calculated from measurements in three separate tracks (tracks 1-3).

| | Cold | Intermediate | Warm |
|---|---|---|---|
| **Snow temperature (°C)** | -10.4 ± 0.2 | -2.5 ± 0.2 | 0 |
| **Air temperature (°C)** | -9.9 ± 0.3 | -2.1 ± 0.3 | 5.2 ± 0.4 |
| **Density (kg/m$^3$)** | 405 ± 43 | 438 ± 65 | 692 ± 80 |
| **Doser snow humidity (%)** | 18 ± 2 | 20 ± 2 | 67 ± 12 |
| **Snow hardness (N/mm$^2$)** | 0.464 ± 0.13 | 0.153 ± 0.027 | 0.085 ± 0.015 |

### 3.1.4 Method for comparing skis on a changing snow surface

When developing a test method for comparing different samples (skis, waxes or configurations), it is important to address the continuously changing snow surface as the number of runs increases. A key challenge in this context is structuring the test sequence for various samples in a way that guarantees equal comparisons. Following the first paper and some additional testing, a set of requirements was formulated for the development of a test method, as outlined in Table 3.3.

To ensure that each sample runs on a relatively equal snow surface, the degree of polishing should be evenly distributed across all the samples. This can be achieved through sequential testing, for example, considering a test with three samples as follows. By testing samples 1, 2, and 3 one time each, and then repeating this sequence five times, instead of testing sample 1 successively five times and then sample 2 five times and so on. However, this introduces some practical challenges by manually switching between the samples 15 times instead of three times. Changing skis, normal loads, or load application points (LAPs) multiple times, rather than running them continuously, introduces a new potential source of error. This error can result from a shift in ski alignment, a difference in applied normal load, or from the adjustment of the bearing angle for the load and LAP tests. Moreover, switching samples consumes additional time.

The testing sequence should also facilitate tracking the degree of polishing on the data. The potential to correct the data based on the polishing trend can help reduce both the differences due to polishing and the standard deviation among each sample. For instance, a common

approach to ski testing is to conduct tests in the sequence 1, 2, 3, 3, 2, 1 to ensure uniform polishing among the samples when comparing the average. While this approach integrates polishing into the test sequence, it can result in a significantly larger standard deviation for sample 1 compared to sample 3.

The number of runs needed to acquire statistically significant data depends on the magnitude of the differences between the samples. However, by utilizing the difference of $\Delta\mu \approx 0.001$ between race-prepared skis, as presented in Breitschädel et al. (2012), we can calculate the number of runs needed to achieve a margin of error for a 95% confidence interval that is lower than this value. As detailed in Paper I, it was determined that more than five runs were needed on dendritic snow, and more than two runs were needed on transformed snow to meet this criterion.

The number of runs in a cycle must be considered because it affects the degree of polishing between the first and last samples. This can to a certain degree be fixed by correcting for the polishing, but that requires linearity in the data. Furthermore, it's important to carefully consider the total number of runs in a track. As the number of runs increase the tracks gets more polished, and may not accurately represent the conditions that skis encounter in real-world scenarios anymore. To maintain the relevance and accuracy of our tests, we genrally limit the total number of runs to less than 100. Moreover, exceeding 100 runs could influence the impact of non-linearity on the polishing curve.

In an initial test, it was observed that the time between runs had a minor impact on the coefficient of friction. To be more specific, friction increased when transitioning from a 0-second wait time to a 10-second wait time between runs. However, no significant difference in friction was noted when the wait time was increased from 10 seconds to 60 seconds.

Table 3.3 Key considerations and mitigating actions for developing a test method to compare the coefficient of friction of skis sliding on snow.

| Considerations | Mitigating actions |
|---|---|
| Spread the degree of polishing among samples | Sequential testing |
| Number of switches between samples | To a minimum, but enough to capture a linear trend |
| Assess and correct data for polishing | At least three points to asses the linearity |
| Number of runs for significant results | Conduct more than five runs per sample |
| Total number of runs in a snow track | Limit to less than 100 to maintain snow track validity |
| Number of samples in a test | Must be determined from the total of 100 runs divided by the required runs per sample |
| Wait time between runs | Ensure a wait time of more than 10 seconds between runs |

### 3.1.5 Use of reference ski to correct for differences between tracks

In Paper III, one of the objectives was to assess the impact of apparent contact area and normal load on friction. Since this involved three different areas and six different normal loads, testing both in the same track presented the challenge of dealing with a substantial testing matrix, with the number of runs exceeding 150. An alternative approach was to run the experiments in three different snow tracks and compare data between the tracks. However, this method introduced potential inaccuracies in the friction levels between the tracks.

As outlined in Paper I, the uncertainty from changing between dendritic snow tracks was 2.48%, which might surpass the differences between individual samples. To correct for this variation, we applied a method to quantify the difference between tracks and subsequently adjusted the data accordingly. The solution was to use a reference ski before the series to measure the initial level of coefficient of friction. The relative differences between the three tracks are reported as the average coefficient of friction of three runs, as outlined in Table 3.4. This relative difference was then applied to adjust the friction coefficients for the subsequent measurements in the other tracks.

Table 3.4 The difference in initial μ between the tracks measured with a reference ski. The middle track was used as a zero value. A positive number denotes that the track was "slower", and the subsequent measurement series was lowered the same amount. A negative number indicates a "faster" track, and the subsequent measurement series is raised the same amount.

| **Snow track** | **1** | **2** | **3** |
|---|---|---|---|
| μ at -10 °C | 0.0567 | 0.0538 | 0.0482 |
| Difference (%) | +5.1 | - | -11.6 |
| μ at -2 °C | 0.0439 | 0.0431 | 0.0423 |
| Difference (%) | +1.8 | - | -1.9 |
| μ at +5 °C | 0.0463 | 0.0617 | 0.0636 |
| Difference (%) | -33.4 | - | +2.9 |

We encountered a particular challenge with this approach at melting temperatures, where the track underwent significant changes over 2 hours of testing, resulting in a 33% difference for one of the tracks, as noted in Table 3.4. This substantial difference raised concerns about relying solely on a reference ski under such conditions. Consequently, we decided to conduct a new set of tests that involved altering both the normal load and contact area within the same snow track. To limit the size of the testing matrix only three normal loads were used for each of the three contact areas.

## 3.2 Development of a rig for measuring contact pressure profiles on skis

The measurement rig was developed to address research objective 2, which was to examine how macroscopic contact parameters change with different loading conditions on a modern ski. When we began investigating the impact of binding movement on cross-country skis, it became evident that quantifying changes in the contact zones was crucial. Initially, we followed the traditional approach of measuring the distance between the ski sole and a rigid surface to determine the camber curve. By using the threshold value of 0.1 mm as the contact criterion, from Breitschädel (2012), the length of the front and rear contact zones was calculated, and the distance between them. However, this method did not provide any information about the pressure distribution within the contact zones. By designing and constructing the rig in-house, we ensured immediate and convenient access for conducting measurements. For comprehensive

details on the construction and application of the rig, please refer to Paper II. Additionally, the wiring configuration and the code for the load cells connected to the Arduino are outlined in Appendix A.

The use of this setup comes with a particular limitation related to the manual operation required for applying the load and adjusting the sliding plate containing the load cells, as depicted in Figure 3.8. To get a force measurement reading every 1 cm, the procedure involves applying the load five times and moving the sliding plate one centimeter four times. These manual operations have the potential to introduce some level of inaccuracy into the measurements.

To investigate the extent of this potential inaccuracy, we conducted three separate measurements on the same ski. Through this testing, we observed that the integrated pressure curve (sum of the loads along the ski) within the contact zones exhibited variations of less than 1%. In other words, the overall pressure measurements were consistent and showed minimal differences between measurements, indicating a reasonable level of precision.

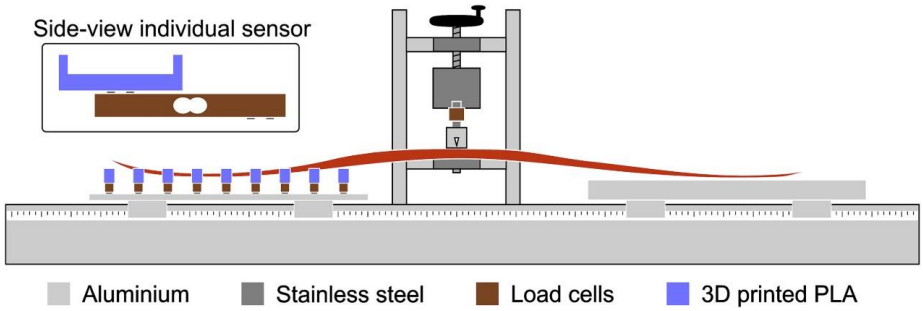


Figure 3.8 Illustration of the developed rig for measuring contact pressure profiles on cross-country skis (Auganæs et al., 2023).

## 3.3 Design of an adjustable test ski

The design of cross-country skis features an arched shape, which results in multiple parameters changing simultaneously when adjusting either the normal load or the point of load application (Kalliorinne et al., 2023b; Mössner et al., 2023). To understand and explain the variations in friction observed on the cross-country ski in Paper II, it became imperative to isolate and precisely control one individual variable at a time. To address this challenge, we developed an adjustable test ski by employing a 1.6-meter-long Rexroth aluminum profile. This ski

framework allowed us to affix 3D-printed sliders of various lengths (20 cm, 30 cm, or 40 cm) and a width of 4.5 cm beneath it, as depicted in Figure 3.9.

Beneath each slider, a 2 mm thick metal sheet was attached, extending 5 cm beyond the front and rear of the sliders. This modification facilitated a smoother and more gradual distribution of pressure, resulting in less plowing and unevenness of the snow track. Additionally, we applied a UHMWPE ski sole material beneath the metal sheets, securing it with double-sided tape. The average surface roughness of the sole material was assessed using a non-destructive elastomeric 3D imaging system (GelSight mobile, GelSight, USA), revealing a $S_a$ value of 1.10 µm.

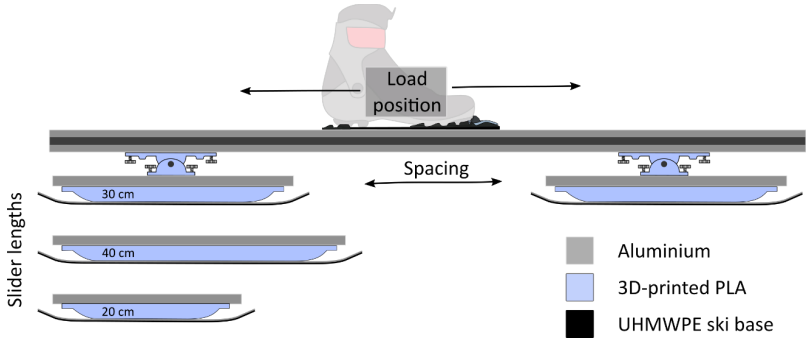


Figure 3.9 Schematic of the adjustable test ski, allowing customized contact zone length, spacing, load, and load application point (Auganæs et al., 2024).

This design enabled us to investigate the effect of load without changes in the apparent contact area. Additionally, we could explore the influence of apparent contact area by varying the areas of the three different sliders while maintaining a constant load. The binding could be moved along the entire length of the ski, allowing us to investigate the load split between the front and rear slider of the ski. Furthermore, we had the flexibility to adjust the spacing between the sliders by moving them along the aluminum profile.

The details of the specific test sequence for each parameter can be found in Paper III. A summary of the test parameters and their corresponding values can be found in Table 3.5. This setup assisted us in addressing research objective 3, which focused on understanding the effect of isolated macroscopic contact parameters on the coefficient of friction.

Table 3.5 Overview of experimental test variables and their selected values. The tested range for each variable is highlighted, while the other variables were kept constant.

| **Test variable** | **Normal force (N)** | **Area ($m^2$)** | **Load split (%)** | **Spacing (cm)** |
|---|---|---|---|---|
| Normal force | **300-800** | 0.018-0.036 | 50 | 60 |
| Contact area | 300-800 | **0.018-0.036** | 50 | 60 |
| Load split | 400 | 0.027 | **5-95** | 60 |
| Spacing | 400 | 0.027 | 50 | **20-100** |

# 4 Results

This chapter presents the main results of the thesis. The results are divided based on the three papers. An additional section details the results of a novel test method for comparing skis. While this chapter highlights the main results, readers are encouraged to refer to the individual papers for a more comprehensive understanding of the results.

## 4.1 Paper I –Precision of the ski-snow tribometer

In this study, the development of the ski-snow tribometer was explained and validated by measuring the friction coefficient of repeated ski runs on laboratory-grown dendritic snow. Tribometer precision contributions from the measurement unit, track position, and snow testbed preparation were determined. The measurement precision was sufficient to distinguish skis with $\Delta\mu \leq 0.001$. The system's accuracy was also tested with a roller ski, and the absolute friction level of the roller ski was comparable to other studies. The change of the snow surface with multiple runs over it was also investigated through the measured coefficient of friction and by 3D surface imaging.

### 4.1.1 Accuracy verification of the measurement system

As the absolute accuracy of the coefficient of friction between skis and snow depends on numerous variables, there is no definitive "gold standard" or reference for calibrating the tribometer. As outlined in Paper I, the friction level of the flat ground ski without wax was almost doubled compared to the waxed race ground ski at a speed of 6 m/s. To mitigate uncertainty arising from the unstable snow surface and different ski preparations, we opted to compare the friction levels by using a roller ski on plywood sheets.

The measured average coefficient of rolling resistance was comparable to two other studies, as illustrated in Figure 4.1 (Ainegren et al., 2008; Schindelwig et al., 2017). This suggests that the measured forces on the tribometer fall within an expected range. The precision of the measurement unit (load cells, data acquisition, and air bearing) was assessed through a 50-run series using a roller ski, as shown in Figure 4.1. The precision of the system was determined by calculating the relative standard deviation in relation to the decreasing linear trendline over a series of 50 runs. This approach involved measuring the standard deviation of the data points

around their respective linear downward trends and expressing this variation as a percentage of the average friction coefficient value. The RSD of the system was found to be 0.73% by using the roller ski.

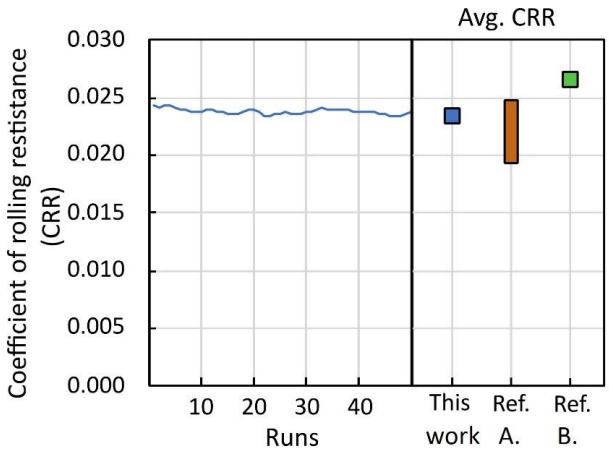


Figure 4.1 Coefficient of rolling resistance for a classic roller ski trough a 50 runs series measured at 6 m/s in the tribometer. The average values are presented alongside those reported by ref A. Schindelwig et al. (2017) and ref B. Ainegren et al. (2008).

### 4.1.2 Precision assessment of the ski-snow tribometer

The measurement precision of the tribometer was categorized into three different levels to distinguish the contribution of variation originating from the snow surface instability (level 1), lateral snow track variations (level 2), and snow testbed preparation (level 3). As shown in Figure 4.2, precision can be considered either as an absolute model or an additive model. In the additive model, precision from each level can be found as the added precision at each level. For new snow, the precision within a track was 1.45%, while the additional precision due to changing between tracks was 1.03%, and the additional precision resulting from testbed preparation was 2.39%. For aged snow, the precision was even lower, with 0.89% at level 1 and 0.28% at level 2.

Comparing the precision of the ski-snow system to the roller ski system, we can note that the precision with the roller ski was 0.72% better than on new snow and 0.16% better than on aged snow. This suggests that the larger fluctuations observed in ski-snow friction measurements primarily stem from the snow surface's instability rather than originating from the measurement

unit of the tribometer. It also demonstrates the tribometer's capability to measure low coefficients of friction with high precision.

The absolute model can be used to assess the total precision on each level. The precision on each level is then the cumulated precision of the tribometer at that level. This can for example be used to determine the number of runs needed to get significant results on each level, or if skis could be compared between tracks or between testbed preparations. For new snow, the precision was 1.45% within one track, 2.48% between four tracks, and 4.87% between testbeds. The uncertainty from changing between tracks or testbeds is thus larger than expected individual differences between similar skis. This implies that a calibration method is needed to be able to compare skis between tracks or testbeds.

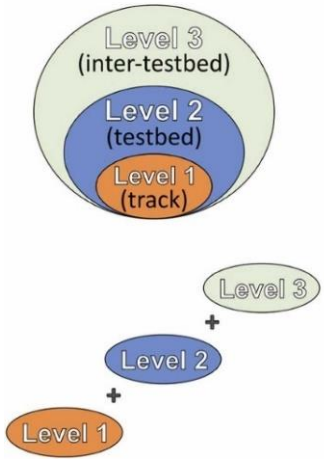


Absolute model

| | New snow | Aged snow |
|---|---|---|
| $\varepsilon_{track}$ [%] | 1.45 | 0.89 |
| $\varepsilon_{testbed}$ [%] | 2.48 | 1.17 |
| $\varepsilon_{inter\text{-}testbed}$ [%] | 4.87 | n/a |

Additive model

| | New snow | Aged snow |
|---|---|---|
| $\varepsilon_{L1}$ [%] | 1.45 | 0.89 |
| $\varepsilon_{L2}$ [%] | 1.03 | 0.28 |
| $\varepsilon_{L3}$ [%] | 2.39 | n/a |

Figure 4.2 An overview of precision is provided across three levels: within a single track, between four tracks, and between testbeds. Precision can be evaluated through both an absolute model and an additive model, which helps analyze the precision contribution at each level (Auganæs et al., 2022).

As outlined in Chapter 2.4, a measurement precision better than $\Delta\mu \leq 0.001$ is essential to differentiate between the averages of very similar skis. To yield statistically significant results, it is required that the margin of error of a 95% CI does not overlap with the mean of another ski. To illustrate this requirement, the number of runs required to achieve this margin of error was calculated, as depicted in Figure 4.3. In the case of new snow, this translates to more than five runs, while for aged snow, it translates to more than two runs.

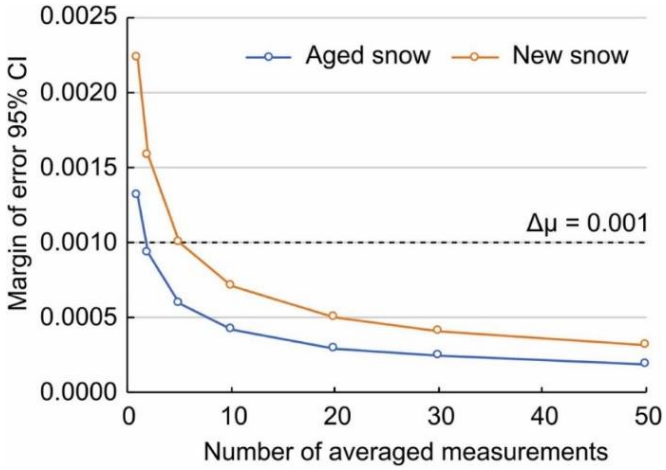


Figure 4.3 The margin of error of a 95% CI vs the number of averaged measurements on new and aged snow. The dotted line represents the threshold for the required number of measurements to achieve a margin of error that is less than $\Delta\mu = 0.001$ (Auganæs et al., 2022).

### 4.1.3 The effect of track polishing

When a ski glides over the snow, the surface changes due to abrasion and/or melting at contact points (Hasler et al., 2022). This fact becomes apparent indirectly through measurements of the friction coefficient and directly through measurements of the surface topography of the snow. Figure 4.4 depicts the impact of snow track polishing on the coefficient of friction over a series of 200 runs. After the first 10 runs, the friction decreased following an exponential decay pattern, signifying that the friction diminishes more rapidly at the beginning of the series before gradually stabilizing at a friction level of approximately $\mu = 0.075$, for this specific ski-snow combination. Another notable trend was the reduction in variability from run 100 and beyond. The RSD between runs 10 and 60 was 2.1%, while it decreased to 1.1% between runs 100 and 150. This observation proves that the tribometer precision is indeed influenced by the snow conditions.

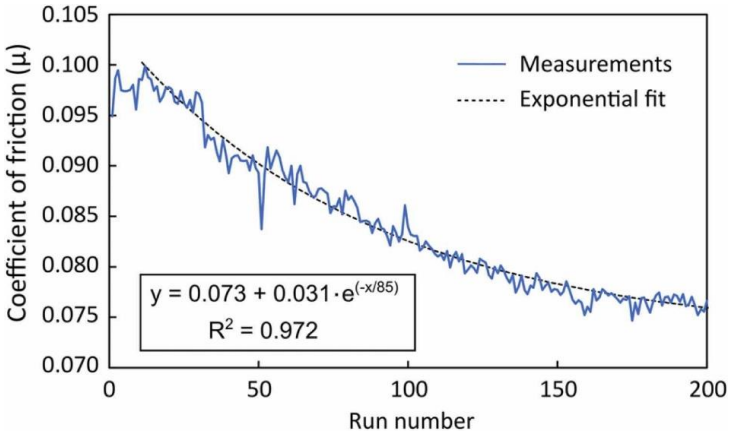


Figure 4.4 The progression of the friction coefficient over a 200-run series on dendritic new snow, at a speed of 6 m/s and snow temperature of -4.1 °C. The fitted curve for runs 11-200 is drawn as a dashed line with an R-squared ($R^2$) value of 0.972 (Auganæs et al., 2022).

The change in snow surface topography was documented using GelSight imaging before the test (Figure 4.5(a)) and after 200 runs (Figure 4.5(b)). In the pre-test image, well-defined contours of snow crystals with sharp edges are visible. However, after 200 runs, a noticeable transformation is observed, characterized by a shift towards more rounded features. This observation is supported by the arithmetic mean peak curvature (SPC) parameter, which decreased from 14.18 $mm^{-1}$ to 7.60 $mm^{-1}$. An increase in the SPC value corresponds to smaller or sharper peak curvatures, while a decrease in the SPC value results in larger or more round peak curvatures.

The density of peaks (SPD) parameter showed a slight increase, going from 1.70 to 2.04 $mm^{-2}$, suggesting abrasion or the fracturing of larger grains into smaller particles. This is further supported by the reduction in the average surface roughness from 30.0 to 19.3 µm, signifying a decrease in the mean height difference from the mean plane. All these different parameters show that the surface became more polished due to the 200 runs of the ski.

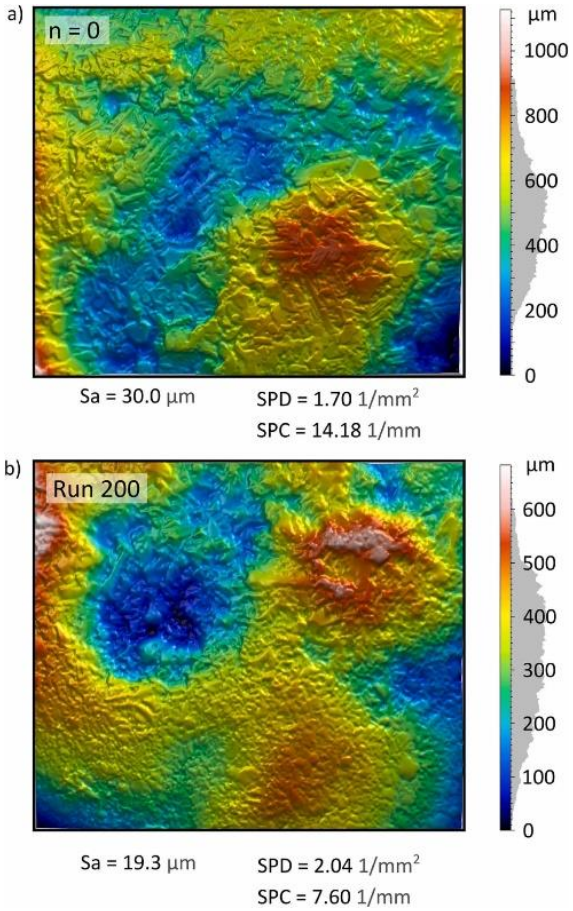


Figure 4.5 Surface topography images of the snow track captured with GelSight before and after 200 runs with the test ski. The real size of the images is 14 × 12 mm, and the running direction of the ski is vertical upwards in the images. The shifting in the images could be caused by inaccuracies in the positioning of the GelSight or a shifting snow surface due to longitudinal deformations in the snow matrix (Auganæs et al., 2022).

## 4.2 Post-processing method to correct for polishing

This section describes the result of a new method developed for the comparison of skis, which involves corrections of the measured coefficient of friction based on the polishing trend. The method was implemented in Paper II and III, and will be described along with an example involving six different skis tested on the same snow track. Each ski underwent three cycles to be able to determine the linear trend of the polishing snow track, as illustrated in Figure 4.6a.

Within one cycle, each ski was tested three times. After three cycles, each ski had undergone nine measurements. This exceeds the earlier stated minimum of five measurements. The advantage of doing three runs (triplicates) was the possibility of discarding data points in the event of significant deviations from the others or if any issues arose during testing. The wait time between each run was set to 30 seconds to ensure that the surface had stabilized before the next run.

After conducting the test, the linear trend for each ski was assessed. In the given example, the extent of polishing on the various skis was determined by the slope of the trendline. It's important to note that the differences between the skis decreased as the snow surface became more polished, as shown in cycle 3 of Figure 4.6a. Averaging the trend lines for each ski allows for establishing a global trend. The slope of this global trend was then used to correct the measured coefficient of friction by incorporating the level of polishing into each run. The equation used for this correction of the coefficient of friction, due to polishing, is as follows:

$$\mu_{cor} = \mu_n - Slope \times n \tag{4.1}$$

where $\mu_{cor}$ represents the corrected coefficient of friction, $n$ is the number of runs and $\mu_n$ is the friction coefficient of the n'th run.

In the provided example, $\mu_{cor}$ for run 1 will have $0.0003 \times 1$ subtracted to it, while run 54 will have $0.0003 \times 54$ subtracted. If the slope is negative the latter runs in the series will be lifted more than the first ones, reducing the impact of polishing between the skis, as illustrated in Figure 4.6b. In other words, the corrected values represent the friction coefficient on an unpolished surface. Consequently, the average friction coefficient is lifted, yet the comparative trend among the skis remains consistent, as seen in Figure 4.6c. Additionally, this correction reduces the standard deviation for each ski, leading to a more stable average. A lower standard deviation also makes the removal of potential outliers less influential on the overall average.

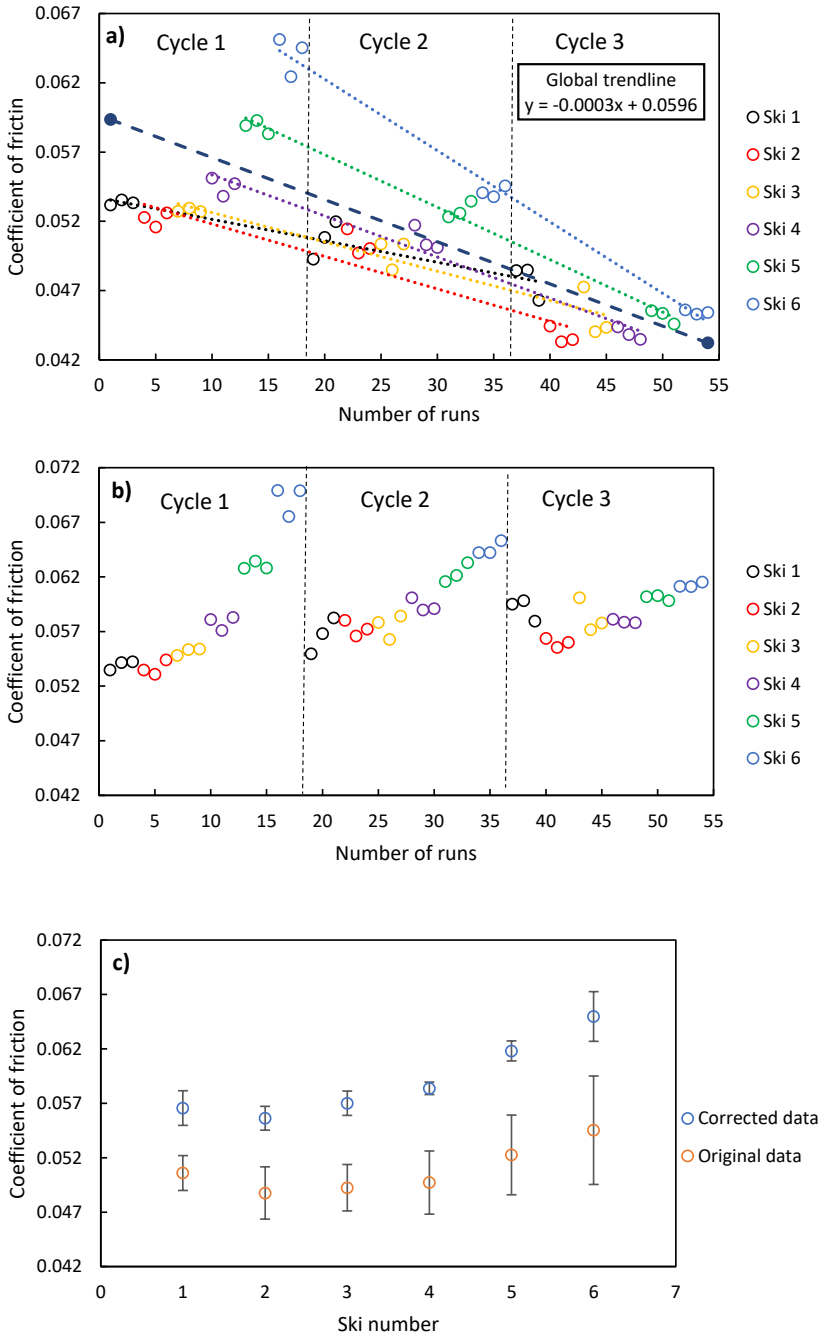


Figure 4.6 Example of the testing sequence and the effect of polishing on the skis. a) Original data with polishing trends and the average global trend. b) Data corrected for polishing. c) Calculated average μ for each sample with corresponding 95% CI.

## 4.3 Paper II – The effect of load and load application point on macroscopic ski contact parameters

### 4.3.1 The effect of normal load

The measured contact pressure profiles for different normal loads are illustrated in Figure 4.7. As the normal load on the ski increased, both the contact length and the peak pressures in the contact zones increased. At the same time, it was identified that the average contact pressure, load split, and spacing between front and rear also changed, as illustrated in Figure 4.8. The increase in contact length showed a linear trend from 200 N to 600 N, but it started to level off as the load reached 800 N. The reason for the change in the trend after 600 N is attributed to the increased stiffness towards the ski's mid-point. The higher bending stiffness in this part of the ski will limit further compression and thus further expansion of the contact zones. Notably, the contact length in the rear zone exhibited a more significant increase than that in the front zone, primarily due to the load application point being positioned 12 cm from the midpoint towards the tail.

Another notable trend was the increase in the average contact pressure. This was due to the average contact length (apparent contact area) not exhibiting the same magnitude of increase as the normal load. For example, as the load was increased from 200 N to 800 N, the apparent contact area increased from 144 $cm^2$ to 294 $cm^2$, an increase of around 100%. Consequently, the average contact pressure (load divided by area) was observed to rise from 12.7 kPa to 25.2 kPa across the loading range of 200 N to 800 N.

Furthermore, the load split shifted towards the rear as the normal load was raised. At 200 N, the load was split 40/60% in front and rear respectively. However, at 800 N, the load split shifted to a 25/75% split in the front and rear, respectively. The final parameter examined was the spacing between the front and rear contact zones, which decreased from approximately 100 cm to 60 cm as the normal load increased from 200 N to 800 N.

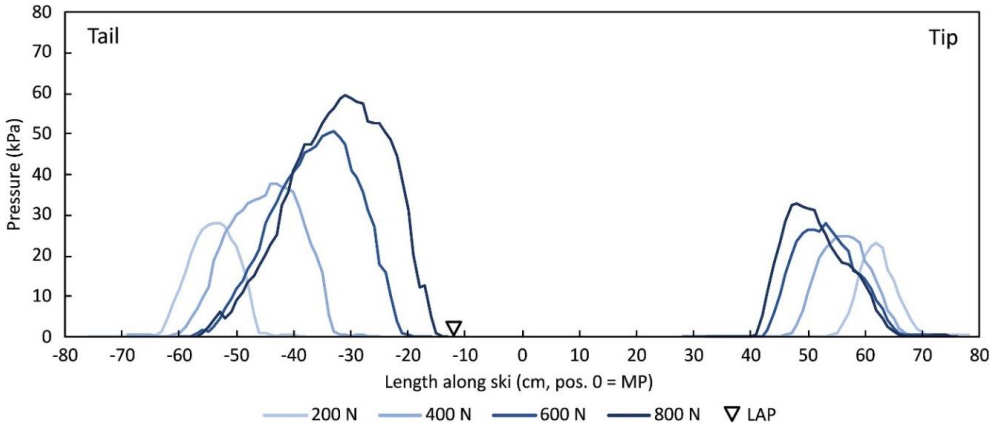


Figure 4.7 Contact pressure profiles for four different normal loads, with the load application point (LAP) 12 cm behind the midpoint (Auganæs et al., 2023).

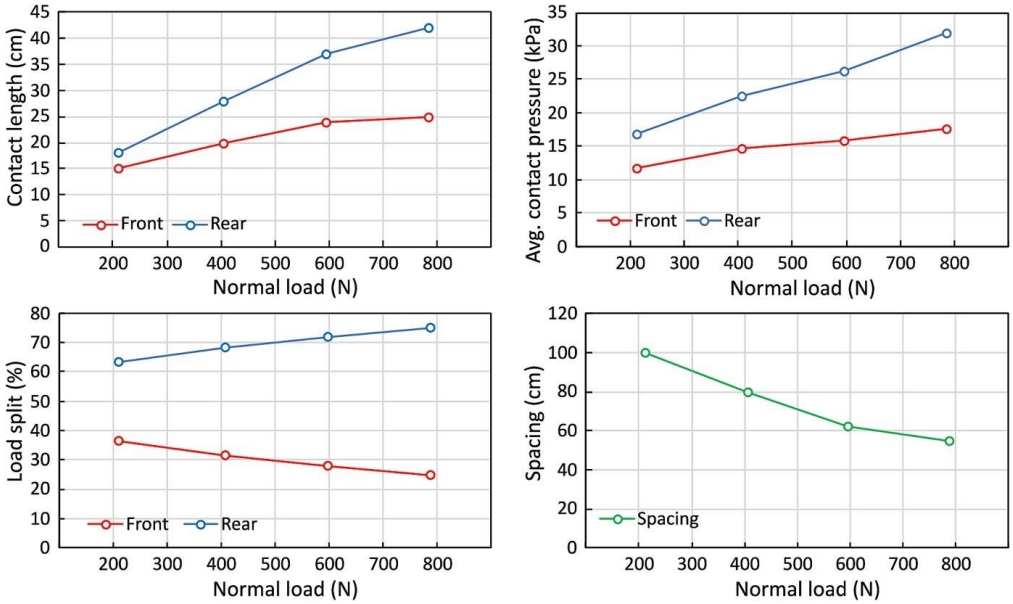


Figure 4.8 Measured contact zone lengths, average contact pressure, load split, and spacing as a function of the normal load (Auganæs et al., 2023).

### 4.3.2 The effect of load application point

The analysis of pressure profiles based on moving the load application point from 2 cm to 22 cm behind the midpoint (MP), is depicted in Figure 4.9. Shifting the LAP towards the rear yields three notable outcomes. Primarily, it increases the load in the rear contact zone, effectively altering the load split. Secondly, this adjustment causes the contact zones at the front and rear to separate further, thus increasing the spacing. The third outcome is a decrease in the length of both contact zones, thus reducing the apparent contact area. At a neutral position, with the LAP positioned 12 cm behind the MP, a front-to-rear load split of 28/72% was observed, with peak pressures occurring at 47 cm ahead of and −33 cm behind the MP. Figure 4.10 provides a more detailed view of how the ski's characteristics evolve with the repositioning of the load application point. It systematically illustrates how each of these parameters adjusts in response to changes in the location where the load is applied, offering a more detailed view of the ski's contact zones characteristics.

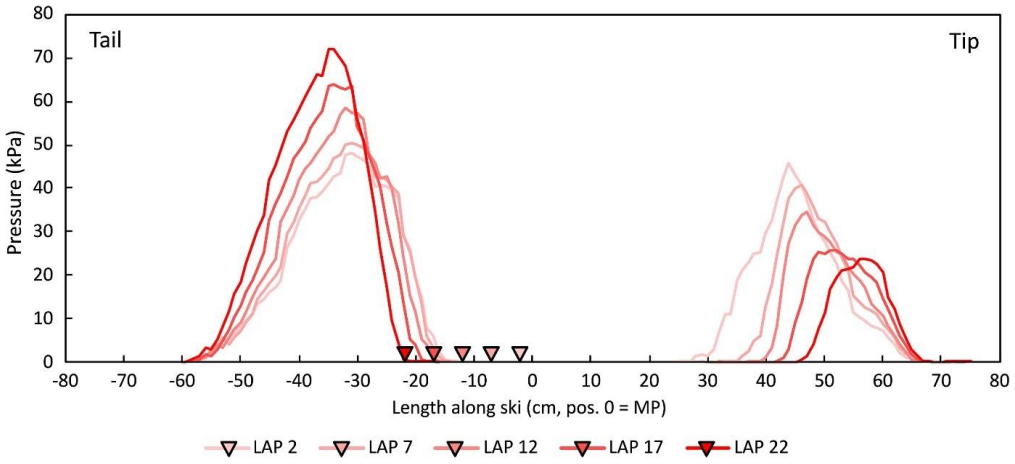


Figure 4.9 Contact pressure profiles of the ski, captured at five distinct load application points, under a consistent normal load of 730 N (Auganæs et al., 2023).

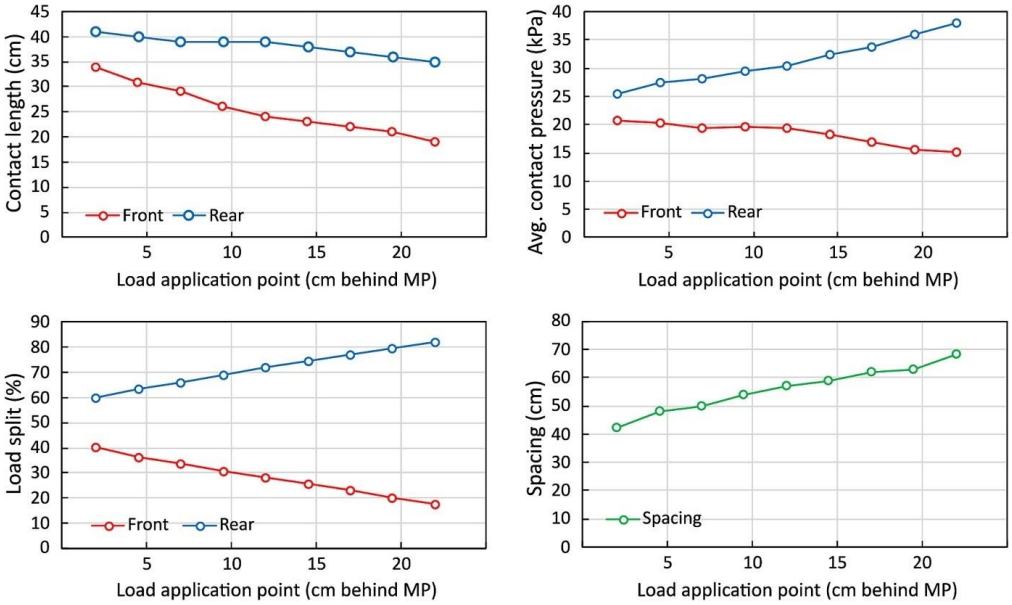


Figure 4.10 Measured contact zone length, pressure, load split, and spacing as a function of the load application point (Auganæs et al., 2023).

## 4.4 Paper III – The effect of isolated macroscopic ski contact parameters on friction

The adjustable test ski made it possible to isolate the macroscopic contact parameters under realistic conditions. The importance of realistic conditions means that variables like speed, load, snow track, and sample size were in the range that can be expected in cross-country skiing. In this way, the observed frictional trends are believed to have a closer proximity to the frictional regimes occurring in ski racing. This resulted in a better understanding of how a change in each parameter affected the friction.

### 4.4.1 The effect of contact pressure

The friction measurements involving normal load and apparent contact area resulted in the calculation of the average contact pressure. The contour plots in Figure 4.11 show the friction coefficient as areas of different color gradients, while the black isolines represent the average contact pressure based on x and y values. At the coldest temperature, an intriguing observation relates to the correlation between the average contact pressure and the friction coefficient. It was shown that the highest friction coincided with regions of low contact pressure, while the

lowest friction occurred in areas with high contact pressures. Notably, the contour lines for the friction coefficient align with the patterns of the contact pressure isolines, particularly for contact pressures below 20 kPa.

At intermediate temperatures, the data clearly shows that friction is predominantly affected by the apparent contact area rather than the normal force applied, as seen in Figure 4.11. This makes the correlation between friction and contact pressure less evident. The friction coefficient exhibited a decreasing trend, from the largest area with the highest load to lower values for the two smaller contact areas. Notably, at this temperature, a minimum friction point was observed, occurring within the range of an apparent contact area of 270 $cm^2$ and a normal force of 600 N.

At the warmest temperature, a strong correlation is evident between the apparent contact area and the friction coefficient. As depicted in Figure 4.11, the highest friction coefficient values align with the largest contact area, and friction decreases as the contact area diminishes. The friction is slightly lower for the normal load of 600 N compared to 300 N and 900 N for all the contact areas.

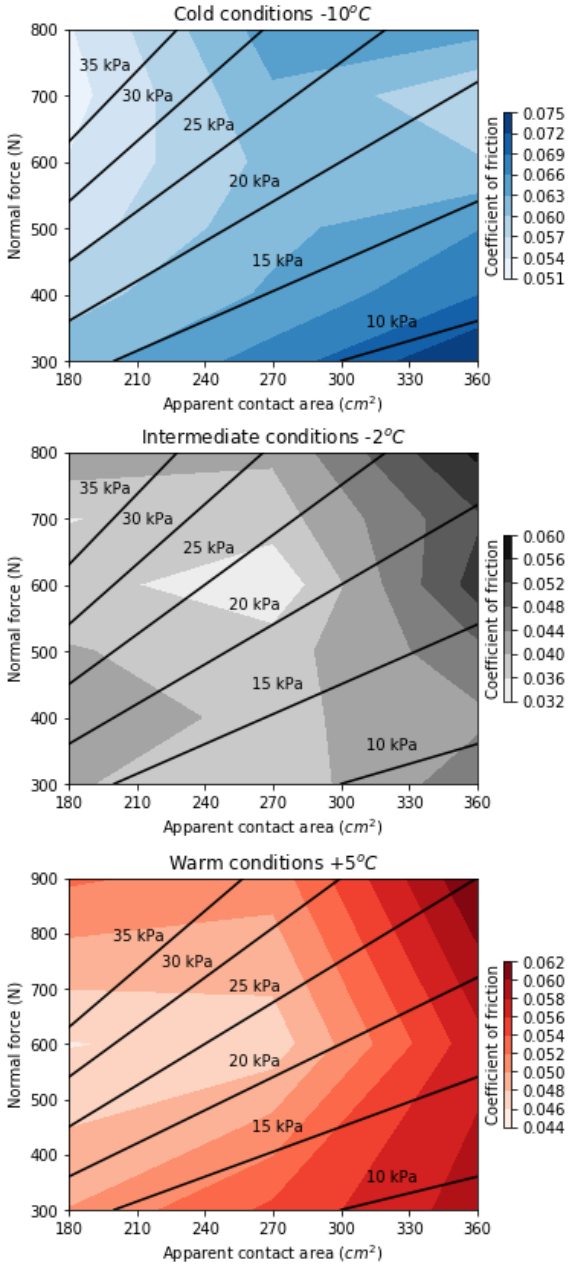


Figure 4.11 The effect of average contact pressure on the friction coefficient at air temperatures of -10 °C, -2 °C and +5 °C. The contour plot illustrates the relationship between the normal force and the apparent contact area, revealing their impact on the friction coefficient. The isolines displayed on the plot provide a visual representation of the average contact pressure's influence on the observed patterns (Auganæs et al., 2024).

### 4.4.2 The effect of load split

As the load application point was moved on the ski, the load split between the front and rear sliders changed accordingly. The impact of load split on the coefficient of friction for three distinct snow conditions is depicted in Figure 4.12. A load split of 95% implies that the applied load is concentrated entirely over the front slider, with the remaining 5% representing the ski's own weight.

In cold conditions, the lowest friction is observed when the load is entirely positioned over either the front or rear slider, as seen in Figure 4.12. This is consistent with the results of the average contact pressure, where a higher contact pressure reduces friction. When starting from the middle of the ski, shifting more of the load towards the front reduces friction slightly compared to having more of the load split towards the rear slider. A relative difference of around 7% is the result of changing the load split from 35% to 65%. This suggests the advantage of concentrating the frictional power towards the front slider to induce a water film earlier along the ski. The frictional power one slider produces on the snow is dependent on the load multiplied by the coefficient of friction and speed. By moving the load application point toward the front or rear, more of the load will be transferred to one of the sliders. The load split can thus be seen as a measure of the distribution of frictional power between the two sliders.

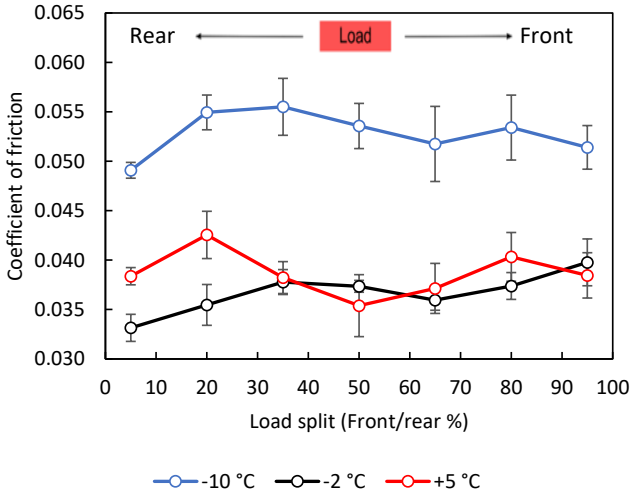


Figure 4.12 The effect of load split between the front and rear slider (5% equals all of the applied load over the rear slider). The tests were conducted using 30 cm sliders, a normal load of 400 N, and a speed of 5 m/s. Error bars are included in the graph to represent one standard deviation in each directions (Auganæs et al., 2024).

Under intermediate conditions, friction increases as the load split transitions from being over the rear slider to being concentrated entirely over the front slider, resulting in a relative difference of around 17%. Contrary to cold temperatures, increased frictional power in the front will potentially lead to the development of a thicker liquid film that increases the real contact area along the slider. This increased real contact area will, in turn, raise the viscous friction for the rest of the slider. A situation that inversely mirrors the behavior noted in colder temperatures.

Under melting conditions, a minimum friction point is observed at a 50% load split, with an increase in friction as the load is shifted toward either the front or rear. Intriguingly, there is a slight decrease in friction when all the load is placed on one slider. This trend exhibits relative symmetry, signifying that there is no discernible difference in shifting the load either forward or backward.

### 4.4.3 The effect of spacing between contact zones

The increasing distances between the ski's front and rear contact zones, consistently indicated a slight yet steady increase in friction, as depicted in Figure 4.13. This trend is particularly uniform in cold and intermediate conditions. At colder temperatures, the data showed about a 5% relative shift in the coefficient of friction when the spacing extended from 20 cm to 100 cm. In contrast, at the warmest temperature, this trend is not as distinct, indicating that either different factors may be affecting the spacing's impact under these warmer conditions, or that spacing plays a less significant role in influencing friction at this temperature.

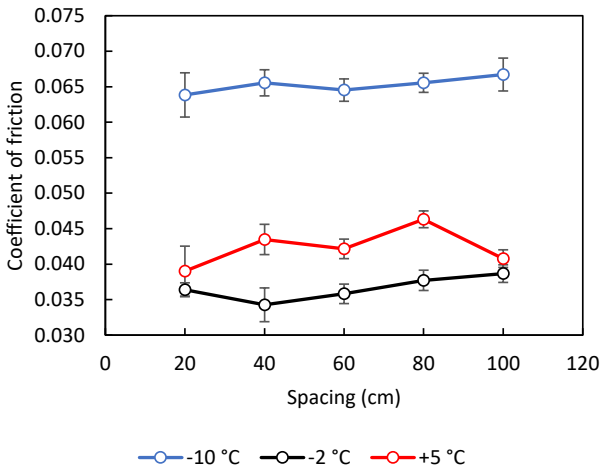


Figure 4.13 The effect of spacing between the front and rear slider on the friction coefficient. The tests were conducted using 30 cm sliders, at a speed of 5 m/s and a normal load of 400 N. The error bars represent one standard deviation in each direction (Auganæs et al., 2024).

# 5 Discussion

The following chapter is segmented into four distinct sections, to ensure a clear and comprehensive discussion of the findings. The first section delves into methodological development, offering insights into the evolution and critical considerations of the laboratory test method used for our experiments. The second section focuses on the measurements of contact pressure profiles on skis. Here, we discuss the intricate details of ski mechanics and how the ski interacts with the snow surface. In the third section, we shift our attention to the effect of isolated contact parameters effect on gliding friction. This part underscores the complexity of ski-snow interaction and the significance of understanding each parameter's contribution. The fourth and final section highlights how the insights from this thesis enhance our understanding and evaluation of ski-snow friction. It discusses the broader implications of our findings for both theoretical knowledge and practical applications, particularly in the context of optimizing ski performance.

## 5.1 Methodological development and considerations for ski testing

Performing repeated friction measurements with a ski sliding over the same snow presents a challenge due to gradual changes in the snow surface caused by mechanisms such as abrasion and/or friction-induced melting (Hasler et al., 2022). This alteration typically results in a decline in the measured coefficient of friction with each pass of the ski. Hasler et al. (2016) documented the change in friction in a series of 50 runs on five different snow tracks. Since the coefficient of friction consistently decreased throughout the series, they determined the best way to calculate the standard deviation by measuring the deviation from the linear trendline of the series. This approach assumes that the least squares fit accurately represents the impact of ski and snow surface changes. It means that any differences between the measured values and the linear fit are not influenced by alterations in the surfaces but are instead attributed to variation in the force measurement unit. The precision was in the end reported as the relative standard deviation, to make the precision independent of the absolute friction level.

We opted to employ this method to assess precision while making some modifications of our own. One notable adjustment involved using a ski with low roughness and no wax during the

measurements. This was implemented to eliminate uncertainties associated with the wax application process on the ski and to attribute any change in the coefficient of friction across runs solely to alterations in the snow surface, rather than potential wax wear. By employing a less optimized ski and utilizing dendritic new snow, the system showcased a relatively high coefficient of friction. Consequently, this led to a noticeable decrease in the coefficient of friction with each subsequent run. Higher friction generates more work on the surface, thereby causing more pronounced changes to the surface for each run.

A question emerged in hindsight regarding the evaluation of the system, specifically regarding the higher friction level compared to tests conducted for Paper II and III. The application of wax to the ski could potentially reduce microroughness or flaws in the ski structure. Additionally, a reduction of the shear force between ski and snow asperities could result in lower work on the surface for each run. This reduction in frictional work could potentially have contributed to a decrease in run-to-run variability (relative standard deviation) of the measured coefficient of friction. However, while waxing the ski could have decreased the relative standard deviation at level 1 (snow surface instability), it is plausible that it might have influenced the precision negatively for levels 2 and 3 (snow track variations and snow testbed variations), due to variations in the ski waxing procedure between each series.

### 5.1.1 Precision

The precision assessment of the ski-snow tribometer highlights a distinct relationship between the snow track surface and the observed run-to-run variability in the friction measurements. Specifically, testing on dendritic new snow exhibited higher standard deviation in comparison to transformed snow conditions. Conversely, when using roller skis on plywood sheets, the variation observed was even lower. It's worth noting that the dendritic structure of new snow is expected to undergo more rapid changes due to factors like abrasion and friction-induced melting compared to older snow, which has undergone some degree of metamorphosis. Furthermore, variations in measurements due to different surface conditions were evident in the 200-run series, where the standard deviation consistently decreased with subsequent runs.

Comparing the precision of 1.45% within a single track found in Paper I, to similar full-scale tribometers, showed slightly higher run-to-run variability. The precision reported in the linear tribometers in Lemmettylä et al. (2021) and Hasler et al. (2016) ranged between 0.6–1.1% and 0.47%, respectively. However, it's essential to consider that our tests were performed on dendritic new snow, in contrast to the rounded artificial snow produced by fan guns. To make

a direct comparison, identical snow conditions and system friction levels are necessary. Even though the variability was higher for our tribometer, the requirement of $\Delta\mu \leq 0.001$ to distinguish between very similar skis can still be met by performing five runs or more. Thus, indicating that the precision of the developed tribometer is sufficient for effective testing and product development.

### 5.1.2 The effect of polishing trend on the precision

The gradual alteration of the snow surface resulting from repeated sliding is often described as "polishing" in the skiing world. This might be due to the snow track becoming shinier when several people have skied on it. However, the appropriateness of using the term "polishing trend" to describe the decreasing or increasing trend in friction can be a subject of discussion. The term "polishing" suggests a process that smoothens and enhances the shine of a surface by rubbing it. Hasler et al. (2022) suggested that mechanical wear and/or melting was the process that contributed to the smoothening of the surface. This process removes material from the asperity's contact spots to nearby valleys. This was observed in their study by a reduction in roughness during a series of 20 runs at snow temperatures of -1.3 °C and -10.7 °C. However, at -19.1 °C, the roughness increased with the number of runs, likely due to the fracturing of entire snow grains.

In Paper I, we also noted a decrease in average surface roughness from 30 µm to 19.1 µm after 200 runs with the ski. The reduction in roughness observed on the snow surface can be attributed to several processes, including plastic deformation, abrasion, or frictional melting (Hasler et al., 2016). These mechanisms collectively result in the smoothing of the snow surface, a phenomenon that significantly impacts the friction between the ski and snow. To maintain clarity and consistency throughout this thesis, we have referred to this collective impact on snow surface as the "polishing trend."

The slope of the polishing curve appears to be dependent on the friction level of the ski-snow system. A ski-snow system with higher friction tends to induce a more pronounced drop in the coefficient of friction for each run. For instance, in Paper I, the unwaxed ski had a high initial coefficient of friction of around 0.09 which dropped 2.5% after 10 runs, while in Paper II, the waxed ski had a lower friction level of around 0.04 and dropped 1% over the same number of runs. The observed polishing trend might be more accurately described by an exponential rather than a linear trend. Initially, the rate of change in friction due to polishing is quite rapid. This rate diminishes over time, indicating that the system approaches a limit where further polishing

has diminishing returns on reducing friction. However, within a certain range, the polishing trend can be approximated with a linear behavior.

Notably, in studies conducted by Lemmettylä et al. (2021) and Sandberg et al. (2023), where the level of coefficient of friction was approximately 0.02, the friction increased with the number of runs despite the surface becoming more visually polished. Despite the snow surface becoming polished, the observed increase in friction could be attributed to an expanded contact area resulting from the ski-snow wear-in or the degradation of ski wax. The polished appearance of snow does not guarantee lower friction. In fact, at lower friction levels, the impact of polishing (resulting in rounder/flatter asperities) may result in less significant changes in friction compared to an increase in the real contact area or the wear effect of wax. This highlights the complex relationship between surface conditions and frictional forces in skiing.

### 5.1.3 Accuracy vs Precision

Ski and wax manufacturers aim to design products that perform optimally across various snow conditions. One aspect of this is testing sliding friction on dendritic snow, which aids in tailoring equipment and wax formulations for optimal performance on such surfaces. Minimizing uncertainty in the development and testing process is therefore an important factor. In Paper I, we've found that the standard deviation can be lowered by conducting tests on snow surfaces that are either “worn in” or made of transformed snow. Further precision is possible by testing on ice (Jakobsen et al., 2023). However, such an approach deviates from the actual snow surface intended for skiing. Despite the potential for improved precision, the transferability or accuracy of the results would be reduced, as illustrated in Figure 5.1. The error bars on the ski sled and snow tribometer indicate that the accuracy can vary depending on how close the snow surface matches the track conditions in the field.

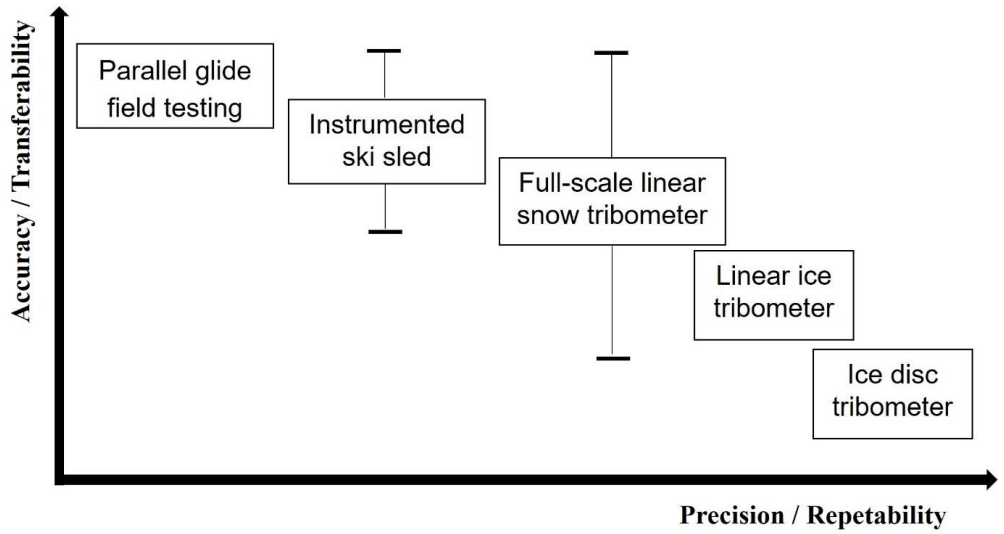


Figure 5.1 Accuracy vs precision for different methods to test ski-snow friction.

To determine the best ski or wax products for race day, the primary objective is to identify the lowest absolute friction value specific to the prevailing snow condition. To achieve this goal, field testing remains essential, offering the highest level of accuracy concerning the surface the ski is intended to perform on. In such cases, the accuracy of the results might be more crucial than attaining high precision. The use of an instrumented sled in the field could potentially increase the precision to some extent, as discussed by Sandberg et al. (2023). However, for product development, the frictional trends for a given input parameter are of greater interest than the absolute friction level. At the same time is it important that the snow surface reflects properties like those in the field to ensure that the frictional trends observed in the tribometer are applicable or valid for the intended use of the product in the field.

A discussion also in field testing is to what degree the snow surface should be run in before starting to test. In the ski comparison example in Chapter 4.2, there is a clear trend that the relative differences between the skis reduced for each cycle. The differences between the skis in the last cycle were much smaller than in the first. This suggests that testing on overly polished or icy surfaces may not accurately reflect a ski's true performance. While such conditions might yield low standard deviations, the differences between the skis are also reduced, potentially masking meaningful performance variations.

### 5.1.4 Comparative analysis of skis on a changing snow surface

The devised method for comparing skis on a changing snow surface proved effective as it evenly distributed the degree of polishing across the samples by repeated sequentially testing. Additionally, the impact of the polishing trend on the data's averages and standard deviations was reduced through corrective adjustments based on the trendline's slope. To the best of the author's knowledge, such a method has not been previously reported in the literature.

A sequential test order was employed to account for changes in the snow surface, balancing the need to spread the polishing effect across different skis, against the uncertainty and additional time introduced by the number of manual changes. As an example, comparing the relative standard deviation of 1.45% from the precision assessment in Paper I, by doing 50 runs with one ski, to the relative standard deviation of around 2.5% in Paper II, indicates an additional source of error from changing the skis three times. However, there is also a statistical difference in comparing the standard deviation for nine runs compared to 50 runs.

The post-processing of the data was performed by correcting the original data by “lifting” it to the same level as the first run in the series. This correction was based on the average polishing trend observed across all the tested skis. One of the primary advantages of this correction was to reduce the effect of polishing on the averages and standard deviations between the skis. However, it should be noted that this correction process had the effect of artificially lifting the reported average coefficient of friction. While the absolute frictional values themselves were not the primary focus, as they tend to vary with specific test conditions, reporting higher values than what was actually measured could potentially lead to confusion for others using the data for comparison purposes.

We also tried the approach of using the trendline from a reference ski before, in the middle, and after the test series to correct for polishing. From this, we learned that the reference ski needed to have the same friction level as the skis in the testing matrix to capture the same degree of polishing between the samples. For example, if the reference ski had high friction levels compared to the tested skis, the slope of the polishing trendline was steeper, and the corrected results were skewed towards the first skis having lower friction. Since the development of the snow surface is dependent on skis performing the “work” on the surface we concluded that it was better to use the trendlines of the skis in the test matrix to evaluate the polishing trend rather than a reference ski. The best results are likely achieved when all skis are fairly uniform in

terms of surface roughness and friction, ensuring that the influence of each ski on the surface for the subsequent ski remains consistent across the test matrix.

## 5.2 Analyzing how normal load and load application point influence macroscopic ski contact parameters

This chapter delves into how the normal load and load application point affected some defined macroscopic contact parameters from the measured pressure profiles of a skating cross-country ski. An observation from the pressure profile measurements was that the macroscopic parameters changed simultaneously when the normal load or LAP was altered. By increasing the normal load, the apparent contact area and the average contact pressure increased, the spacing got shorter and the load split shifted towards the rear. These changes across multiple parameters made it challenging to establish a direct relationship between these parameters and the measured gliding friction. Notably, the frictional changes in response to changes in normal load were minimal across all temperatures tested. This was particularly unexpected in colder conditions, where previous research using small-scale sliders suggested a potential load dependency on the friction coefficient.

The complexity of the load response arises from the design of the cross-country ski, where the apparent contact area is dependent on the normal load. Interestingly there seems to be a missing link between the friction measurements on simplified sliders (constant apparent contact area) and the combined response between load and apparent area on a cross-country ski. For example, Buhl et al. (2001) suggest that a heavier skier benefits from a lower coefficient of friction at snow temperatures below -10 °C. This is true if the apparent contact area stays constant, however, that is not the case for a cross-country ski. This might be one of the reasons that we did not observe any changes in friction for higher loads on the cross-country ski at the cold temperature.

When adjusting the LAP towards the tail of the ski, several changes occurred: the apparent contact area decreased, leading to an increase in average contact pressure. Additionally, the spacing between the front and rear zones expanded and as expected, the load split shifted more toward the rear contact zone. These adjustments collectively contributed to a reduction in friction, observable in both cold and warm snow conditions. The predominant factor thought to

drive this decrease in friction is the reduced apparent contact area, although it's acknowledged that additional factors might also affect friction to some degree.

Building on the initial findings regarding the effects of normal load and LAP on macroscopic contact parameters, our investigation further unravels the complexities inherent in cross-country ski design and its interaction with snow. Despite the small frictional changes across temperatures, it becomes evident that the interaction between load and the apparent contact area on a cross-country ski differs significantly from that on simplified sliders.

### 5.2.1 Potential for more information from pressure profiles

An aspect that has not been thoroughly explored is the shape of the pressure profiles. The pressure profiles of skis often exhibit a degree of asymmetry, as seen in Figure 4.7. The starting point of the front zone indicates a more gradual pressure increase owing to lower bending stiffness, while the end of the front zone appears more abrupt. Conversely, the rear zone demonstrates a steep pressure increase at the beginning, followed by a more gradual decrease toward the ski's tail. Analyzing these pressure profiles raises questions about how the contact zones should be defined.

Typically, the contact zone length is defined where the distance to the sole is less than 0.1 mm or where pressure starts to increase. However, the actual shape of the pressure profile, for two skis with equally defined contact lengths, may differ significantly. In the example in Figure 5.2, both profiles have the same contact length and average contact pressure, but the increase in pressure and peak pressure are different. Thus, it might be beneficial to begin reporting parameters like contact length above 50% pressure to get more information from the area carrying most of the load. Parameters such as skewness and the slope of the pressure increase/drop could capture more of the curve's shape and offer valuable insights into evaluating ski design. For instance, in the development of the adjustable model ski, it was discovered through trial and error that a certain gradual pressure increase is necessary to avoid snow-plowing effects.

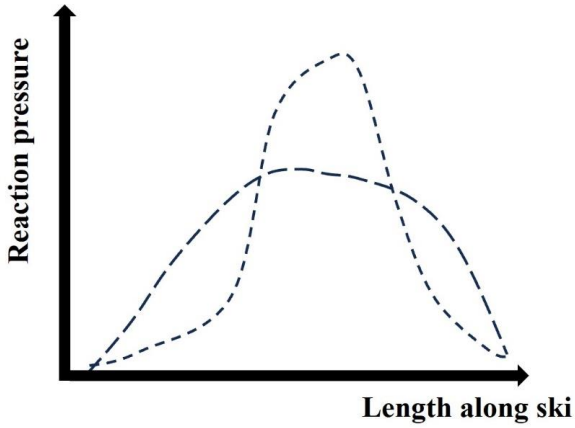


Figure 5.2 Example of two imaginary pressure profiles, that would result in the same defined contact length and average contact pressure.

Contact zone characterization should also be seen in context with snow hardness. Studies by Mössner et al. (2023) and Kalliorinne et al. (2022) have shown the dependence of snow hardness on the apparent contact area and peak pressures. With softer snow, the load from the ski will be distributed over a larger area due to the displacement of the ski into the snow. Due to the metrological parameters and sintering time after preparation, the snow hardness seen in cross-country tracks can vary a lot (Moldestad, 1999). Furthermore, the diverse methods used to characterize snow hardness make it challenging to compare values. The mentioned study by Kalliorinne et al. (2022) used the Youngs modulus from a compression test (MPa), while Mössner et al. (2013) reported the hardness as the displaced volume of snow from a drop test ($N/mm^3$), and Wolfsperger et al. (2021) reported the hardness as penetration resistance from a drop test (N). As we move forward, it's imperative to adopt more consistent and comprehensive methods for characterizing snow conditions, which will, in turn, make it possible to evaluate pressure profiles based on snow conditions.

### 5.2.2 Contact pressure profiles and the elasticity of snow

Due to the delayed elastic response of snow, the characteristics of the contact zones on a gliding ski might be different compared to static measurements. This phenomenon arises from the viscoelastic properties of snow, behaving as a combination of a viscous fluid and an elastic solid under stress (Wolfsberger et al., 2019). Under repetitive loading and unloading, such as a ski repeatedly passing over the same spot, the snow will “slowly” regain its original shape and

volume over time rather than instantaneously springing back or showing perfect elastic behavior (Theile et al., 2009), as illustrated in Figure 5.3.

The process begins with the compression of the snow in the front contact zone as the ski exerts force upon it. This is followed by an unloading phase where the force exerted by the ski diminishes. Subsequently, as the rear zone passes over the same point, there is a reloading phase. Due to the rear contact zone carrying the most load, this second loading phase will compress the snow to a larger magnitude than the front contact zone. The chart effectively captures the cyclical nature of the snow's compression and the subsequent recovery as the ski moves over it, highlighting the unique mechanical interaction between the ski and the snow surface.

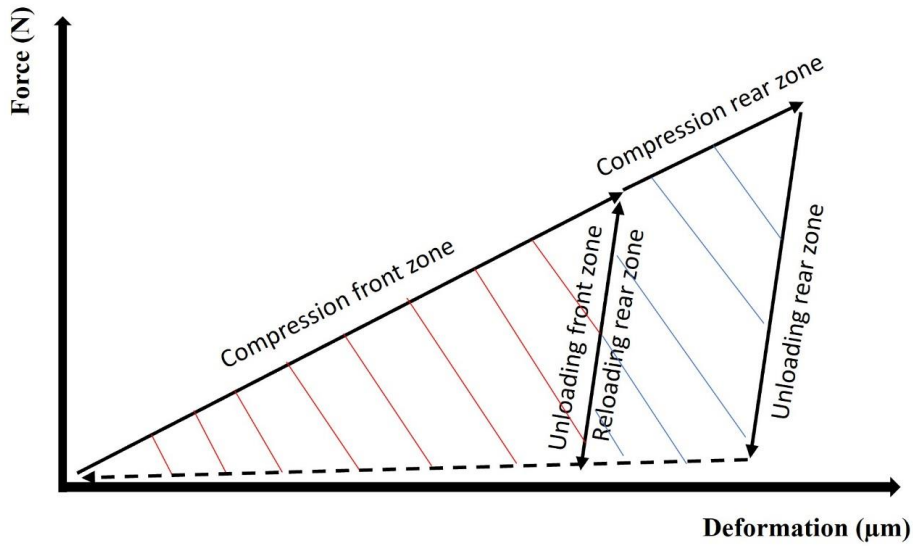


Figure 5.3 The delayed elastic response of snow under the dynamic loading of a gliding ski. The grid lines in red and blue illustrate the compression work done by the front and rear zones, respectively. (adapted from (Mössner et al., 2023) and (Theile et al., 2009))

Transferring this behavior to the measurement of contact pressure profiles suggests that the contact area behind the peak pressure within the contact zones on a gliding ski could experience a more rapid decrease in pressure due to this delayed elastic response, as illustrated in Figure 5.4. The degree of delayed elastic response impact on the pressure distribution is contingent on the snow's hardness and the extent of delayed elasticity within the snow matrix. In the work of Theile et al. (2009), who measured repeated loading on hard snow samples (Young's modulus

of 1200 MPa), the delayed elastic recovery was only 20 µm, and the frictional work going to the snow compression was shown to be negligible. With such small deformations, the change in the contact profiles would be very small.

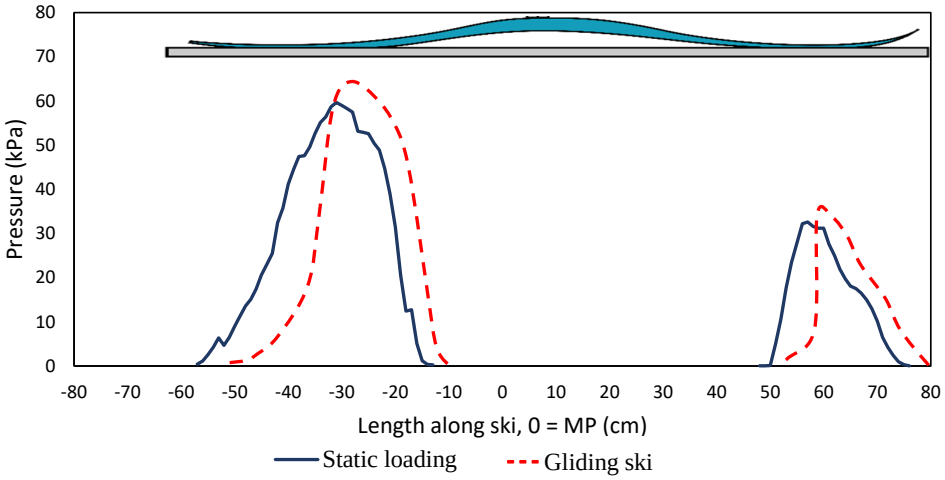


Figure 5.4 Reaction pressure between the ski and snow for static loading (blue line), and imaginary pressure for a gliding ski where the snow exhibits a delayed elastic response (dashed red line). MP equals the mid-point or balance point of the ski.

The measurements of contact pressure profiles have shown to give more information about the contact zones of the ski compared to the more traditional camber curve method. While the camber curve still gives important information for the application of grip wax in classical skiing, there is more potential in evaluating pressure profiles when focusing on gliding. There is even further potential to introduce new parameters to better explain the profiles, beyond the scope of what was presented in Paper II.

Additionally, there is a potential for standardizing snow hardness measurements concerning skiing tracks, and especially cross-country tracks. Standardization might narrow the range of values currently observed in various studies, facilitating a better comparison of results across different research methodologies. This could lead to a more cohesive understanding of how snow hardness affects the apparent contact area and ultimately the ski-snow friction.

## 5.3 The effect of isolated macroscopic ski parameters on friction

In the subsequent sections, the effect of average contact pressure and load split on the friction coefficient are discussed together and categorized for each testing temperature. This approach is taken due to the distinct frictional mechanisms prevailing at different temperatures. By dissecting the frictional behavior at different temperatures, we can better understand and optimize skis for their intended environmental conditions. Conversely, the impact of spacing on friction will be treated separately, as the response to spacing changes has shown to be consistently similar across the range of temperatures tested.

### 5.3.1 Cold temperatures

At the cold temperature of -10 °C the measured coefficient of friction was observed to be highest for all the tested parameters (up to $\mu = 0.07$), compared to the other temperatures. The liquid-like layer is thinner at low temperatures (Dash et al., 2006), and the initial contact with the ski is believed to consist mostly of boundary contacts with relatively high friction. In this friction regime, the contact points experience a higher friction force, primarily due to the formation of stronger surface adhesion bonds (Kietzig et al., 2010). As the ski slides over the snow asperities the repeated contact will generate frictional heat that can increase the liquid-like layer thickness and thus reduce friction (Colbeck, 1992).

The frictional power generated by the ski, as given in equation (2.5, is measured in joules per second. An increase in frictional power equates to a greater amount of energy being transferred to the snow per unit of time. This explanation has been used in studies that observed a reduction in the coefficient of friction for higher sliding speeds or increased normal force, particularly in cold temperature conditions (Bäurle et al., 2006; Oksanen & Keinonen, 1982).

#### 5.3.1.1 Normal load, apparent contact area, and average contact pressure

At the coldest temperature tested (-10 °C), the measurements revealed a distinct correlation between average contact pressure and the coefficient of friction. One method to modify the contact pressure involves adjusting the normal force. This relationship between normal force and the coefficient of friction has previously been documented on small-scale sliders in studies by Oksanen and Keinonen (1982) and Buhl et al. (2001).

Less focus has been given to the effect of the apparent contact area of the ski or slider on the coefficient of friction, maybe due to the early experimental results from Bowden and Hughes (1939) that indicated the apparent area to have little influence on the coefficient of friction.

However, Bäurle et al. (2006) showed that smaller apparent areas of contact resulted in lower coefficients of friction. They attributed this to the fact that the frictional energy released per unit area was greater for a slider subjected to a higher normal force or possessing a smaller apparent contact area.

In other words, this means that a higher average contact pressure is beneficial for increased frictional power per area. In theory, an increase in the average contact pressure can lead to the following scenarios for the contact spots, as illustrated in Figure 5.5:

1. The number of contact spots remains constant; therefore, existing contacts need to carry a higher load, which in turn leads to more frictional heating of these contacts.
2. The number of contact spots increases and the load is divided equally among new and existing contacts. Therefore, each contact will carry the same load as before, which leads to the same degree of heating.

In reality, there is likely a mix between these two scenarios depending on the roughness and hardness of the surfaces. The elevated peaks on the snow surface will experience higher contact pressure as the ski compresses the snow, while additional contacts will be formed due to the compression. Contacts enduring higher loads will consequently experience increased heating, thereby offering improved lubrication.

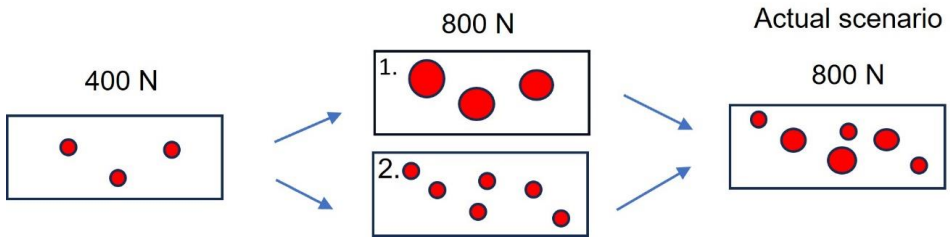


Figure 5.5 Example of development of contact points on the snow surface when doubling the normal load. The same situation would apply for reducing the apparent contact area.

According to the hypothesis that suggests increased frictional heat per unit area for higher contact pressures, it appears insignificant how the average pressure is modified, as was seen from the contour plots in Figure 4.11. In our study, we noted a 14% reduction in the coefficient of friction when either the contact area was halved from 360 $cm^2$ to 180 $cm^2$, or the normal force was doubled from 300 N to 600 N. However, at the highest contact pressures, reducing the apparent contact area seems to have a more pronounced effect. This is aligned with the

findings of Bäurle et al. (2006) who reported a 35% relative decrease in the coefficient of friction when the contact area was reduced from 2 cm² to 0.8 cm². In contrast, an increase in load from 21 N to 52 N in their study resulted in a smaller reduction of 19% in the coefficient of friction.

It is important to note that Bäurle et al. (2006) altered the contact area by widening the slider, not lengthening it, which means the added area did not directly slide over the same snow contact points. However, since the study used a pin-on-disc setup there could be an effect of sliding over the same area for each rotation. When the area is increased by lengthening, the added area may benefit from pre-heated contact points, leading to a lesser increase in friction. This might explain why Bäurle et al. (2006) observed a more significant reduction in friction by altering the apparent contact area than in our study. Additionally, they operated at contact pressures in the range of 10 times higher than our study.

At cold temperatures, the ski with the highest average contact pressure of 35 kPa exhibited the best performance, suggesting that even higher pressures might further reduce friction. The apparent contact area of the shortest sliders on the adjustable ski is approximately 30% shorter than that of a typical cross-country ski subjected to a normal force of 800 N. This indicates that skate cross-country skis could potentially reduce the apparent contact area under similar snow conditions, primarily to minimize the coefficient of friction. However, it's essential to acknowledge that there are limits to increasing the contact pressure, and this adjustment must take into account the snow's hardness. If the pressure exceeds the resistance against deformation (indicated by the hardness), one expects the friction to increase again. The outcomes of our study may appear to contradict those of Breitschädel (2014), who found that the Norwegian national team generally favored skis with slightly longer contact zones (resulting in a larger apparent contact area) for cold conditions. However, athletes' preferences for skis with longer contact zones do not necessarily imply a lower coefficient of friction. Ski selection also factors in subjective elements such as how the skis feel, with stability being a key criterion when selecting skating skis. Furthermore, the wide range of snow conditions encountered in the field may offer an alternative explanation for athletes' preferences.

#### 5.3.1.2 Load split

The results from the load split also show the benefit of a higher contact pressure, as explained above. Moving most of the load (80% or more) onto one of the two sliders results in lower friction. In addition, there was a decreasing trend by moving the load from 20% to 100% over

the front slider. The advantage of shifting the load forward from the center as opposed to backward could be explained by the hypothesis of Moldestad (1999). He proposed that at cold temperatures or low snow humidity, it might be advantageous to apply increased pressure at the initiation of the contact area in the front zone. This approach aims to shorten the length of "dry friction" by inducing lubrication earlier along the slider. Consequently, the remaining section of the ski (rear zone) would then encounter pre-heated contact points with a thicker liquid-like layer, and thus lower friction, as illustrated in Figure 5.6. In contrast, by having more of the load split onto the rear slider more of the frictional heat would be produced in this zone. Creating better lubrication at the rear of the ski, will thus not benefit the front ski.

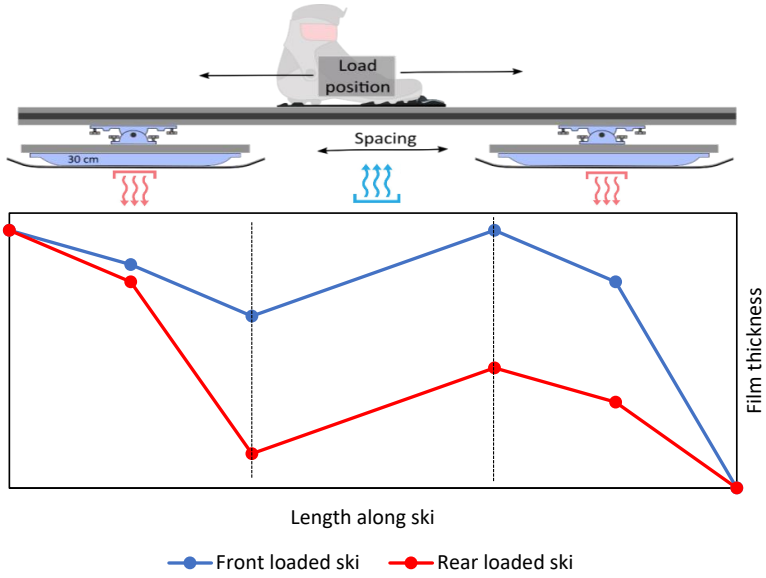


Figure 5.6 Illustration of lubrication film development on a snow asperity as a ski slides over it. Initially, frictional heating occurs at the front slider, followed by a cooling phase in the gap between the sliders, and subsequent heating at the rear slider. The blue line represents a ski that has a load split towards the front and the red a ski that has a load split towards the rear.

The load split results at cold temperatures in Study III differ from the findings observed in Study II, which employed a cross-country ski. In Study II, a gradual reduction in the coefficient of friction was observed as the load split shifted from 40% to 18% (with the load application point moving toward the rear of the ski). However, it's important to highlight that this adjustment in load application point on a cross-country ski also had an impact on the

apparent contact area, introducing some uncertainty regarding the specific influence of load split on friction in the previous study.

Interestingly, the result from Study III suggests that the typical placement of the binding or load application point on cross-country skis, resulting in a load split of around 30%, may not be optimal for minimizing friction when considering load split in cold conditions.

### 5.3.2 Intermediate temperatures

At a temperature of -2 °C, our measurements indicated the lowest friction levels, likely because the snow grains already possess a thicker liquid-like layer (Kietzig et al., 2010). Given this understanding, one might expect that the influence of variations in the normal load or the apparent contact area would show less impact on the coefficient of friction, compared to cold conditions. This was true for the test of normal load, where we observed that the coefficient of friction remained consistent despite variations in the normal load. However, the apparent contact area had a surprisingly significant effect on the friction coefficient in these conditions. Figure 4.11 showed that at -2 °C the friction was higher at the larger apparent contact areas.

Comparing the results to the study of Bäurle et al. (2006), conducted at -5 °C, it was also observed that the friction coefficient was influenced by the size of the apparent contact area, especially for smaller areas under high contact pressure. They noted that as the contact area increased, its impact on the friction coefficient diminished and ultimately became negligible, particularly when the contact pressure dropped to 100 kPa or less. This leads us to anticipate that, in our study, the apparent contact area would exert a relatively minor effect on friction at pressures below this value. The mechanism behind the apparent contact area dependency under these intermediate conditions remains unclear. It's possible that the snow surface became so smooth that an increase in the apparent contact area actually led to an increase in the real contact area, which is a situation that typically does not occur at a constant load.

Our findings at intermediate temperatures also demonstrated that moving the load toward the rear slider resulted in reduced friction. In these milder conditions, the liquid-like layer is believed to be closer to an optimal thickness for friction reduction. Thus, transferring additional load to the front slider increases frictional work in this area, possibly leading to an even thicker liquid film. This, in turn, could increase the friction for the rest of the slider, a situation that inversely mirrors the behavior noted in colder temperatures.

All in all, our results suggest that a ski operating at intermediate temperatures should feature a reduced apparent contact area, have its load application point shifted towards the rear, and incorporate a short spacing to achieve optimal gliding performance.

### 5.3.3 Warm temperatures

At melting snow conditions ($T_{air}$ = +5 °C), our measurements revealed a significant relationship between the friction coefficient and the apparent contact area, likely attributable to viscous friction from excess water on the snow surface. When excess water is present, we assume that the ski base structure is filled with water, and the relative real contact area is close to 100%. In this situation, the friction force is largely dependent on viscous shear, and the extent of the apparent contact area between the surfaces plays a pivotal role in determining the friction coefficient.

The decrease in the coefficient of friction for the load increase from 300 N to 600 N in Figure 4.11, can be explained by constant friction force due to a relative real contact area close to 100%. Beyond 600 N the coefficient of friction started to increase again, possibly due to water being squeezed out from between contacts at higher pressures (Bäurle, 2006). The squeeze-out will reduce the film thickness between the ice asperities and the ski base leading to a higher viscous shear force. The removal of water with low viscosity might also increase the viscosity of the remaining lubrication layer, due to the higher viscosity of the liquid-like layer (Dash et al., 2006).

Snow conditions similar to the ones tested at warm temperatures in the lab can be encountered in ski racing when there are significant temperature fluctuations, such as transitioning from sub-zero temperatures at night to above-freezing temperatures and the onset of radiation from the sun in the morning (Wagner & Horel, 2011). Under such conditions, the surface snow may contain free water due to the onset of melting, while the underlying bulk snow remains cold and retains its structural strength. However, over time with warm temperatures, the bulk snow will start to soften, and the bearing strength of the surface will reduce. Higher average contact pressures might then lead to more plowing and different frictional trends would be observed.

### 5.3.4 Spacing

The distance between the ski's contact zones affects the time gap between the front and rear sliders contacting the snow surface. Our measurements, taken at three different temperatures, indicated an increase in friction with longer spacing. One potential explanation is that the snow has more time to cool down between the passage of the front slider and the subsequent passage

of the rear slider over the same snow asperities. After the front slider makes contact, certain points on the snow heat up, and there is a brief period for these spots to cool down before the rear slider passes over them. However, the time difference between the sliders only varies from 0.04 s to 0.2 s, corresponding to spacing from 20 cm to 100 cm (at a speed of 5 m/s). Whether this short variance in cooling time could result in an overall 5% increase in total friction is questionable.

Hasler et al. (2021) measured a rapid exponential decrease in snow temperature from -1.5 °C to -3.4 °C within the first four seconds after a ski pass. Although this duration is considerably longer than the interval between the sliders in this study, it's plausible that a cooling duration might affect friction to some degree. However, the almost identical friction trends observed in both cold and intermediate conditions challenge this cooling hypothesis. If the cooling effect was a dominant factor, we would expect to see a more marked increase in friction in colder conditions, which was not the case in our findings.

Another potential explanation involves the energy dissipation resulting from the compression work on the snow matrix. Snow displays a delayed elastic response, indicating that compressed snow requires time to restore its initial shape (Theile et al., 2009). Therefore, the duration between the front and rear slider could impact the extent of snow recovery. A longer duration allows for more recovery of the snow, implying that the rear slider has to do a larger compression work. For example, if the snow fully recovers, the rear slider would have to perform the same amount of compression work as the front slider.

In research conducted by Theile et al. (2009), the delayed elastic recovery of snow after repeated loading was quantified as 20 µm, observed under a contact pressure of up to 150 kPa on very hard snow with Young's modulus of 1200 MPa. Complete recovery of the snow was noted after one minute. The energy lost in the hysteresis loop due to repeated loading and unloading of the snow was $860 \times 10^{-6}$ J, corresponding to the energy lost to compaction of around $10^3$ mm$^2$ of snow. By comparing the energy loss in the delayed elastic response of the snow in their study to the total frictional energy of the ski in our study, we can estimate how much energy is used for compaction. The sliding ski with a width of 45 mm and a speed of 5 m/s will compact $2.3 \times 10^5$ mm$^2$/s of snow. The calculated energy lost to compaction for the ski would then be around 0.2 J/s. In contrast, the theoretical total energy dissipation of a ski ($P_{friction} = \mu v F_N$) sliding at 5 m/s, with a friction coefficient (µ) of 0.06 and a normal force ($F_N$) of 400

N, would be 120 J/s. Thus, the energy lost to snow compaction constituted only about 0.15% of the total energy dissipation.

Given this minimal energy loss to compaction and the short recovery time of 0.2 seconds between the sliders in our study, it appears improbable that the delayed elastic recovery of the snow significantly contributes to the variations in friction coefficient observed in relation to spacing. However, it's worth noting that Theile et al. (2009) conducted their study on snow with Young's modulus ten times higher than that found in the compression test of artificial snow by Lintzen and Edeskär (2014). This disparity suggests that the compression work in the study of Theile et al. (2009) might be less than what was the case in our study or actual field conditions.

## 5.4 Implications

The developed tribometer for testing skis has the potential to significantly enhance precision and efficiency in product testing, while also offering a reasonable degree of accuracy. This can contribute, for example, to the further development of new fluorine-free products for the skiing industry. Currently, conducting comprehensive tests of skis and products can be time-consuming and resource intensive. From a practical standpoint, implementing the proposed ski testing methodology could lead to a substantial reduction in testing efforts within the industry. By enhancing precision and gaining a deeper understanding of how various factors influence friction, manufacturers can streamline their testing processes, ultimately saving time and resources while still producing high-quality products.

The contact zones of a ski should be characterized with the help of pressure profiles to accurately assess key parameters linked to friction mechanisms, such as the average contact pressure, peak contact pressure, the slope of the pressure increase, load split between front and rear, etc. A deeper understanding of the snow's dynamic response could help bridge the knowledge gap between static contact zone measurements and the pressure profiles observed from a gliding ski. By quantifying how pressure is distributed across contact zones and its correlation to friction, engineers can make informed decisions about ski design modifications to optimize for reduced friction. Adopting a more scientific approach to choosing skis, based on an understanding of the pressure profiles, skiers can achieve a more personalized and optimized skiing experience.

The current ski design, which incorporates a degree of self-regulating contact pressure, offers advantages in terms of performance across a wide range of snow conditions. Given the significant variations in snow conditions, the ability to tune the ski to match these conditions is crucial. However, the tuning possibilities are constrained by an interconnected response of the macroscopic contact parameters. While the current ski design performs well in various conditions, there is potential for further friction reduction by making more extensive adjustments to the macroscopic ski contact parameters than currently feasible. For the specific conditions tested in Paper III, the following recommendations are summarized in Table 5.1.

In cold temperatures, increasing the average contact pressure emerges as a crucial design objective. Since the normal load exerted by athletes in a gliding position is constant, the only way to enhance pressure is by reducing the apparent contact area. Additionally, it's beneficial to distribute a greater portion of the load toward the ski's front zone. For intermediate temperatures, our results indicate that friction can be reduced by decreasing the apparent contact area, shifting more load towards the rear, and reducing the spacing between contact zones. In warmer conditions, the data suggest that the most impactful parameter is minimizing the apparent contact area, along with maintaining a balanced load split of 50/50%.

Table 5.1 Recommendations for macroscopic ski parameter at three different snow temperatures (Auganæs et al., 2024).

| | Parameter recommendations at each temperature (H = high, M = medium, L = low) | | |
|---|---|---|---|
| Parameter | Cold | Intermediate | Warm |
| Normal force (300-800 N)* | H | M | M |
| Contact area (180-360 $cm^2$) | L | L | L |
| Avg. pressure (10-35 kPa) | H | M | M/H |
| Load split (5-95%) | H | L | L |
| Spacing (20-100 cm) | L | L | L |

*This parameter is not possible to alter in the design process for skis, which is why we also report apparent contact area and average contact pressure. However, this value is of interest when comparing gliding performance between skiers of different weight classes.

While it might not be possible to combine all the recommendations of parameters to the current design of a cross-country ski, it can give a ski designer some pointers on what to focus on.

Another implication from this is the potential of a new ski design that allows for individual tuning of parameters. Envision a ski where the length of each contact zone, bending stiffness of connection material, pressure distribution in each contact zone, and surface roughness can all be individually tailored. Such customization would allow for significant improvements through more specific adjustments tailored to the prevailing snow conditions.

# 6 Conclusion and further work

## 6.1 Conclusions

- The developed ski-snow tribometer allows for year-round testing of cross-country skis on both new and aged snow at high speeds (up to 10 m/s). The accuracy of the measurement system has been determined and the precision within a single track, between tracks, and between different testbeds have been documented. Adequate precision was obtained with repeated measurements within one snow track, which allows for distinguishing between skis or glide products of very similar performance ($\Delta\mu \leq 0.001$).

- The snow surface changed with repeated ski runs, becoming less rough and more rounded features as the number of runs increased. The measured coefficient of friction gradually decreased through a series of 200 runs. The change from run to run was largest at the start and gradually decreased as the friction level stabilized after around 160 runs. One should note that the polishing curve is a system response dependent on the absolute level of the friction coefficient.

- A test method has been developed to compensate for the effect of the changing snow surface between different skis. This involved testing the skis sequentially and using the linear trend line of the skis for a leveling correction. These approaches were shown to reduce the polishing effect on the averages and the standard deviations between the skis.

- The normal load affected the apparent contact area and average contact pressure in the contact zones of the cross-country ski. A doubling of the normal load led to an approximately 50% increase in the area, meaning that the average contact pressure also increased. Another aspect that changed was the split of load between the front and rear zones, and the spacing between them. The effect of normal load on the coefficient of friction on a cross-country ski was small. Of the three temperatures tested only a distinct

difference was seen at warm air temperatures of +5 °C, where the friction decreased for higher normal loads.

- The load application point naturally controls the split of load between the front and rear zones. Moving the load application point backward from the middle reduced the overall contact area due to less compression of the ski. Mainly the front zone got smaller and was moved toward the tip of the ski. The effect of load application point on the coefficient of friction showed significant differences both at cold and warm temperatures, while no significant changes were seen at intermediate temperatures. At cold temperatures, there was a steady decrease in friction when moving the LAP towards the rear. At warm temperatures, the friction coefficient had a maximum point for a LAP around 7-12 cm behind the midpoint and decreased for binding positions in front or rear of this.

- At cold temperatures, the average contact pressure correlated well with a decrease in the coefficient of friction. Altering the pressure through normal load or the apparent contact area produced almost the same effect on the friction coefficient. Under warmer and intermediate snow conditions, it was consistently observed that the apparent contact area was the most critical factor influencing the coefficient of friction.

- The load split between the front and rear contact zones showed distinct frictional trends depending on the temperature. At cold temperatures, it was beneficial to move more of the load towards the front slider, to induce a lubrication layer earlier along the slider. At intermediate temperatures, the opposite behavior was seen. At warm temperatures, there was a distinct minimum for having the load split 50/50. The effect of spacing between the contact zones showed a tendency for a reduction in friction for shorter spacing, for the three tested snow temperatures.

## 6.2 Further work

Further work should address the understanding of the delayed elastic response on snow tracks “relevant” for cross-country skiing. This could potentially highlight differences between the contact zones measured under static loading and those under the dynamic conditions of a sliding ski. Additionally, there's an opportunity to develop a standardized approach for measuring snow hardness and/or compression in the field, that more accurately simulates the dynamic pressure application of a ski. Traditional methods, like drop tests, assess snow hardness through sudden impacts, which do not fully represent the gradual pressure changes and distribution patterns experienced during actual skiing.

Based on the findings related to the potential friction reduction of different parameters presented in the third paper, it would be interesting to develop a ski where the apparent contact area is not load-dependent. This would allow for a greater degree of freedom in tuning individual parameters to suit prevailing snow conditions. From a practical performance perspective, examining the friction on edging skis warrants attention. During the skating phase of cross-country skiing, a significant portion of the glide phase occurs on the edge, a phenomenon that, to my knowledge, has not yet been investigated. With the developed tribometer, achieving this would require a relatively simple modification.

Exploring the Design of Experiments within the product development process presents an interesting opportunity, particularly to determine if the developed testing method is sufficiently reliable for identifying trends and relationships across different input variables and friction. Furthermore, investigating the effect of adjusting the ski base roughness along the ski to potentially match it with the pressure distribution presents an intriguing line of inquiry for future research.

# Bibliography


Ainegren, M., Carlsson, P., & Tinnsten, M. (2008). Rolling resistance for treadmill roller skiing. *Sports Engineering*, *11*(1), 23. https://doi.org/10.1007/s12283-008-0004-1

Almqvist, A., Pellegrini, B., Lintzen, N., Emami, N., Holmberg, H.-C., & Larsson, R. (2022). A Scientific Perspective on Reducing Ski-Snow Friction to Improve Performance in Olympic Cross-Country Skiing, the Biathlon and Nordic Combined. *Frontiers in Sports and Active Living*, *4*, 844883. https://doi.org/10.3389/fspor.2022.844883

Ambach, W., & Mayr, B. (1981). Ski gliding and water film. *Cold Regions Science and Technology*, *5*, 59-65.

Auganæs, S. B., Buene, A. F., & Klein-Paste, A. (2022). Laboratory testing of cross-country skis – Investigating tribometer precision on laboratory-grown dendritic snow. *Tribology International*, *168*, 107451. https://doi.org/10.1016/j.triboint.2022.107451

Auganæs, S. B., Buene, A. F., & Klein-Paste, A. (2023). The effect of load and binding position on the friction of cross-country skis. *Cold Regions Science and Technology*, *212*, 103884. https://doi.org/10.1016/j.coldregions.2023.103884

Auganæs, S. B., Buene, A. F., & Klein-Paste, A. (2024). Experimental investigation into the effect of macroscopic cross-country ski parameters on gliding friction. *Cold Regions Science and Technology*, *225*, 104264. https://doi.org/https://doi.org/10.1016/j.coldregions.2024.104264

Bowden, F. P. (1953). Friction on Snow and Ice. *Proceedings of the Royal Society of London Series a-Mathematical and Physical Sciences*, *217*(1131), 462-478. https://doi.org/DOI 10.1098/rspa.1953.0074

Bowden, F. P., & Hughes, T. P. (1939). The mechanism of sliding on ice and snow. *Proceedings of the Royal Society of London Series a-Mathematical and Physical Sciences*, *Volume 172*(949).

Breitschädel, F. (2012). Variation of Nordic Classic Ski Characteristics from Norwegian national team athletes. *Procedia Engineering*, *34*, 391-396. https://doi.org/https://doi.org/10.1016/j.proeng.2012.04.067

Breitschädel, F. (2014). *Technical aspects to improve performance in crosscountry skiing* [Doctoral dissertation, Norwegian university of science and technology.

Breitschädel, F., Berre, V., Andersen, R., & Stjernström, E. (2012). A comparison between timed and IMU captured Nordic ski glide tests. *Procedia Engineering*, *34*, 397-402. https://doi.org/10.1016/j.proeng.2012.04.068

Breitschädel, F., Haaland, N., & Espallargas, N. (2014). A Tribological Study of UHMWPE Ski Base Treated with Nano Ski Wax and its Effects and Benefits on Performance. *Procedia Engineering*, *72*, 267-272. https://doi.org/https://doi.org/10.1016/j.proeng.2014.06.048

Breitschädel, F., Klein-Paste, A., & Løset, S. (2010). Effects of Temperature Change on Cross-Country Ski Characteristics. *Procedia Engineering*, *2*, 2913-2918. https://doi.org/10.1016/j.proeng.2010.04.087

Budde, R., & Himes, A. (2017). High-resolution friction measurements of cross-country ski bases on snow. *Sports Engineering*, *20*(4), 299-311. https://doi.org/10.1007/s12283-017-0230-5

Buene, A. F., Auganæs, S. B., & Klein-Paste, A. (2022). Effect of Polydimethylsiloxane Oil Lubrication on the Friction of Cross-Country UHMWPE Ski Bases on Snow. *Frontiers in Sports and Active Living*, *4*. https://doi.org/10.3389/fspor.2022.894250

Buhl, D., Fauve, M., & Rhyner, H. (2001). The kinetic friction of polyethylen on snow: The influence of the snow temperature and the load. *Cold Regions Science and Technology*, *33*, 133-140. https://doi.org/10.1016/S0165-232X(01)00034-9

Bäckström, M., Dahlen, L., Tinnsten, M., & Estivalet, M. (2009). Essential Ski Characteristics for Cross-Country Skis Performance (P251). In *The Engineering of Sport 7* (pp. 543-549). https://doi.org/10.1007/978-2-287-09413-2_66

Bäurle, L. (2006). *Sliding friction of polyethylene on snow and ice* [Doctoral dissertation, Swiss Federal Institute of Technology Zurich]. 10.3929/ethz-a-005210667

Bäurle, L., Kaempfer, T. U., Szabó, D., & Spencer, N. D. (2007). Sliding friction of polyethylene on snow and ice: Contact area and modeling. *Cold Regions Science and Technology*, *47*(3), 276-289. https://doi.org/10.1016/j.coldregions.2006.10.005

Bäurle, L., Szabó, D., Fauve, M., Rhyner, H., & Spencer, N. D. (2006). Sliding friction of polyethylene on ice: tribometer measurements. *Tribology Letters*, *24*(1), 77-84. https://doi.org/10.1007/s11249-006-9147-z

Böttcher, R., Seidelmann, M., & Scherge, M. (2017). Sliding of UHMWPE on ice: Experiment vs. modeling. *Cold Regions Science and Technology*, *141*, 171-180. https://doi.org/10.1016/j.coldregions.2017.06.010

Colbeck, S. C. (1988). The Kinetic Friction of Snow. *Journal of Glaciology*, *34*(116), 78-86. https://doi.org/10.3189/S0022143000009096

Colbeck, S. C. (1992). A Review of the Processes That Control Snow Friction.

Colbeck, S. C. (1993). Bibliography on snow and ice friction.

Colbeck, S. C. (1994). Bottom temperatures of skating skis on snow. *Medicine and science in sports and exercise*, *26*(2), 258-262. https://doi.org/10.1249/00005768-199402000-00019

Colbeck, S. C. (1997). Capillary bonding of wet surfaces-the effects of contact angle and surface roughness. *Journal of Adhesion Science and Technology*, *11*(3), 359-371.

Colbeck, S. C., & Warren, G. (1991). The thermal response of downhill skis. *Journal of Glaciology*, *37*(126), 228-235.

Dash, J. G., Rempel, A. W., & Wettlaufer, J. S. (2006). The physics of premelted ice and its geophysical consequences. *Reviews of Modern Physics*, *78*(3), 695-741. https://doi.org/10.1103/RevModPhys.78.695

Federolf, P., Auer, M., Fauve, M., Lüthi, A., & Rhyner, H. (2006, 2006//). Subjective Evaluation of the Performance of Alpine Skis and Correlations with Mechanical Ski Properties. The Engineering of Sport 6, New York, NY.

Federolf, P., Scheiber, P., Rauscher, E., Schwameder, H., Lüthi, A., Rhyner, H.-U., & Müller, E. (2008). Impact of skier actions on the gliding times in alpine skiing. *Scandinavian Journal of Medicine & Science in Sports*, *18*(6), 790-797. https://doi.org/https://doi.org/10.1111/j.1600-0838.2007.00745.x

Fierz, C., R.L, A., Y, D., P, E., Greene, E., McClung, D., Nishimura, K., Satyawali, P., & Sokratov, S. (2009). *The international classification for seasonal snow on the ground (UNESCO, IHP (International Hydrological Programme)–VII, Technical Documents in Hydrology, No 83; IACS (International Association of Cryospheric Sciences) contribution No 1)*.

Giesbrecht, J. L., Smith, P., & Tervoort, T. A. (2010). Polymers on snow: Toward skiing faster. *Journal of Polymer Science Part B: Polymer Physics*, *48*(13), 1543-1551. https://doi.org/10.1002/polb.22033

Giudici, H., Fenre, M., Klein-Paste, A., & Rekila, K.-P. (2017). A Technical Description of LARS and Lumi: Two Apparatus for Studying Tire-Pavement Interactions. *Route/Road Magazine*.

Glenne, B. (1987). Sliding friction and boundary lubrication of snow. *Journal of Tribology*, *109*(4), 614-617. https://doi.org/10.1115/1.3261520

Hasler, M., Jud, W., & Nachbauer, W. (2021). Snow Temperature Behind Sliding Skis as an Indicator for Frictional Meltwater. *Frontiers in Mechanical Engineering*, *7*, 738266. https://doi.org/10.3389/fmech.2021.738266

Hasler, M., Mössner, M., Jud, W., Schindelwig, K., Gufler, M., van Putten, J., Rohm, S., & Nachbauer, W. (2022). Wear of snow due to sliding friction. *Wear*, *510*, 204499. https://doi.org/10.1016/j.wear.2022.204499

Hasler, M., Schindelwig, K., Mayr, B., Knoflach, C., Rohm, S., van Putten, J., & Nachbauer, W. (2016). A Novel Ski–Snow Tribometer and its Precision. *Tribology Letters*, *63*(3). https://doi.org/10.1007/s11249-016-0719-2

International ski federation. (2021). *The international ski competition rules (ICR)*. https://assets.fis-ski.com/image/upload/v1624284540/fis-prod/assets/ICR_CrossCountry_2022_clean.pdf

Jakobsen, L., Auganaes, S. B., Buene, A. F., Sivebaek, I. M., & Klein-Paste, A. (2023). Dynamic and static friction measurements of elastomer footwear blocks on ice surface. *Tribology International*, *178*, 108064. https://doi.org/https://doi.org/10.1016/j.triboint.2022.108064

Johnson, J., & Schneebeli, M. (1999). Characterizing the microstructural and micromechanical properties of snow. *Cold Regions Science and Technology*, *30*, 91-100. https://doi.org/10.1016/S0165-232X(99)00013-0

Kalliorinne, K., Hindér, G., Sandberg, J., Larsson, R., Holmberg, H.-C., & Almqvist, A. (2023a). Characterisation of the Contact between Cross-Country Skis and Snow: On the Multi-Scale Interaction between Ski Geometry and Ski-Base Texture. *Lubricants*, *11*, 427. https://doi.org/10.3390/lubricants11100427

Kalliorinne, K., Hindér, G., Sandberg, J., Larsson, R., Holmberg, H.-C., & Almqvist, A. (2023b). The impact of cross-country skiers' tucking position on ski-camber profile, apparent contact area and load partitioning. *Proceedings of the Institution of Mechanical Engineers, Part P: Journal of Sports Engineering and Technology*, 17543371221141748. https://doi.org/10.1177/17543371221141748

Kalliorinne, K., Sandberg, J., Hindér, G., Larsson, R., Holmberg, H.-C., & Almqvist, A. (2022). Characterisation of the Contact between Cross-Country Skis and Snow: A Macro-Scale Investigation of the Apparent Contact. *Lubricants*, *10*, 279. https://doi.org/10.3390/lubricants10110279

Karlöf, L., Smevold, T., Tretterud, O. B., & Zupan, M. (2007). *Swix test protocol for testing of glide products*. https://swixracing.us/nordic/pdf/swix-test-protocol-for-testing-of-glide-products.pdf

Kietzig, A.-M., Hatzikiriakos, S. G., & Englezos, P. (2010). Physics of ice friction. *Journal of Applied Physics*, *107*(8). https://doi.org/10.1063/1.3340792

Kuroiwa, D. (1977). The Kinetic Friction on Snow and Ice. *Journal of Glaciology*, *19*(81), 141-152. https://doi.org/10.3189/S0022143000029233

Kuzmin, L. (2010). *Interfacial kinetic ski friction* [Doctoral dissertation, Mid Sweden University].

Kuzmin, L., & Fuss, F. (2013). Cross country ski technology. In *Routledge Handbook of Sports Technology and Engineering* (pp. 171-188). Routledge.

Lemmettylä, T., Heikkinen, T., Ohtonen, O., Lindinger, S., & Linnamo, V. (2021). The Development and Precision of a Custom-Made Skitester [Original Research]. *Frontiers in Mechanical Engineering*, *7*(36). https://doi.org/10.3389/fmech.2021.661947

Lever, J. H., Asenath-Smith, E., Taylor, S., & Lines, A. P. (2021). Assessing the Mechanisms Thought to Govern Ice and Snow Friction and Their Interplay With Substrate Brittle Behavior. *Frontiers in Mechanical Engineering*, *7*. https://doi.org/10.3389/fmech.2021.690425

Lever, J. H., Taylor, S., Hoch, G. R., & Daghlian, C. (2019). Evidence that abrasion can govern snow kinetic friction. *Journal of Glaciology*, *65*(249), 68-84. https://doi.org/10.1017/jog.2018.97

Lever, J. H., Taylor, S., Song, A. J., Courville, Z. R., Lieblappen, R., & Weale, J. C. (2018). The mechanics of snow friction as revealed by micro-scale interface observations. *Journal of Glaciology*, *64*(243), 27-36. https://doi.org/10.1017/jog.2017.76

Lintzén, N. (2013). *Mechanical properties of artificial snow* [Doctoral dissertation, Luleå tekniska universitet].

Lintzen, N., & Edeskär, T. (2014). Uniaxial Strength and Deformation Properties of Machine-Made Snow. *Journal of Cold Regions Engineering*, *29*, 04014020. https://doi.org/10.1061/(ASCE)CR.1943-5495.0000090

Luchsinger, H., Kocbach, J., Ettema, G., & Sandbakk, O. (2017). Comparison of the Effects of Performance Level and Sex on Sprint Performance in the Biathlon World Cup. *International journal of sports physiology and performance*, *13*, 1-24. https://doi.org/10.1123/ijspp.2017-0112

Lutz, J., Gebhard, A., Zipp, F., & Schuster, J. (2023). Investigation of the impact of the fluorine-content of ski wax on the friction between ice and ski base using a novel tribometer. *Tribology International*, *187*, 108705. https://doi.org/https://doi.org/10.1016/j.triboint.2023.108705

Moldestad, D. A. (1999). *Some aspects of ski base sliding friction and ski base structure* [Doctoral dissertation, Norwegian university of science and technology].

Moxnes, J. F., Sandbakk, O., & Hausken, K. (2014). Using the power balance model to simulate cross-country skiing on varying terrain. *Open Access Journal of Sports Medicine*, *5*, 89-98. https://doi.org/10.2147/OAJSM.S53503

Mössner, M., Hasler, M., & Nachbauer, W. (2021). Calculation of the contact area between snow grains and ski base. *Tribology International*, *163*, 107183. https://doi.org/10.1016/j.triboint.2021.107183

Mössner, M., Innerhofer, G., Schindelwig, K., Kaps, P., Schretter, H., & Nachbauer, W. (2013). Measurement of mechanical properties of snow for simulation of skiing. *Journal of Glaciology*, *59*(218), 1170-1178. https://doi.org/10.3189/2013JoG13J031

Mössner, M., Schindelwig, K., Heinrich, D., Hasler, M., & Nachbauer, W. (2023). Effect of load, ski and snow properties on apparent contact area and pressure distribution in straight gliding. *Cold Regions Science and Technology*, *208*, 103799. https://doi.org/10.1016/j.coldregions.2023.103799

Nachbauer, W., Kaps, P., Hasler, M., & Mössner, M. (2016). Friction Between Ski and Snow. In F. Braghin, F. Cheli, S. Maldifassi, S. Melzi, & E. Sabbioni (Eds.), *The Engineering Approach to Winter Sports* (pp. 17-32). Springer New York. https://doi.org/10.1007/978-1-4939-3020-3_2

Nilsson, J., Karlöf, L., & Jakobsen, V. (2013). A new device for measuring ski running surface force and pressure profiles. *Sports Engineering*, *16*(1), 55-59. https://doi.org/10.1007/s12283-012-0109-4

Oksanen, P., & Keinonen, J. (1982). The mechanism of friction of ice. *Wear*, *78*(3), 315-324. https://doi.org/10.1016/0043-1648(82)90242-3

Pellegrini, B., Stöggl, T. L., & Holmberg, H.-C. (2018). Developments in the Biomechanics and Equipment of Olympic Cross-Country Skiers. *Frontiers in physiology*, *9*, 976-976. https://doi.org/10.3389/fphys.2018.00976

Petrenko, V. F., & Whitworth, R. W. (1999). *Physics of ice*. OUP Oxford.

Reynolds, O. (1901). *Papers on Mechanical and Physical Subjects: 1881-1900* (Vol. 2). The University Press.

Rogowski, I., Leonard, D., Gauvrit, J.-Y., & Lanteri, P. (2007). Influence of fluorine-based additive content on the physical and physicochemical properties of ski gliding wax. *Cold Regions Science and Technology*, *49*(2), 145-150.

Rohm, S., Knoflach, C., Nachbauer, W., Hasler, M., Kaserer, L., van Putten, J., Unterberger, S. H., & Lackner, R. (2016). Effect of Different Bearing Ratios on the Friction between Ultrahigh Molecular Weight Polyethylene Ski Bases and Snow. *ACS Applied Materials & Interfaces*, *8*(19), 12552-12557. https://doi.org/10.1021/acsami.6b02651

Rohm, S., Unterberger, S. H., Hasler, M., Gufler, M., van Putten, J., Lackner, R., & Nachbauer, W. (2017). Wear of ski waxes: Effect of temperature, molecule chain length and position on the ski base. *Wear*, *384-385*, 43-49. https://doi.org/https://doi.org/10.1016/j.wear.2017.05.004

Sandbakk, Ø., Solli, G. S., Talsnes, R. K., & Holmberg, H.-C. (2021). Preparing for the Nordic Skiing Events at the Beijing Olympics in 2022: Evidence-Based Recommendations and Unanswered Questions. *Journal of Science in Sport and Exercise*, *3*(3), 257-269. https://doi.org/10.1007/s42978-021-00113-5

Sandberg, J., Kalliorinne, K., Hindér, G., Holmberg, H.-C., Almqvist, A., & Larsson, R. (2023). A novel free-gliding ski tribometer for quantification of ski-snow friction with high precision. *Tribology Letters*. https://doi.org/https://doi.org/10.1007/s11249-023-01781-w

Schindelwig, K., Hasler, M., van Putten, J., Rohm, S., & Nachbauer, W. (2014). Temperature Below a Gliding Cross Country Ski. *Procedia Engineering*, *72*, 380-385. https://doi.org/10.1016/j.proeng.2014.06.065

Schindelwig, K., Mössner, M., Hasler, M., & Nachbauer, W. (2017). Determination of the rolling resistance of roller skis. *Proceedings of the Institution of Mechanical Engineers, Part P: Journal of Sports Engineering and Technology*, *231*(1), 50-56. https://doi.org/10.1177/1754337116628719

Shapiro, L., Johnson, J., Sturm, M., & Blaisdell, G. (1997). Snow Mechanics: Review of the State of Knowledge and Applications. *Cold Regions Research and Engineering Laboratory (U.S.)*, 40.

Stachowiak, W. G., & Batchelor, W. A. (2006). Engineering Tribology 1 - 9. https://doi.org/https://doi.org/10.1016/B978-075067836-0/50002-X

Szabo, D., & Schneebeli, M. (2007). Subsecond sintering of ice. *Applied Physics Letters*, *90*, 151916-151916. https://doi.org/10.1063/1.2721391

Takeda, M., Nikki, K., Nishizuka, T., & Abe, O. (2010). Friction of the short model ski at low velocity. *Journal of Physics: Conference Series, 258*. https://doi.org/10.1088/1742-6596/258/1/012007

Theile, T., Szabo, D., Luthi, A., Rhyner, H., & Schneebeli, M. (2009). Mechanics of the Ski–Snow Contact. *Tribology Letters, 36*(3), 223-231. https://doi.org/10.1007/s11249-009-9476-9

Wagner, W., & Horel, J. (2011). Observations and simulations of snow surface temperature on cross-country ski racing courses. *Cold Regions Science and Technology, 66*(1), 1-11. https://doi.org/https://doi.org/10.1016/j.coldregions.2010.12.003

Wolfsberger, F., Rhyner, H., & Schneebeli, M. (2019). *Slope preparation and grooming. A handbook for practitioners*. Davos, WSL Institute for Snow and Avalanche Research SLF.

Wolfsperger, F., Meyer, F., & Gilgien, M. (2021). The Snow-Friction of Freestyle Skis and Snowboards Predicted From Snow Physical Quantities. *Frontiers in Mechanical Engineering, 7*. https://doi.org/10.3389/fmech.2021.728722

# Paper I

Tribology International 168 (2022) 107451

Contents lists available at ScienceDirect

Tribology International

journal homepage: www.elsevier.com/locate/triboint

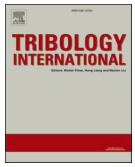

# Laboratory testing of cross-country skis – Investigating tribometer precision on laboratory-grown dendritic snow

Sondre Bergtun Auganæs, Audun Formo Buene *, Alex Klein-Paste

*Department of Civil and Environmental Engineering, Norwegian University of Science and Technology, Høgskoleringen 7a, 7034 Trondheim, Norway*

ARTICLE INFO

*Keywords:*
Ski-snow sliding friction
High-speed measurements
Ski testing
Snow topography

ABSTRACT

Small differences in ski-snow friction results in large time gaps, and glide testing is therefore an important part of racing. To test ski-snow friction without the influence of changing weather, snow conditions and skier position is therefore valuable. In this study, a full-scale ski-snow tribometer was developed and we investigated the degree of precision obtainable for different snow types, speeds, between separate ski tracks and snow surface preparations. The precision within new snow test tracks was 1.45%, and changing between parallel tracks added another 1.03% to the precision. Measurements across several dendritic snow testbeds were associated with a further 2.39% contribution to the precision. On aged snow, better precision was obtained within and between tracks on the same snow surface.

## 1. Introduction

Minimizing ski-snow friction continues to be an active field of research, recently driven by an international ban on fluorine-containing waxes and ski bases [1]. As the industry searches for fluorine-free alternatives, there is a need for good testing facilities that provide representative data for various snow conditions. But the quantification of ski-snow friction in a precise and representative way is still a challenge. Today, manufacturers mostly rely on full-scale field testing when evaluating new skis, waxes, and preparation techniques. Field-tests offer valuable information on friction optimization but are inhibited by factors such as changing environmental conditions (e.g. changes in temperature, wind, solar radiation and snow conditions) and variations in the skier's position. To determine the coefficient of friction from field tests, one needs to separate air drag and gliding resistance. This makes it difficult to obtain high precision values from field measurements [2]. Moxnes et al. [3] showed that a decrease in the coefficient of friction, $\mu$, from 0.037 to 0.030, reduced the finishing time for a skier by 5.9% over a simulated 5 km race. Such differences are of great significance, considering the time difference that separates first to tenth place in a world cup race often is less than 4.5% [4]. Breitschädel et al. [5] estimated that a resolution of $\mu \pm 0.001$ was needed to distinguish between race-prepared skis.

Laboratory studies of friction between snow or ice and sliders of various materials have been investigated by several researchers over the years [6–10]. This has increased our knowledge about the dominating friction mechanisms. The most common laboratory set-up is the "pin on disc", where a disc of snow or ice is rotated, and a pin with the sample material is pressed vertically down on the disc while the friction force is measured. The benefit of these setups is that realistic speeds (several m/s) can be achieved, but the specimen runs repeatedly in the same track causing severe polishing. The sample size of this method is also limited, which makes it difficult to study the complex friction effects on long sliders such as a full-size ski [11]. A third issue is the increasing build-up of meltwater in the snow, and consequently the snow is often replaced by ice, although this is likely to affect the friction mechanisms. Meltwater may also be moved radially outwards due to centrifugal forces [2].

The linear tribometer is another common laboratory set-up for friction measurements. Here, a test sample is pressed against snow or ice and moved linearly for a given distance while the forces are measured. This allows testing on relatively fragile types of snow and limits the issue of polishing. Several researchers have applied linear tribometers at low speeds around 0.1–1 m/s [12–15]. To the authors' knowledge, only two tribometer studies reported in the open literature have used high speeds ($>$ 4 m/s) and full-size skis [16,17]. They used artificial snow, produced by snow canons, which produces snow consisting of mainly rounded grains.

Freshly fallen snow has a more dendritic structure, compared to snow produced by snow canons or older natural snow that has been

* Corresponding author.
*E-mail address:* audun.f.buene@ntnu.no (A.F. Buene).

https://doi.org/10.1016/j.triboint.2022.107451
Received 11 October 2021; Received in revised form 15 December 2021; Accepted 12 January 2022
Available online 15 January 2022

transformed and groomed [18]. When compressed and prepared into a ski track many dendrites fracture, leaving a surface with many small asperities of relatively sharp curvature. Since snow on the ground is inherently unstable, these asperities will smoothen and over time transform into older snow of larger, and more rounded crystals. To test ski friction on dendritic snow is of interest for ski and wax manufacturers because it is important to have high performing products for this type of snow. Scientifically, the friction on dendritic snow is of interest as it challenges our understanding of how quickly the contact points transform due to fracture, melting, abrasion and viscoelastic deformations.

Using naturally fallen dendritic snow for laboratory studies is challenging due to large variations in the microstructure. This leads to uncertainties that are difficult to quantify without large test data sets.

Laboratory-grown dendritic snow provides better control and can produce the same type of snow repeatedly [19,20].

Recently we have modified our existing linear track [20] to accommodate for friction measurements with full-size cross-country skis at speeds up to 8 m/s. In this paper, we describe the development of our linear tribometer and applied it to determine precision on testbeds made with laboratory-grown dendritic snow.

## 2. Method

### 2.1. Description of the tribometer

The main components of the tribometer are illustrated in Fig. 1. The mobile carriage is connected to an electrical servo motor by a belt drive. The track is 8.80 m long, with an effective tribometer stroke length of 6.50 m (due to the ski protruding from the front and back of the carriage). During a run, there will be a phase of acceleration, constant speed, and deceleration. The length of the constant speed phase will vary from 2.50 to 5.50 m depending on the chosen acceleration of the motor. The apparatus has been described in more detail in [20]. The carriage consists of a fork, an air bellow (PM/31022, IMI Norgren, Norway), linear air bearing (Dovetail-Series 150 mm * 300 mm, OAV, USA), two vertical load cells (U9C 1 kN, HBM, Germany), a horizontal load cell (S2M 100 N, HBM, Germany) and a system for data acquisition and transmission (T7-PRO 16-bit, LabJack, USA). Signals from the three load cells are acquired by the microcontroller and transmitted by an ethernet cable to the control room, with an effective resolution of 1000 Hz. The position of the carriage is obtained from the encoder on the servo motor. The function of the linear bearing is to prevent that the horizontal load cell is loaded by vertical forces. The vertical load is applied by pressurizing the air bellow. The vertical force can be adjusted from 50 N to 800 N. The applied load is distributed over the entire length of the binding with the center of mass approximately 12 cm behind the front of the binding. This correlates well with a skier's weight distribution and center of mass over the ski.

The applied force from the air bellow is transmitted via the fork to the two vertical load cells sitting on top of the linear air bearing. The ski is connected to the bottom part of the air bearing that can slide in a "frictionless" manner, and the angle of the bearing is zeroed with an adjustment screw and a digital level (PLR 50 C, Bosch, Germany). The resistance force that occurs when the ski is drawn across the snow surface is measured by a horizontal load cell placed between the housing and the slider of the air bearing.

### 2.2. Calculation of the coefficient of friction and vibrational analysis

A run consists of an acceleration phase, a constant speed phase and a deceleration phase, as illustrated in Fig. 2(a). The acceleration profile of the motor is a sinusoidal ramp (S-ramp), so in the second half of

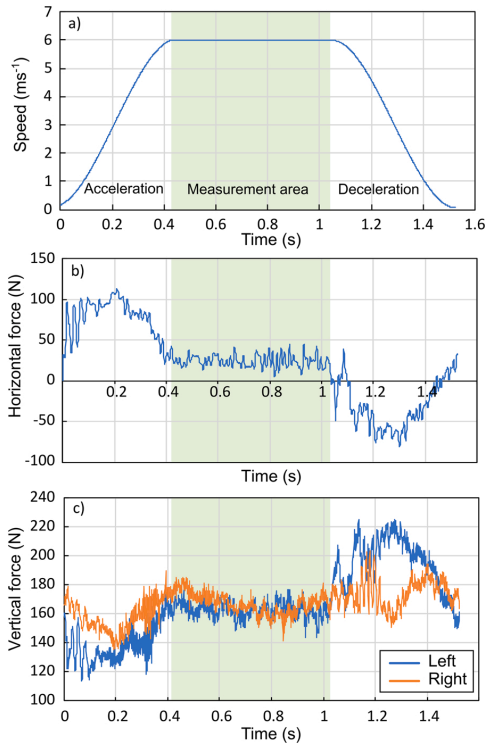


**Fig. 2.** Illustration of the collected data a) Carriage speed, b) horizontal force, c) vertical force. The highlighted area is the measurement area.

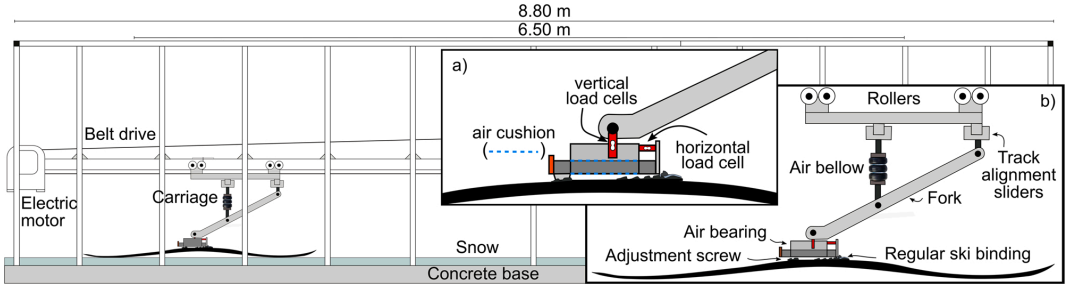


**Fig. 1.** Schematic of the friction track with the carriage optimized for cross-country skis. Insert a) shows the 'frictionless' sliding air bearing and the position of the load cells while insert b) shows the detailed components of the carriage.

acceleration, the motor controller gradually decreases the acceleration until the desired speed is achieved. This reduces the impact of inertia from the transition between the acceleration and measurement phase. As a visible peak in Fig. 2(b), the horizontal force during the acceleration is significant due to the added inertia force of the ski and slider (approximately 3.6 kg). The inertia force during the constant speed phase is assumed to be zero. The air drag of a related setup was measured by Hasler et al. [16] to be 0.075 N at a speed of 5 m/s. Considering an average friction force of 20 N, the air drag would be less than 0.4% of the total force and thus assumed negligible.

The measured horizontal force $F_f$ is assumed to consist of only the ski-snow friction force, while the normal force $F_N$ consist of:

$$F_N = F_{V1} + F_{V2}$$

where $F_{V1}$ and $F_{V2}$ are the forces from the two vertical load cells. These are illustrated in Fig. 2(c).

Calculation of $\mu$ is obtained by taking the arithmetic mean of the horizontal force $\overline{F}_f$ divided by the vertical force $\overline{F}_N$ in the measurement area. As significant vibrations are occurring in the transitions between the three phases of operation (acceleration, measurement and deceleration), 50 data points were removed at the start and end of the measurement area to reduce the impact of these transitions on the data quality.

$$\mu = \overline{F}_f \quad / \overline{F}_N$$

The vibrational analysis was performed in a script written in R, utilizing the spectral package. The function spectrum(x) performs a spectral analysis by a fast Fourier transform of the force data as a function of time and returns the spectral density of the data in hertz. The largest peak is identified, and the frequency of this peak is reported as the major frequency of the force data. The average amplitude is calculated from the root-mean-square (RMS) of the force data adjusted for its mean (i.e. force – mean(force)). The average amplitude is then estimated from RMS $\bullet 2^{1/2}$.

### 2.3. Snow testbed preparation and characterization

Dendritic snow with a density of 50–80 kg/m$^3$ was produced in a snow machine as described by Giudici et al. [20]. It was produced inside a cold room at −20 °C for approximately 24 h before the snow was harvested and moved to the friction lab with a temperature of −3 °C. The specific surface area of freshly harvested snow has been measured earlier to be about 50 m$^2$/kg [21]. The dimensions of the snow testbed were 8.80 m in length, 30 cm in width and 50 mm deep. The lowest 45 mm consisted of transformed snow that was planed to a level base. The top 5 mm consisted of freshly produced dendritic snow that was compressed to a density of 300 kg/m$^3$. To reach this density the fresh snow was first distributed evenly inside a frame (dimensions 30 × 30 × 2 cm) which was moved along until a 2 cm layer of fluffy new snow covered the hard snow base. Manual compaction of this layer with a plate and subsequent sintering concluded the snow bed preparation procedure. Sintering of the track was performed at −3 °C for 16 h while covered by 50 mm thick XPS Styrofoam plates to reduce unwanted sublimation. For the rest of this paper, the following terms will be used for clarity. The track is a single lane with room for one cross-country ski. A testbed consists of four parallel tracks, as shown in Fig. 3. During this study, a single base layer was used. Hence the term preparation refers only to the preparation of the 5 mm thick top layer.

For tests on aged snow, a testbed prepared as described above was left for five days at −3 °C under XPS insulating plates. Then, the top 5 mm of this "aged" snow layer was scraped off with a steel blade. This snow was subsequently sieved with a 7 mm metal sieve before it was placed back inside the track and leveled with the steel blade to a smooth surface. The track was left to sinter for 16 h at −3 °C.

The snow was characterized by measuring the snow temperature in the middle of the track and snow density in 1-meter increments in the measurement area (SLF snow sensor, FPGA company GmbH, Switzerland). The snow was characterized with five measurements before and five measurements after the tests for each track (N = 40 for each testbed). The average values of all tracks for each preparation are given in Table 1. The surface topography of the snow was documented before and after a measurement series with a non-destructive elastomeric 3D imaging system (GelSight mobile, GelSight, USA), and the obtained images were analyzed using Digital Surf MountainsMap 9.0 software. To calculate the roughness parameters, the ISO 25178 standard [22] was used with a Gaussian S-filter of 2.5 μm. For the arithmetic mean peak curvature (Spc) and density of peaks (Spd) a wolf pruning of 5% of $S_z$ was used.


**Fig. 3.** Showing one testbed with four tracks.

### 2.4. Ski surface

A single skating ski (Redline 2.0 Regular 192 cm, Madshus, Norway) was used for the precision assessments. To minimize any changes in the structure between tests, it was decided alongside the ski manufacturer to flat grind the running surface of the ski. This is the second-last stage of the actual production process, just before stone grinding. This results in a very smooth surface. The surface topography of the ski sole was measured in the pressure zones in the front and rear of the ski with the elastomeric 3D image system, illustrated in Fig. 4. The surface roughness $S_a$ was measured to be 1.6 μm before and 1.6 μm after 1500 runs, suggesting there is little or no measurable wear of the sole material. The Spc and Spd value increased slightly, indicating more peaks and sharper peaks. If there had been significant wear these parameters are expected to drop between the measurements. The choice of not stone grinding the ski was made to exclude the possibility that the ground structure would wear gradually and thereby add additional uncertainty to the study. In the same line of reasoning, it was decided to not wax the ski because the wear of wax and variation in application would influence the development of the friction coefficient through a series. With these precautions in place, we assume that variations in friction coefficient due to the wear of the ski sole structure are negligible within the whole study.

To complement the speed tests with a ski of normal race performance, a race grind skating ski (Redline 2.0 Regular 192 cm, Madshus, Norway) was used. The ski was waxed with a base wax (Swix PS6, Brav, Norway) topped with a high-performance wax (Swix Marathon Pure, Brav, Norway) polished by a rotowool brush. The roughness $S_a$ was measured to be 3.0 μm, the SPD 9.5 mm$^{-2}$ and the SPC was 2.8 mm$^{-1}$.

**Table 1**
Showing the average temperature and snow conditions for the different tests ± one standard deviation.

| | Speed test | Polishing test (n = 200) | Testbed 2 New snow | Testbed 3 New snow | Testbed 4 New snow | Testbed 5 Aged snow |
|---|---|---|---|---|---|---|
| T air (°C) | -2.9 ± 0.35 | -2.8 ± 0.2 | -2.8 ± 0.1 | -2.9 ± 0.2 | -3.0 ± 0.2 | -3.0 ± 0.2 |
| T snow (°C) | -4.0 ± 0.3 | -4.1 ± 0.2 | -4.8 ± 0.3 | -4.2 ± 0.3 | -4.4 ± 0.2 | -3.9 ± 0.2 |
| RH (%) | 50.5 ± 3.5 | 51.8 ± 2.2 | 44.3 ± 2.0 | 52.3 ± 2.6 | 49.1 ± 1.9 | 42.2 ± 4.9 |
| Initial density (kg m$^{-3}$) | 296 ± 16 | 307 ± 13 | 397 ± 10 | 312 ± 19 | 334 ± 19 | 451 ± 14 |
| Final density (kg m$^{-3}$) | 345 ± 29 | 378 ± 29 | 469 ± 6 | 381 ± 12 | 382 ± 14 | 492 ± 20 |

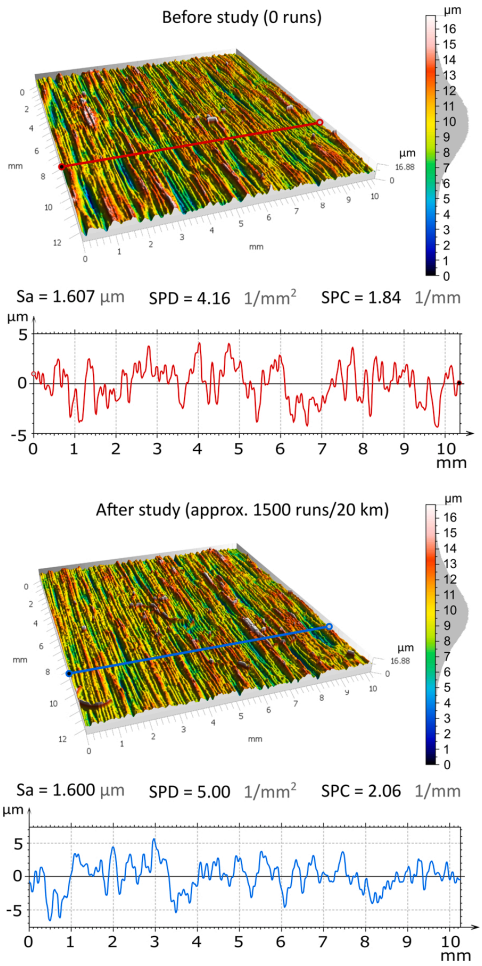


**Fig. 4.** The surface topography of a ski sole before and after the study, with corresponding height distributions. The z-axis is magnified by 5% for ease of visualization. The extracted profile is drawn though the highest point of each image.

### 2.5. Measurement protocol

Before each measurement series, there was a run-in protocol for each track. First, one run at 1 m/s was performed without any additional vertical load to check the test setup. Then, the vertical load of 330 N was applied, and the speed was increased by 1 m/s for each run until the desired testing speed was reached. For testing at 6 m/s, the run-in protocol totaled six runs at 1–6 m/s. The load of 330 N was chosen because it is approximately half of the recommended skier weight for the test ski and should resemble the load on one ski from outdoors glide testing. Between each run the ski waited 20 s in home position before the next run. This was done to minimize the build-up of frictional heating and meltwater in the track and to mimic the industry field-testing procedures.

The overall precision of the tribometer will vary depending on which level is being investigated. At level 1 we look at single tracks, and the precision obtained here reflects the precision of the friction measurement unit of the tribometer. Level 2 looks at parallel tracks within one testbed, and the precision obtained from these measurements includes the inaccuracies from level 1 in addition to the effect of changing the position of the ski within the testbed. Lastly, at level 3 we investigate the precision between different testbeds prepared with snow produced in different batches. The inaccuracies obtained here will include contributions from levels 1 and 2 in addition to a combined contribution from the snow production and snow testbed preparation. Detailed descriptions of the different precision calculations at the three levels are given below.

#### 2.5.1. Effect of track polishing and speed

In comparison to snow tracks outside, also tribometer snow tracks polish over time until an ice-like surface is obtained. The development of coefficient of friction was investigated in a dedicated test by continuing with repetitive runs beyond 50 runs until stabilization of the $\mu$ was observed. This test was performed on dendritic snow at 6 m/s, with a run-in protocol of the track consisting of six runs at increasing speeds from 1 m to 6 m/s.

The effect of speed was investigated in another dedicated test by running the test ski one time at each speed from 1 m/s to 8 m/s repeatedly, until six measurements were obtained for each speed (see Fig. 7(a)). Before the test, a run-in protocol of eight runs with 330 N load at increasing speed from 1 m/s to 8 m/s was performed. The precision reported for the various speeds were calculated from Eq. (1) modified for six datapoints.

#### 2.5.2. Measurement precision within single tracks – Level 1

To assess the precision of the friction measurements within single tracks, 50 consecutive runs were performed per track. After a few runs (1−4), a decrease in $\mu$ could be approximated by a linear trendline. The level 1 precision of the tribometer was estimated from the variation of the measurement series around their linear trendlines ($\mu_{\text{fit}}$), as a standard deviation ($\sigma_{\text{track}}$). Dividing $\sigma_{\text{track}}$ by the average $\mu$ for the series gives the relative standard deviation ($\varepsilon_{\text{track}}$) reported in percent for each track. Eq. (1) is used to calculate $\sigma_{\text{track}}$ for one track.

$$\sigma_{\text{track}} = \sqrt{\frac{1}{46}\sum_{i=5}^{50}(\mu_i - \mu_{\text{fit,i}})^2} \quad (1)$$

#### 2.5.3. Measurement precision within testbeds – Level 2

Moving the ski to other parallel tracks within the same testbed introduces a new variable affecting the precision of the tribometer. To determine the precision within testbeds, the test ski was run 50 times in each of the tracks. A common linear trendline ($\mu_{\text{fit}}$) was calculated from all the tracks of the testbed, and the standard deviation of all $\mu$ measurements of each run $i$ was then calculated around the value of $\mu_{\text{fit,i}}$. Averaging over all runs gives the Eq. (2) for the modified standard

deviation $\sigma_{testbed}$. Dividing $\sigma_{testbed}$ by the average testbed $\mu$ value, a relative value for the standard deviation ($\varepsilon_{testbed}$) was obtained.

$$\sigma_{testbed} = \sqrt{\frac{1}{46N}\sum_{j=1}^{N}\sum_{i=5}^{50}(\mu_{i,j} - \mu_{fit,i})^2} \quad (2)$$

To isolate the variation in the testbed from the variation in the measurement unit, we subtract the variation from level 1 in the following way: $\varepsilon_{L2} = \varepsilon_{testbed} - \varepsilon_{track}$.

#### 2.5.4. Measurement precision between testbeds – Level 3

To determine the contribution to the measurement precision from the snow quality and snow bed preparation, i.e. between different testbeds, we employed a methodology similar to level 2. The linear fit for all measurements in all the tracks of all the testbeds ($\mu_{fit}$) was found, and the standard deviation of the $\mu$ measurements ($\sigma_{inter\text{-}testbed}$) was calculated around this line, Eq. (3). Dividing $\sigma_{inter\text{-}testbed}$ by the average of the linear trendline, a relative value for the standard deviation ($\varepsilon_{inter\text{-}testbed}$) was obtained.

$$\sigma_{inter-testbed} = \sqrt{\frac{1}{46NM}\sum_{k=1}^{M}\sum_{j=1}^{N}\sum_{i=5}^{50}(\mu_{i,j,k} - \mu_{fit,i})^2} \quad (3)$$

The uncertainties contributing to $\varepsilon_{inter\text{-}testbed}$ are variations in the measurement unit, effects from changing the track position and the snow quality and testbed preparation. By subtracting the separate contributions calculated for levels 1 and 2 we obtain a value for the variation between different testbeds: $\varepsilon_{L3} = \varepsilon_{inter\text{-}testbed} - \varepsilon_{track} - \varepsilon_{testbed}$.

#### 2.5.5. Roller ski measurements

To assess the accuracy of the tribometer it is important to compare absolute $\mu$ values to other studies. To do this, a 50 run test with a classic roller ski (IDT Sports, Norway) with rubber wheels number 2 was performed. The surface of the track was 21 mm thick plywood plates, and the room temperature was 20 °C. The binding and the rest of the measurement setup was identical to the measurements performed on snow, but instead of calculating the coefficient of friction, the same calculation yields the coefficient of rolling resistance (CRR) for the roller ski. In contrast to measurements on snow, no run-in protocol was used, but a 20 s delay in 'home'-position between subsequent measurements was employed to reduce heat build-up. The effect of speed on CRR of the roller ski was performed in an analogous fashion to the speed test on snow.

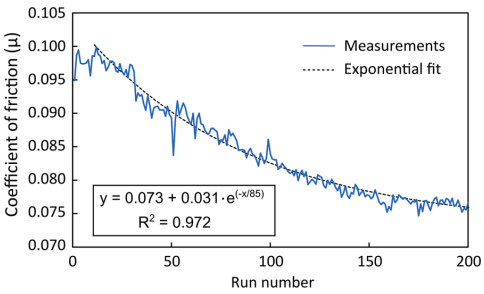


**Fig. 5.** Development of friction coefficient through a 200 runs series at a speed of 6 m/s. The fitted curve for runs 11–200 is drawn as a dashed line with an $R^2$ value of 0.972.

## 3. Results and discussion

### 3.1. Effect of track polishing

The effect of track polishing is illustrated in Fig. 5 by plotting the measured friction coefficient for successive runs in the same track. In this particular case (fresh snow, $v = 6$ m/s, $T_{snow} = -4.1$ °C), the friction level stabilized after 200 runs. After the first 10 runs, the friction coefficient decreased gradually in a path that could be described as an exponential decay function, where the friction level stabilized just below $\mu = 0.075$. The $R^2$ value of the exponential fit was 0.972. In the first part of the experiment (runs 11–50) the $R^2$ value for the exponential fit was 0.875 while that of the linear fit was 0.882. Based on this, the changes in the snow surface within the first 50 runs could be approximated with a linear fit.

The drop in friction coefficient from 0.099 to 0.075 equals a relative difference of 25%. Another noticeable trend was the increase in precision from run 100 and outwards. The precision from run 10–100 was 1.9%, while it was 1.2% for run 100–160. This observation proves that the tribometer precision is in fact dependent on the snow conditions.

Topography images captured with the GelSight illustrate contours of

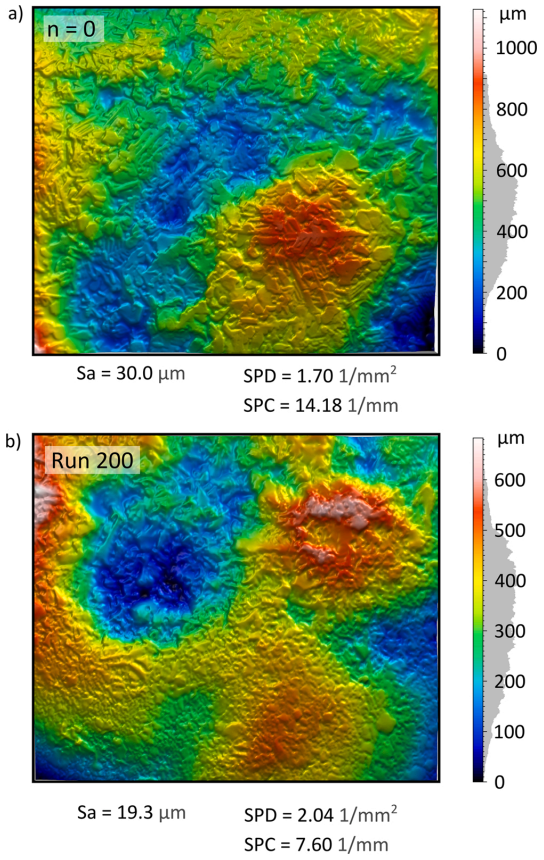


**Fig. 6.** 3D topography GelSight images of the snow track surface before and after 200 runs of the test ski on new snow. The real size of the images is 14 by 12 mm, and the running direction of the ski is vertical upwards in the images. The shifting in the images could be caused by inaccuracies in the positioning of the GelSight or a shifting snow surface due to longitudinal deformations in the snow matrix.

snow crystals and defined grains before the test (Fig. 6(a)) and after 200 runs (Fig. 6(b)). After 200 runs more rounded features are visible. This is supported by the SPC parameter (arithmetic mean peak curvature) that was about halved (from 14.18 $mm^{-1}$ to 7.60 $mm^{-1}$), meaning that the peaks have increased in roundness. The average surface roughness ($S_a$) decreased from 30.0 to 19.3 μm, meaning that the track lost roughness. The density of peaks (SPD parameter) increased slightly (from 1.70 to 2.04 $mm^{-2}$), which might be due to abrasion and fracture of dendritic plates and larger grains into smaller grains.

### 3.2. Effect of speed

The coefficient of friction varies depending on the speed of the ski, and ideally the tribometer measurements should be performed at the same speeds as in competitions. However, as test speeds increase, so do the forces and impacts from acceleration, deceleration, and irregularities in the track surface. Fig. 7(a) shows six subsequent sets of speed tests at speeds of 1–8 m/s. The averaged friction values at the different speeds are plotted in Fig. 7(b). The first general observation is the increase in friction with speed. For the flat grind and race grind skis at speeds of 2 m/s up to 8 m/s the friction increases approximately linearly with speed, similar to the data reported by Hasler et al. [16] However, a marked transition is observed below 2 m/s, which could point towards a change of frictional regime. While the friction coefficients of the non-waxed flat grind ski are generally very high, the waxed race grind ski displayed absolute μ levels only slightly higher than those reported by Hasler et al. [16]. The slope of the increasing friction, as seen in Fig. 7 (b) is very different between skis with a flat grind and a racing ski. For the speed range of 2–8 m/s, the friction coefficient of the race ski increased by 50% while the flat grind ski increased its friction by 150%. The much steeper slope of the flat grind ski is attributed to the larger increase in contact area between the ski and the snow as the thickness of the meltwater film increases with frictional power.

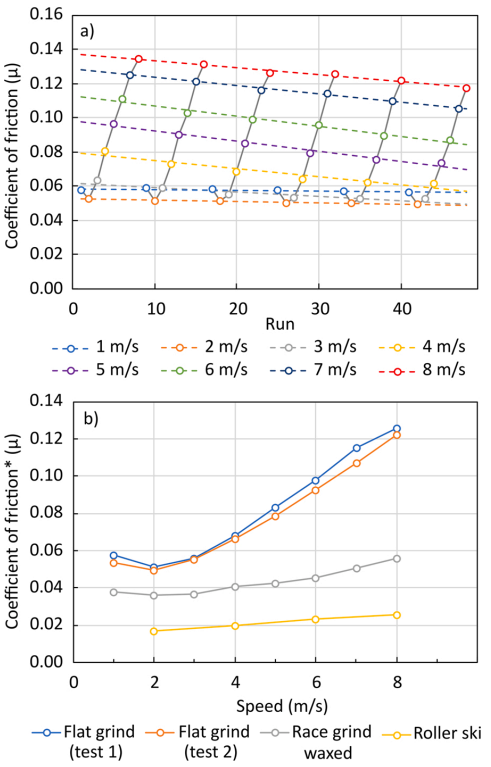


**Fig. 7.** (a) Measurement series showing the effect of speed on friction coefficient for an unwaxed flat grind ski (test 1). The dashed lines are the trendlines for the different speeds (1–8 m/s). (b) Summary of friction coefficient vs. speed for the flat grind ski (two repeated tests), a waxed ski with a racing grind and a classic roller ski. * Coefficient of rolling resistance (CRR) for the roller ski measurements.

The standard deviations ($\sigma_{track}$), relative standard deviations ($\varepsilon_{track}$), main vibrational frequency and oscillation amplitudes for the different speeds on new snow are reported in Table 2. The $\sigma_{track}$ and $\varepsilon_{track}$ first increase to 4 m/s before decreasing towards 8 m/s. The main vibrational frequency decreases with speed in both the vertical and horizontal directions and stabilize around 20 Hz for the higher speeds. We interpret this frequency to be a property of the spring system consisting of the electric motor belt-drive, test ski and the air bellow. Both horizontal and vertical oscillation amplitudes were strongly affected by increasing speed.

### 3.3. Accuracy assessment

Assessing the absolute accuracy of a full-scale ski-snow linear tribometer is a challenge. As the friction level variations for different snow surfaces and ski properties (grind, wax, length etc.) are generally large, comparisons of friction values from different studies are inherently uncertain. To complement such comparisons and to omit the uncertainty associated with the snow, we have tested the rolling resistance of a classic roller ski. The coefficients of rolling resistance at 2, 4, 6 and 8 m/s are reported in Fig. 7(b). The average CRR value at 6 m/s of 0.0237 is within the range of 0.019–0.025 reported by Schindelwig et al. [23], while Ainegren et al. [24] report slightly higher CRR values of 0.027. This indicates the accuracy of the reported tribometer is acceptable at the friction level of a roller ski, which is generally comparable to that of a racing cross-country ski. The standard deviation of the 50 roller ski runs at 6 m/s was 0.000227, a value which is 63% lower than the lowest value obtained for a track on new snow. This equates to a precision of 0.96%, indicating that the tribometer can achieve high precision also at lower friction levels.

### 3.4. Measurement precision within single tracks

The precision within single tracks was determined for ten separate tracks of new snow and four tracks of aged snow. On two occasions the collected data needed to be discarded due to technical problems with the tribometer. The results are given in Table 3. The standard deviations $\sigma_{track}$ and relative standard deviations $\varepsilon_{track}$ are calculated for each track. For new snow, the precision within a single track varies between 0.83%

**Table 2**
Average coefficient of friction, standard deviation, relative standard deviation, main oscillation frequency and amplitude for measurements (n = 6) at 1–8 m/s on new snow. The total downforce was 300–320 N.

| Speed [m/s] | Avg. $\mu$ | $\sigma_{track}$ [$10^{-4}$] | $\varepsilon_{track}$ [%] | Vertical oscillation | | Horizontal oscillation | |
|---|---|---|---|---|---|---|---|
| | | | | Freq. [Hz] | Amp. [N] | Freq. [Hz] | Amp. [N] |
| 1 | 0.057 | 5.8 | 1.0 | 71.4 | 4.7 | 71.4 | 8.9 |
| 2 | 0.050 | 2.0 | 0.40 | 1.4[a] | 3.0 | 50.0 | 9.5 |
| 3 | 0.056 | 15.0 | 2.68 | 42.9 | 4.8 | 42.9 | 10.1 |
| 4 | 0.068 | 20.0 | 2.94 | 40.7 | 7.3 | 40.7 | 11.1 |
| 5 | 0.083 | 13.5 | 1.63 | 20.1 | 7.5 | 27.2 | 12.6 |
| 6 | 0.097 | 12.5 | 1.29 | 20.0 | 11.4 | 20.0 | 18.3 |
| 7 | 0.115 | 6.9 | 0.60 | 19.3 | 12.7 | 23.1 | 19.2 |
| 8 | 0.126 | 9.0 | 0.72 | 22.1 | 18.1 | 20.8 | 23.5 |

[a] The software written to analyze the oscillations struggled at low speeds due to poorly defined vibrations.

**Table 3**
Standard deviation and relative standard deviation of the difference between the measured μ and μ calculated from the linear fit.

| Track | Testbed 2 New snow | | | Testbed 3 New snow | | | Testbed 4 New snow | | | Testbed 5 Aged snow | | |
|---|---|---|---|---|---|---|---|---|---|---|---|---|
| | μ | $\sigma_{track}$ [$10^{-4}$] | $\varepsilon_{track}$ [%] | μ | $\sigma_{track}$ [$10^{-4}$] | $\varepsilon_{track}$ [%] | μ | $\sigma_{track}$ [$10^{-4}$] | $\varepsilon_{track}$ [%] | μ | $\sigma_{track}$ [$10^{-4}$] | $\varepsilon_{track}$[%] |
| 1 | – | – | – | 0.0804 | 19.7 | 2.45 | 0.0828 | 14.0 | 1.69 | 0.0753 | 6.1 | 0.81 |
| 2 | 0.0787 | 8.5 | 1.08 | 0.0795 | 15.5 | 1.95 | 0.0843 | 7.0 | 0.83 | 0.0747 | 7.1 | 0.95 |
| 3 | 0.0795 | 6.6 | 0.83 | 0.0754 | 15.0 | 1.99 | 0.0851 | 7.4 | 0.87 | 0.0759 | 6.6 | 0.87 |
| 4 | 0.0732 | 7.5 | 0.97 | – | – | – | 0.0868 | 14.5 | 1.67 | 0.0755 | 7.1 | 0.94 |

and 2.45%, with an average of 1.45%. In comparison, the variation on aged snow within a single track was smaller and less varied with $\varepsilon_{track}$ values between 0.81% and 0.95%.

Even though the general change in snow surface is accounted for by basing the precision calculations on the linear evolution of the $\mu$, the random changes from run to run are assumed to be higher for new snow compared to aged snow. The aged snow consisted of transformed and rounded grains, as seen in Fig. 8(c). This likely provides a mechanically more stable surface, compared to the more fragile new snow. When the contact points are better connected to the rest of the snow matrix, measurements with less variability are expected.

The dendritic structure of new snow is expected to change more rapidly when the surface is subjected to pressure, abrasion, melting and refreezing of water, compared to old snow that has already gone through some metamorphosis. The average drop in $\mu$, from run 5–50, was 12% for new snow, while for aged snow the drop was 9%. The more rapidly changing $\mu$ of the new snow surfaces is likely attributed to more compression and fracture of large grains into smaller pieces, and a rearrangement of crystals, all causing a reduction in the pore space. This is supported by the density measurements, where new snow displays an 18% density increase over 50 runs. In comparison, the density of the aged snow only increased by 9% for the same number of runs.

The surface topography of the new snow testbed before the test (Fig. 8(a)) comprised of clear dendritic features like elongated crystals. These features are less visible after 50 runs, as seen in Fig. 8(b). The aged snow testbed had already more rounded features before the test (Fig. 8 (c)) and appeared more polished and flatter after the 50 runs (Fig. 8(d)). The development in SPD and SPC for both comparisons are not in the direction expected, but as the changes are small this could be an effect of minute changes in sensor position, variations in vertical force during imaging or shifting of snow grains.

The reported precision within one track for the linear tribometers of Lemmettylä et al. [17] and Hasler et al. [16], was 0.6–1.1% and 0.47% respectively. Our precision on this level (1.45%) was slightly lower, but one needs to account for the fact that our tests were conducted on dendritic new snow, and for a direct comparison identical snow

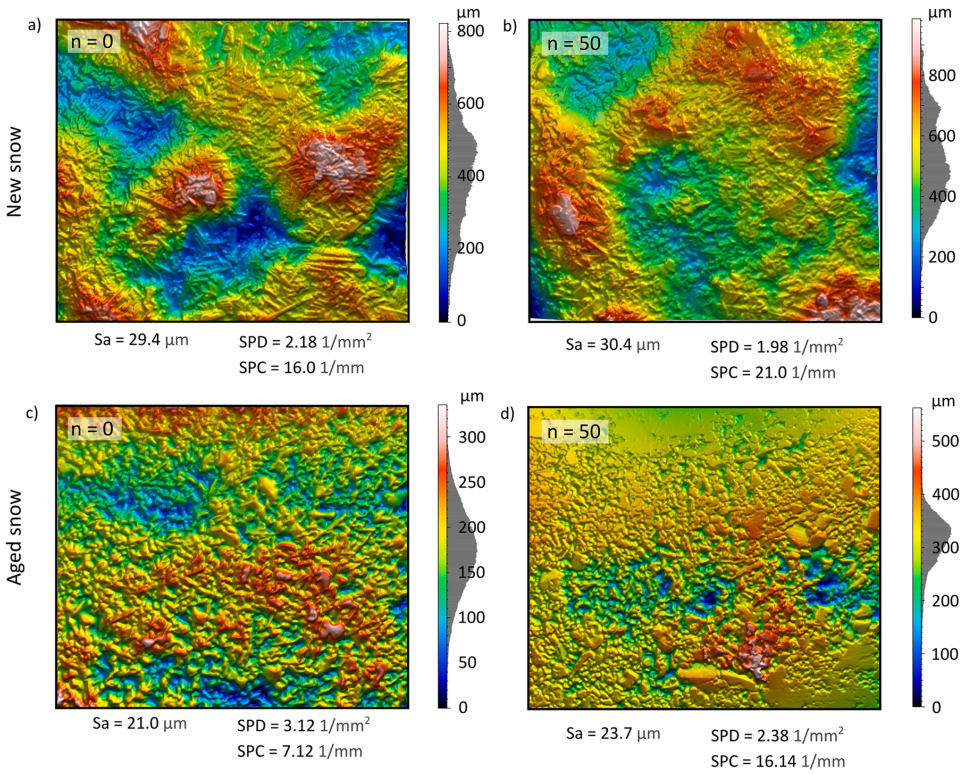


**Fig. 8.** 3D topography GelSight images of the snow track surface before and after 50-run measurements on new and aged snow. The real size of the images is 14 by 12 mm, and the running direction of the ski is vertical upwards in the images. Shifting snow and inaccuracies in the placement of the sensor may cause the images before and after to be slightly shifted.

conditions and friction levels are required.

### 3.5. Measurement precision within one testbed

On the surface of one testbed there is space for up to four parallel tracks that are prepared in the same operation with the same batch of snow. While this increases the sample capacity, the effect of changing tracks on the tribometer precision was unknown. The development in coefficient of friction for all tracks for three new snow testbeds and one aged snow testbed is shown in Fig. 9. In general, the coefficient of friction initially increases from start to run 2–5, before a gradually decreasing trend is observed for the rest of the tests.

On new snow (testbeds 2–4), the variations around each testbed trendline, $\varepsilon_{testbed}$ were 1.77%, 3.29% and 2.38%, with an average value of 2.48%. The difference between precision levels 1 and 2 for new snow is attributed to lateral inhomogeneities in the snow surface from the manual preparation. In comparison, for the aged snow testbed, the $\varepsilon_{testbed}$ of 1.17% was only moderately elevated compared to the $\varepsilon_{track}$ precision of 0.89%. This suggests achieving more homogenous tracks is easier with the preparation method for aged snow compared to the method used for fresh snow. Due to the sticky nature of the new snow, achieving an even distribution across the testbed was a challenge, while aged snow could be evenly distributed with a steel blade leading to a more homogenous snow layer.

The other report of a full-scale tribometer for cross-country skis with parallel snow tracks is by Hasler et al. [16]. They reported an average relative standard variation $\varepsilon_{ss}$ (ss - contributions from ski and snow) between five parallel tracks of 1.64% on artificial snow, at average $\mu$ levels about half of the values in this work.

### 3.6. Precision between new snow testbeds

For larger studies or studies over time, it is desirable to compare data from different testbeds and therefore of interest to document the reproducibility of testbeds. The data presented in Fig. 9 can also be used to calculate the precision between different testbeds (level 3). Using the method reported in Section 2.5.4 gave a value for the relative standard variation between testbeds of 4.87%. This accounts for the variation in the measurement unit, track position, snow quality and testbed preparation.

Lemmettylä et al. [17] determined the snow and ski to have the largest influence on the tribometer precision, reporting variation values ranging from 10.4% to 16.7% between different testbed preparations at 4 m/s at $\mu$ levels of 0.01–0.03. This is the only other account of the reproducibility of snow testbeds for full-scale ski tribometers.

### 3.7. Precision contributions and practical implications

Having established the relative standard deviations at the three different precision levels, one can determine the separate contributions

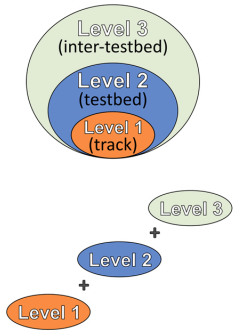


Absolute model

| | New snow | Aged snow |
|---|---|---|
| $\varepsilon_{track}$ [%] | 1.45 | 0.89 |
| $\varepsilon_{testbed}$ [%] | 2.48 | 1.17 |
| $\varepsilon_{inter\text{-}testbed}$ [%] | 4.87 | n/a |

Additive model

| | New snow | Aged snow |
|---|---|---|
| $\varepsilon_{L1}$ [%] | 1.45 | 0.89 |
| $\varepsilon_{L2}$ [%] | 1.03 | 0.28 |
| $\varepsilon_{L3}$ [%] | 2.39 | n/a |

**Fig. 10.** The two models for viewing the precisions of the three levels, absolute precisions, and additive precisions. The average values at the different levels and snow conditions are reported.

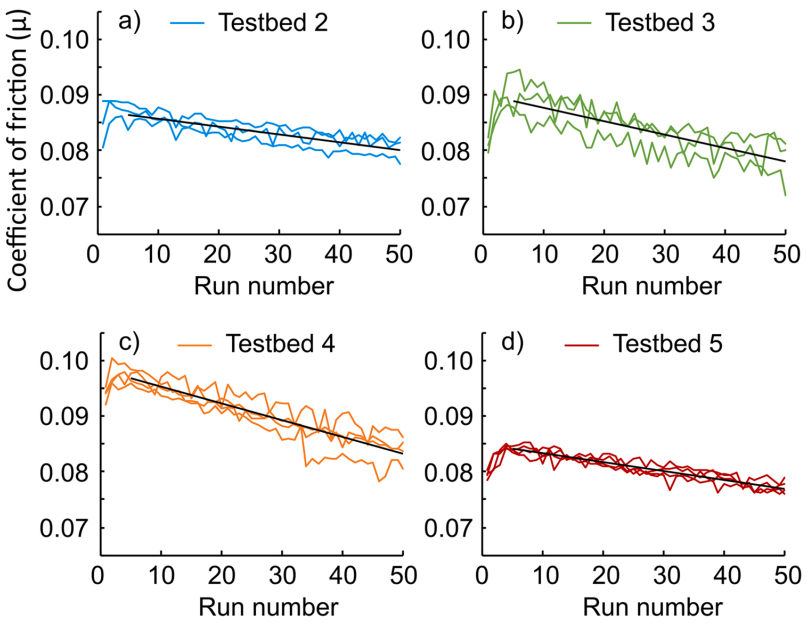


**Fig. 9.** Development of three testbeds on new snow (testbed 2–4) and one testbed on aged snow (testbed 5). Dashed lines represent the linear trendlines for each testbed from run 5–50.

from each of the levels under the assumption that the variations are additive. Fig. 10 shows the two models for viewing the precisions, either as absolute or additive. The level 1 precision describes the variation observed within single tracks and is the highest level of precision obtainable with this tribometer. Another way to view this is as a minimum measurement error associated with all measurements, which can only be reduced by increasing the number of measurements. When changing tracks within a testbed or changing between testbeds, new sources of variation are introduced. By subtracting the variation determined for the lower levels the contributions at each level can be determined. The absolute values and the individual additive contributions per level have been calculated and reported in Fig. 10.

#### 3.7.1. Precision level 1 – one track

The precision calculated at level 1 for new snow ($\sigma_{track}$ 11.6 $\cdot 10^{-4}$ and $\varepsilon_{track}$ 1.45%) is above the requirement postulated by Breitschädel et al. [5] and tested by Budde and Himes [25]. The implication of this is that repeated measurements are needed to reach sufficient precision. The margin of error (expressed in a 95% confidence interval) when multiple measurements of the same ski in the same track are averaged is shown in Fig. 11. A sufficient margin of error on new snow can be obtained by averaging five measurements. The higher precision obtained on aged snow ($\sigma_{track}$ 6.7 $\cdot 10^{-4}$ and $\varepsilon_{track}$ 0.89%) means to reach the same margin of error by averaging only two repeated measurements.

In the authors' opinion, the maximum number of runs in a single track is not necessarily limited to 50. As shown in Fig. 5, reliable data can be obtained for series up to 200 runs and probably even further, albeit at track conditions closer to ice than fresh new snow. When measuring different skis in the same track, a reference ski may be used before and after the measurement series to establish the overall polishing trend of the track, and the $\mu$ values adjusted accordingly. Errors related to track polishing can also to a certain extent be amended by cycling or reversing the order of the test skis.

#### 3.7.2. Precision level 2 – one testbed

There are many advantages of several parallel tracks on the same testbed with the same snow preparation. For this tribometer, it implies a fourfold increase in the number of measurements, which can allow large studies such as design of experiment (DoE) studies. The additive precision contribution obtained within new snow testbeds ($\varepsilon_{L2}$ 1.03%) is the variation attributed to changing the position of the ski. To compensate for this source of error, one can use a reference ski before and after the measurements in each track, so the variation in $\mu$ levels of the different tracks may be eliminated. For the testbed prepared with aged snow, the $\varepsilon_{L2}$ contribution was only 0.28%. This means the precision within a testbed of aged snow is better than the average precision within a single track on new snow.

#### 3.7.3. Precision level 3 – between testbeds

The precision obtained between different snow beds/preparations will depend on the snow production and track preparation. The average relative standard deviation between different snow beds of new snow was 4.87%, while the additive precision contribution of the different snow beds ($\varepsilon_{L3}$) was 2.39%. This precision is too low to perform meaningful comparisons between testbeds without a strong method of inter-testbed calibration. While a single ski could serve the purpose as a calibration ski, we believe no ski is perfectly constant over long periods and distance skied. We do however believe that the snow conditions are similar enough between testbeds to achieve high precision when measuring relative differences in performance. Consequently, with the current precision of the tribometer, ski products can be benchmarked against reference products from season to season, accelerating the learning in glide product development.

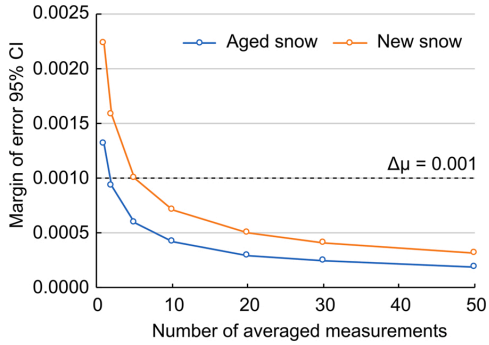


**Fig. 11.** Margin of error vs. number of averaged measurements on new and aged snow.

## 4. Conclusion

Performing repeatable friction measurements on any system undergoing change is challenging, and ski-snow friction measurements are no exception. The metamorphism of the snow is most pronounced for small, dendritic particles, commonly referred to as new or fresh natural snow. The need for precise measurements on this type of snow led us to develop a tribometer in conjunction with a dendritic snow machine.

The precision of the tribometer on new snow is divided into three levels. The highest precision currently achieved for this setup can be obtained when doing measurements within a single ski track. Here, the average relative standard deviation for measurements was 1.45%. The second level of precision describes the repeatability of parallel tracks within one testbed, and the relative contribution to the precision from this level was 1.03% for new snow. The last level of precision is that between measurements from different testbeds. The relative contribution to the overall precision from this level was 2.39%. With five or more repeated measurements, the precision within tracks is sufficient to separate skis with performance differences in $\mu$ of 0.001, providing the measurements come from the same track. Between tracks, a calibration ski may be used to increase precision, but this may not be feasible between testbeds over longer periods. The absolute tribometer accuracy was found to be in line with previous studies on both cross-country and roller skis.

We expected aged new snow to yield measurements of higher precision, as its features are less aggressive and are transforming at a much slower rate than freshly produced dendritic snow. The average relative standard deviation within test tracks on aged snow was 0.89%, while the contribution to the precision from changing tracks was only 0.28%. The lower variation between tracks was attributed to the better preparation method available for aged snow compared to new snow.

The ski-snow tribometer in the NTNU Snowlab allows testing of cross-country skis year-round on new and aged snow. Adequate precision was obtained which should allow distinguishing between skis or glide products of very similar performance ($\Delta\mu < 0.001$). Further improvements in precision, vibration reduction and measurement protocols will help accelerate the ski technology development and aid in the transition to a fully fluorine-free sport in the near future.

## Funding sources

This work is funded by the Norwegian Research Council (NFR) through the Nano2glide consortium, project number 296540.

## Declaration of Competing Interest

The authors declare that they have no known competing financial

interests or personal relationships that could have appeared to influence the work reported in this paper.

## Acknowledgments

The authors would like to thank the Nano2glide consortium (Brav, Madshus, IDT Sports, Olympiatoppen and SINTEF). We would also like to thank the mechanical workshop at IBM-NTNU and the technical staff at the Department of Civil and Environmental Engineering. Especially Senior engineer Per Asbjørn Østensen deserves a big thanks for all his work on the electronics of the track.

## References

[1] International ski federation. The international ski competition rules (ICR). 2021. p. 25.
[2] Nachbauer W, Kaps P, Hasler M, Mössner M. Friction between ski and snow. In: Braghin F, Cheli F, Maldifassi S, Melzi S, Sabbioni E, editors. The Engineering Approach to Winter Sports. New York, NY: Springer New York; 2016. p. 17–32.
[3] Moxnes JF, Sandbakk O, Hausken K. Using the power balance model to simulate cross-country skiing on varying terrain. Open Access J Sports Med 2014;5:89–98. https://doi.org/10.2147/OAJSM.S53503.
[4] Luchsinger H, Kocbach J, Ettema G, Sandbakk O. Comparison of the effects of performance level and sex on sprint performance in the biathlon world cup. Int J Sports Physiol 2017;13:1–24. https://doi.org/10.1123/ijspp.2017-0112.
[5] Breitschädel F, Berre V, Andersen R, Stjernström E. A comparison between timed and IMU captured Nordic ski glide tests. Procedia Eng 2012;34:397–402. https://doi.org/10.1016/j.proeng.2012.04.068.
[6] Bäurle L, Szabó D, Fauve M, Rhyner H, Spencer ND. Sliding friction of polyethylene on ice: tribometer measurements. Tribol Lett 2006;24:77–84. https://doi.org/10.1007/s11249-006-9147-z.
[7] Bowden FP, Hughes TP. The mechanism of sliding on ice and snow. Proc R Soc Lond 1939;172.
[8] Buhl D, Fauve M, Rhyner H. The kinetic friction of polyethylen on snow: The influence of the snow temperature and the load. Cold Reg Sci Technol 2001;33:133–40. https://doi.org/10.1016/S0165-232X(01)00034-9.
[9] Takeda M, Nikki K, Nishizuka T, Abe O. Friction of the short model ski at low velocity. J Phys Conf Ser 2010;258:258. https://doi.org/10.1088/1742-6596/258/1/012007.
[10] Kuroiwa D. The kinetic friction on snow and ice. J Glaciol 1977;19:141–52. https://doi.org/10.3189/S0022143000029233.
[11] Colbeck SC. A review of the processes that control snow friction. Hanover, NH: US army corps of engineers. Cold Reg Res Eng 1992;40.
[12] Bowden FP. Friction on snow and ice. Proc R Soc Lon Ser-A 1953;217:462–78. https://doi.org/10.1098/rspa.1953.0074.
[13] Montagnat M, Schulson EM. On friction and surface cracking during sliding of ice on ice. J Glaciol 2003;49:49–396.
[14] Wolfsberger F, Szabo D, Rhyner H. How to glide well on wet snow? Can roughness and hydrophobicity lower friction of polymers on snow? Gliding 2020;2:6–14.
[15] Böttcher R, Seidelmann M, Scherge M. Sliding of UHMWPE on ice: experiment vs. modeling. Cold Reg Sci Technol 2017;141:171–80. https://doi.org/10.1016/j.coldregions.2017.06.010.
[16] Hasler M, Schindelwig K, Mayr B, Knoflach C, Rohm S, van Putten J, et al. A novel Ski–Snow tribometer and its precision. Tribol Lett 2016;63:63. https://doi.org/10.1007/s11249-016-0719-2.
[17] Lemmettylä T, Heikkinen T, Ohtonen O, Lindinger S, Linnamo V. The development and precision of a custom-made skitester. Front Mech Eng 2021;7:7. https://doi.org/10.3389/fmech.2021.661947.
[18] F. Wolfsperger, H. Rhyner, M. Schneebeli. Slope preparation and grooming. A handbook for practitioners: Davos, WSL Institute for Snow and Avalanche Research SLF.; 2019.
[19] Schleef S, Jaggi M, Löwe H, Schneebeli M. An improved machine to produce nature-identical snow in the laboratory. J Glaciol 2014;60:94–102. https://doi.org/10.3189/2014JoG13J118.
[20] Giudici H, Fenre M, Klein-Paste A, Rekila K-P. A technical description of LARS and Lumi: two apparatus for studying tire-pavement interactions. Route/Road Mag 2017.
[21] Wåhlin J, Klein-Paste A. Influence of microstructure on the consolidation of compressed snow. J Cold Reg Eng 2015;29:29. https://doi.org/10.1061/(asce)cr.1943-5495.0000080.
[22] International organization for standardization. ISO 25178–2:2012 Geometrical product specifications (GPS) — Surface texture: Areal — Part 2: Terms, definitions and surface texture parameters. 2012.
[23] Schindelwig K, Mössner M, Hasler M, Nachbauer W. Determination of the rolling resistance of roller skis. Proc Inst Mech Eng, Part P: J Sports Eng Technol 2017;231:50–6. https://doi.org/10.1177/1754337116628719.
[24] Ainegren M, Carlsson P, Tinnsten M. Rolling resistance for treadmill roller skiing. Sports Eng 2008;11:23–9. https://doi.org/10.1007/s12283-008-0004-1.
[25] Budde R, Himes A. High-resolution friction measurements of cross-country ski bases on snow. Sports Eng 2017;20:299–311. https://doi.org/10.1007/s12283-017-0230-5.

# Paper II

Cold Regions Science and Technology 212 (2023) 103884

Contents lists available at ScienceDirect

Cold Regions Science and Technology

journal homepage: www.elsevier.com/locate/coldregions

# The effect of load and binding position on the friction of cross-country skis

Sondre Bergtun Auganæs, Audun Formo Buene, Alex Klein-Paste *

*Department of Civil and Environmental Engineering, Norwegian University of Science and Technology, Høgskoleringen 7a, 7034 Trondheim, Norway*

ARTICLE INFO

*Keywords:*
Cross-country ski
Ski pressure distribution
Load conditions
Ski-snow friction

ABSTRACT

This study investigates the effect of moving the binding and adjusting the normal load on friction for a modern cross-country ski. The binding was moved 10 cm forward and backward from the normal position. The results showed that moving the binding backward on the ski reduced the friction at cold (−10 °C) and warm air temperatures (+5 °C). At intermediate temperatures (−2 °C), neither changes to the binding position nor the total load affected the friction coefficient. Measurement of pressure zone profiles revealed that moving the binding backward reduced the apparent contact area, increased the average contact pressure, increased the peak pressure in the rear zone and increased the spacing between the front and rear contact zones of the ski.

## 1. Introduction

Over the last century, cross-country skiing has evolved from a necessary means of winter transport to a recreational activity and international sport. More recent developments in snow track preparation and artificial snow production have led to more compact and homogenous tracks, which enables faster skiing on shorter and narrower skis (Lintzén, 2016). Modern skis are complex constructions consisting of different layers of carbon and composite materials with an arced profile that compresses during loading. The most common method to determine the ski camber profile is to compress the ski onto a flat surface and measure the distance between the ski sole and the surface while increasing the normal load (Breitschädel et al., 2010). Such measurements along the entire length of the ski yield the contact zones, the camber height and other ski characteristics. The bending stiffness of the ski dictates how much of the sole will be in contact with the snow surface for a given load. A stiffer ski will in general have shorter contact zones compared to a softer ski with the same applied load (Breitschädel et al., 2010). The length of the contact zones or the apparent contact area (contact zone length × ski width) of the ski is thus adjusted to the prevailing snow conditions. For example will longer contact zones reduce the average contact pressure, which is favorable when the snow track is soft, as the friction component from compaction and plowing is reduced (Mössner et al., 2021). However, when the snow hardness is high, shorter contact zones might be favorable due to less solid-to-solid contact. Also when the snow humidity is high, the contact area should be reduced to avoid large zones of wet friction (Nachbauer et al., 2016).

In skiing, the center of pressure beneath the foot varies with the skiing discipline, gradient and throughout a glide and push-off cycle. A study on skating technique on roller skis found that the center of pressure (COP) in the ski boot moved from behind the middle of the foot during the glide, to some centimeters in front of the middle during the push-off cycle (Hoset et al., 2013). Another study measured the plantar pressure in the ski boot in the downhill tucking position to be 16 cm behind the balance point (Kalliorinne et al., 2023). When ski manufacturers and retail stores measure ski characteristics, the load is usually applied 8 cm behind the balance point of the ski (I. o. f. standardization, 1985). The load application point (LAP) alongside the mechanical ski properties and snow hardness dictates contact pressure profiles and the load split between the front and rear contact zones (Schindelwig et al., 2014; Bäckström et al., 2009; Nilsson et al., 2013; Mössner et al., 2023). By moving the ski binding, the LAP can be adjusted along the length of the skis. In classic cross-country skiing, moving LAP forward reduces the camber height which increases the contact between the snow and the grip wax, skin or imprinted pattern. While this improves grip it may also affect the gliding friction negatively and thus classic skiers must find a suitable compromise. However, for skating skis, it is unclear how moving the binding alters the overall friction of the ski. Binding adjustments for skating skis seem to be more targeted towards tuning the feeling of the ski, as it is perceived by the athletes. Among Norwegian athletes and coaches there appears to be a perception that moving the binding forward increases stability when the racetrack is hard or icy, and moving the binding backward on soft snow makes the ski float better.

The athletes themselves can also move the center of mass over the skis by changing their position. On alpine skis, Federolf et al. (Federolf et al., 2008) found that leaning backward in a tucked alpine position moved the

* Corresponding author.
*E-mail address:* alex.klein-paste@ntnu.no (A. Klein-Paste).

https://doi.org/10.1016/j.coldregions.2023.103884
Received 13 March 2023; Received in revised form 28 April 2023; Accepted 8 May 2023
Available online 11 May 2023

force application point on the binding by 16 cm compared to forward-leaning. However, they found no significant difference in glide times. Nilsson et al. (Nilsson et al., 2013) conducted a similar study for cross-country skis identifying that backward leaning increased the peak force in the rear contact zone by 18%. However, the length of the contact zones and position of peak force were largely unchanged. The glide times with backward leaning were 0.2% faster compared to a centered tuck position, but the results were not statistically significant ($p = 0.145$). As demonstrated by these reports, large uncertainties are often associated with glide tests performed outside with skiers adjusting their position.

A common theory in ski-snow friction assumes that dry friction occurs at the initial contact between the ski base and snow. The friction process generates heat, which creates a thin water layer that lubricates the contact spots (Bowden and Hughes, 1939). It is believed that the friction changes along the ski, by gradually building up a lubricating film from initial dry contact to a mixed-lubricated contact regime. The thickness of this water film is critical because it determines whether dry friction, lubricated friction or capillary suction is dominating the contact spots. The rate at which this film develops is dependent on snow parameters like temperature, liquid-water content, hardness and roughness (Moldestad, 1999). Also, ski parameters like speed, pressure distribution and base structure are contributing. Researchers have tried to measure and model the heat generation, water film thickness and real contact area (Mössner et al., 2021; Schindelwig et al., 2014; Hasler, and J. W, W. Nachbauer., 2021; Colbeck, 1992; Bäurle et al., 2007; Theile et al., 2009). However, at relevant speeds and loads, a lot is still unknown about the real contact area between ski and snow, because it is hard to measure directly (Hasler, and J. W, W. Nachbauer., 2021). The complexity of the tribological system means the heat production over the length of the ski depends on the friction coefficient, which again depends on the thickness of the water film.

Studies of sliders on snow have shown the friction force to be proportional to the normal load, at least for temperatures between −1 °C to −8 °C (Nachbauer et al., 2016; Buhl et al., 2001). Below this temperature, Buhl et al. (Buhl et al., 2001) found that increasing the load led to a decrease in the friction coefficient. At higher temperatures, Bäurle et al. (Bäurle et al., 2006) found that the friction coefficient decreased with increasing load for slider experiments on ice. They also showed that a smaller apparent contact area reduced friction at colder temperatures. This contrasts the findings of Eriksson and Nupen (Eriksson and Nupen, 1955) who demonstrated how increasing the slider length reduced the coefficient of friction. Colbeck (Colbeck, 1992) explained this by a thickening of the water film along the length of the ski. He derived the fraction of the length of the slider that is dry, showing that the proportion of dry versus lubricated sliding is higher for a model ski versus a full-length ski. From this hypothesis, Moldestad (Moldestad, 1999) suggested that in the case of cold temperatures or low snow humidity, it would be beneficial to induce higher pressure at the start of the front zone to decrease the dry friction length and induce lubrication earlier along the ski.

Modern cross-country skis are complex tribological sliders to study due to their design with two contact zones that vary with normal load and load application point. To the author's knowledge, no previous research has investigated the friction of a slider with two separate contact zones with different loads sliding over the same snow or ice surface. Using the high-precision tribometer developed by our group (Auganæs et al., 2022), the current study investigates the effect of the load and load application point on the friction coefficient of a modern cross-country skating ski. We further attempt to explain this with correlation to pressure distribution measurements within the contact zones.

## 2. Method

This section is divided into three parts. 1) Development of a rig for measuring contact pressure profiles. 2) Preparation of ski and snow surfaces and meteorological parameters. 3) The protocols for the friction measurements on a regular cross-country ski with a custom moveable binding.

### 2.1. Development of rig for measuring contact pressure profiles

Skiing consists of dynamic movements and therefore the normal load on the ski will vary through a glide and push-off cycle. When the load is changed or the load application point is moved on the ski, several parameters change at the same time. Most notably will the load split between the front and rear contact zones change, but it may also affect the distance between the two contact zones, their lengths and pressure distribution (Mössner et al., 2023). To quantify these changes, we built a rig to measure the pressure zones of a ski, as seen in Fig. 1. On top, there is a vice screw with a 2000 N (U9C 2 kN, HBM, Germany) load cell connected to an Arduino and a screen displaying the applied force onto the ski. The load from the vise screw is transferred to the ski with an aluminum block with an area of 45*45 mm. One contact zone of the ski is placed on top of 9 loadcells rated for 100 N (10 kg straight bar, SparkFun Electronics, USA) spaced 5 cm apart, and the other zone rests on an aluminum profile of the same height. The load cells were first calibrated individually with known weights of 50 g and 1000 g. 3D-printed PLA plastic support cradles (15 mm * 50 mm) were attached to each load cell. To achieve vertical alignment of the load cells, the two outermost cells were fixed, and a rigid aluminum beam was positioned across them. The remaining load cells were aligned vertically to the same level as the aluminum beam by tensioning the adjustment screws. To validate the rig, a rigid beam with a uniformly distributed load was placed across the sensor array to ensure approximately similar readings from each load cell. To avoid imprints from the plastic supports onto the ski sole a 1.0 mm flexible rubber strip was placed over the supports. This also helped reduce any difference in vertical misalignment.

The vertical deflection of an individual load cell was measured by loading it with 100 N from the screw vice. This caused a deflection of 0.05–0.1 mm measured by feeler gauges. This deflection can be converted into an estimate of snow hardness. The volume displacement (50 mm length, 45 mm width and 0.05–0.1 mm depth) under a load of 100 N corresponds to a hardness of 0.45–0.9 $Nmm^{-3}$.

To increase resolution, the sliding plate with the sensor array can be moved while the ski remains in the same position. This way, the resolution can be increased significantly. For this study, five separate measurements were performed with 1 cm increments yielding a force measurement resolution of 1 cm. To ensure that the entire load of the contact zone was measured, the two outermost load cells were checked to read approximately zero for each measurement. After the front zone was measured the ski was turned, and the rear contact zone was measured in the same way.

The threshold definition of contact was set at any reading above 0.5 N in the pressure distribution, and the contact lengths were calculated accordingly. The force resolution for a single load cell is 0.02 N. The sum of the forces from the front and rear contact zones was approximately the same as the total applied load by the vice screw. For the test of normal load, the LAP was set to 12 cm behind MP, and the ski was loaded by 200 N increments from 200 N to 800 N. For the test with different binding positions, the LAP was moved in 2.5 cm steps from 2 cm to 22 cm behind MP, with the normal load of 730 N.

### 2.2. Preparation of ski and snow surfaces and meteorological parameters

A single skating ski (Redline 2.0 192 cm, Madshus, Norway) with a medium stone grind was used for the entire study. The ski binding was a commercial Rottefella Move Tune Skate, with a custom 3D-printed part allowing 20 cm of binding adjustment instead of 3.5 cm. The surface topography of the sole was measured in the front and rear contact zones and the average $S_a$ was found to be 3.02 μm. To ensure comparable glide performance, the ski was cleaned and waxed before each test. First, Swix base cleaner was rubbed onto the ski with Fiberlene fibrous cloth and agitated with a nylon brush and left to dry for 5–10 min. After that, a dry Fiberlene fibrous cloth was used to wipe the sole, before roto steel brushing twice (1500 rpm, 0.5 m/s). The next step was to apply HS6,

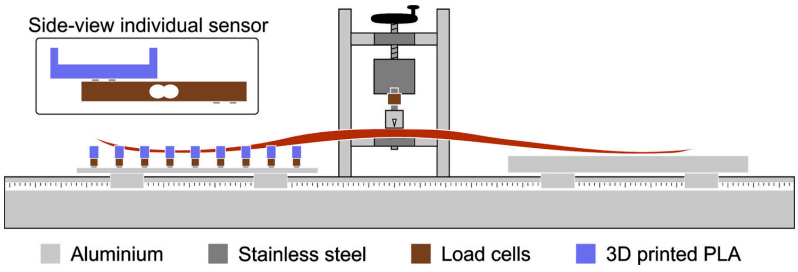


**Fig. 1.** Side view of the developed rig for measuring contact pressure profiles on cross-country skis.

HS7 or HS8 liquid spray wax for snow temperatures −10 °C, −2 °C and 0 °C respectively, and leave it to dry for 15 min. The last step was to polish the surface with a roto nylon brush.

The preparation of the dendritic snow track at −10 °C was performed as described in a previous study by Auganæs et al. (Auganæs et al., 2022). In short, dendritic snow was produced at −20 °C, before the fresh snow was evenly distributed and compacted by running a 30 cm wide compaction board at low speed over the snow, and then left to sinter for 16 h. The preparation of one snow bed consists of four single tracks that can be utilized for testing. One single track was used for the test of binding position and one track for the test of normal load. After the testing at −10 °C, the temperature in the lab was raised to −2 °C, and the two unused tracks were left to sinter below covers for 16 h. These two tracks are referred to as intermediate conditions.

To prepare the snow track for warm conditions ($T_{air}$ = +5 °C), the top layer of snow from previous testing was scraped and removed for sieving. Afterward, the snow was placed back into the track and leveled using a steel blade. The snow was then left to sinter for 16 h at a temperature of −2 °C, before the air temperature was set from −2 °C to +5 °C, four hours before testing. This increased humidity and water content of the top snow layer. The snow was characterized by measuring the snow temperature in the middle of the track, and snow density and humidity in 0.5 m increments (SLF snow sensor, FPGA company GmbH, Switzerland and Doser snow moisture meter 011, GmbH, Germany). The average meteorological values for three separate tests on cold and intermediate and two tests on warm conditions are given in Table 1.

### 2.3. Friction measurement protocol for cross-country ski

The friction measurements were performed in the full-scale linear tribometer, where a ski is mounted to a carriage and driven 6.5 m over a snow track. The setup and precision of the tribometer are reported in Auganæs et al. (Auganæs et al., 2022), and the updated data acquisition system is reported in Buene et al. (Buene et al., 2022). Before each measurement series, there was a run-in protocol, as visualized in Fig. 2. First, the load was increased from 100 N to 700 N while the speed was set at 1 m/s. Then when fully loaded with 700 N, the speed was increased up to 6 m/s and lastly, six runs were performed with full load and speed to run the track in. To reduce the differences in impact from polishing between samples, all test configurations were cycled/repeated three times to distribute the effects of polishing over all samples. During the tests, track polishing was observed by decreasing COF for each cycle.

**Table 1**
Average temperature and snow conditions for the test on different temperatures. With the following ± one standard deviation.

| | Cold | Intermediate | Warm |
|---|---|---|---|
| $T_{snow}$ (°C) | −10.6 ± 0.1 | −2.7 ± 0.7 | 0 ± 0.1 |
| $T_{air}$ (°C) | −9.9 ± 0.2 | −2.0 ± 0.1 | 5.1 ± 0.2 |
| $\rho_{snow}$ (kg/m$^3$) | 453 ± 54 | 457 ± 35 | n/a* |
| Snow humidity (%) | 20 ± 3 | 20 ± 1 | 70 ± 20 |

* Outside reliable measurement range.

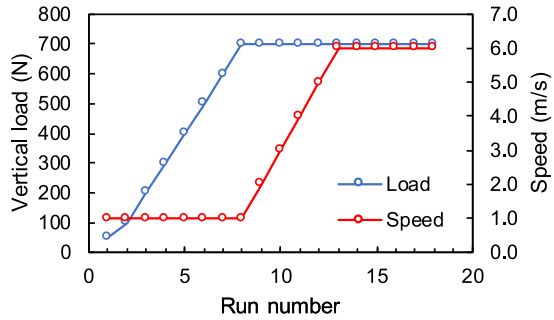


**Fig. 2.** Run-in protocol of the snow track before each measurement series.

This was corrected for using a linear fit of the polishing for each series, see Auganæs et al. (Auganæs et al., 2022) for details.

To investigate the impact of binding position on friction, the measurement series began with the binding pin placed 10 cm in front of the Mass Point (MP) - the balance point for the ski and a widely used reference position. As shown in Fig. 3, when the binding is in the neutral position, the center of pressure (COP) for a shoe size EU 42 is located 12 cm behind the binding pin. This means that shifting the binding from 10 cm in front to 10 cm behind the neutral position is equivalent to moving the load application point from 2 cm to 22 cm behind MP. After performing three runs in the tribometer the binding was moved 2.5 cm by turning the adjustment wheel two revolutions. The test series was performed by doing nine runs in each position with LAP placed 2–22 cm

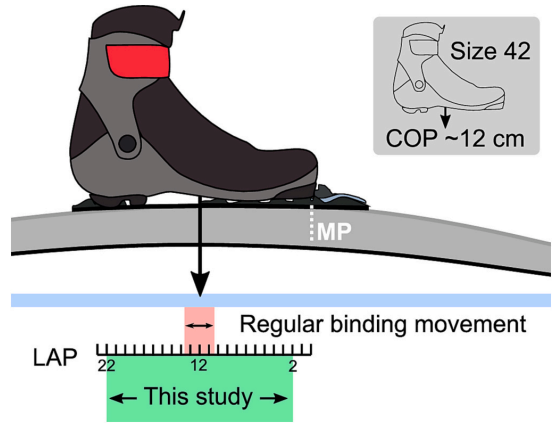


**Fig. 3.** Relation between the load application point and binding position. The center of pressure (COP) for a size EU 42 ski boot is approximately at 12 cm behind the binding pin.

behind MP in increments of 2.5 cm. Each test series was repeated three times for cold and intermediate temperatures ($n_{runs} = 27$) and two times for warm temperatures ($n_{runs} = 18$). Due to the arced top surface of the ski, movement of the binding changed the angle between the ski and the boot. In the tribometer, the ski is mounted beneath an air bearing with horizontal and vertical load cells. Because of the change in this angle, the horizontal and vertical load cells had to be aligned each time the binding was moved using an adjustment screw and a digital level.

The test series for the effect of the normal load was performed by conducting nine runs for each normal load starting from 800 N and decreasing to 200 N in 100 ± 10 N increments. Each test series was repeated three times at cold and intermediate temperatures ($n_{runs} = 27$) and two times at warm temperatures ($n_{runs} = 18$). The absolute COF measurements are reported as the average values for the separate test series performed at each temperature.

To compare the relative changes between temperatures, the deviations from the series average in percent were calculated with Eq. (1). Here, $p$ denotes the parameter (load or LAP), $i$ denotes the value of the parameter (LAP 2–22 or load 200–800 N) and $s$ denotes the test series (s = 1–3 for $T = -10$ and $-2$ °C or s = 1–2 for T = +5 °C). The reported values for ΔCOF are then the average $\Delta COF_p(i)$ across all series $s$ at a given temperature.

$$\Delta COF_p(s,i) = \frac{\mu_p(s,i) - \overline{\mu}_p(s)}{\overline{\mu}_p(s)} \times 100\%$$

## 3. Results

### 3.1. Contact pressure profiles for different normal loads

The measured contact pressure profiles for the different applied normal loads are shown in Fig. 4. The results of the experiments

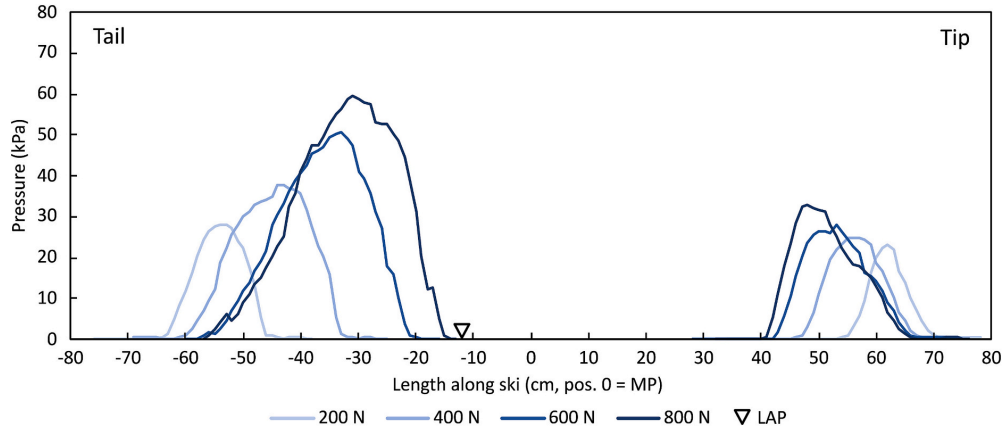


**Fig. 4.** Contact pressure profiles for four different normal loads, with the load application point 12 cm behind MP.

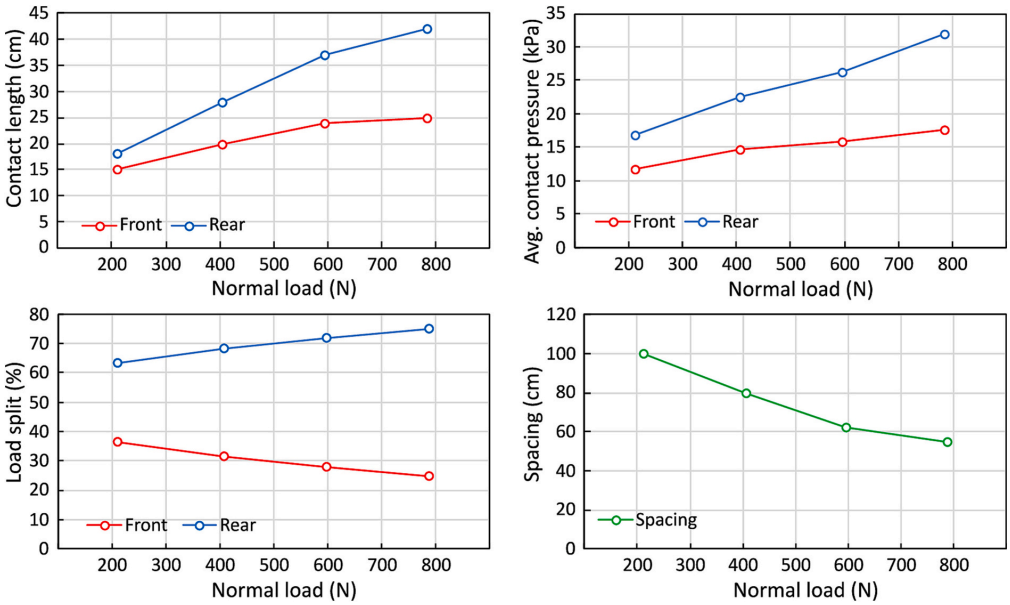


**Fig. 5.** Measured contact zone lengths, pressures, load split and spacing as a function of the normal load.

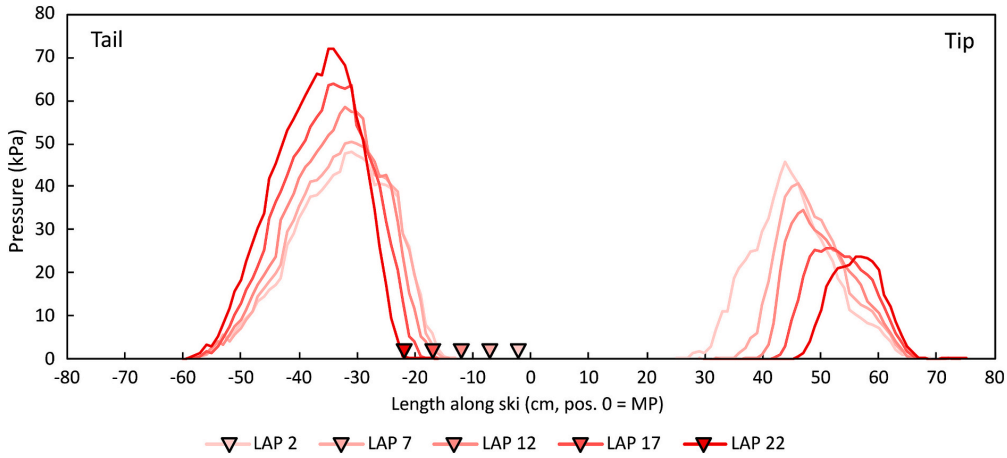


**Fig. 6.** Contact pressure profiles of the ski at five different load application points, with a normal load of 730 N.

demonstrated a non-linear correlation between the load and the contact lengths (apparent contact area). As the normal load was increased from 200 N to 800 N, the contact lengths and average contact pressure increased. The contact zones also moved towards the center of the ski. As expected, a doubling of the normal load did not lead to a doubling of the apparent contact area. Therefore, the average contact pressure was observed to increase from 12.7 kPa rising to 25.2 kPa over the loading cycle of 200–800 N. A more detailed view of how the different ski characteristics changed is illustrated in Fig. 5. These include a higher load split towards the rear zone and a shorter spacing distance between the two zones as the normal load increases. There is a discontinuity in the trends around 600 N, where the increase in contact lengths starts to flatten out, resulting in steeper increase in contact pressure. Also, the movement of the two zones towards the midpoint (spacing) becomes less pronounced beyond 600 N. These results show how the ski-snow pressure is altered by increasing the load for this ski.

### 3.2. Contact pressure profiles for different load application points

The pressure profiles were analyzed based on the movement of the LAP from 2 cm to 22 cm behind the MP, and the results are shown in Fig. 6. Moving the load application point backward has three effects. The first and most obvious is that the load on the rear contact zone increases, altering the load split. Secondly, it causes the front and rear pressure zones to move further away from each other. The third effect was a reduction in the length of both contact zones. In the neutral position with the LAP located 12 cm behind MP, a 28/72% front/rear load split was recorded, with the peak pressures detected at 47 cm and − 33 cm

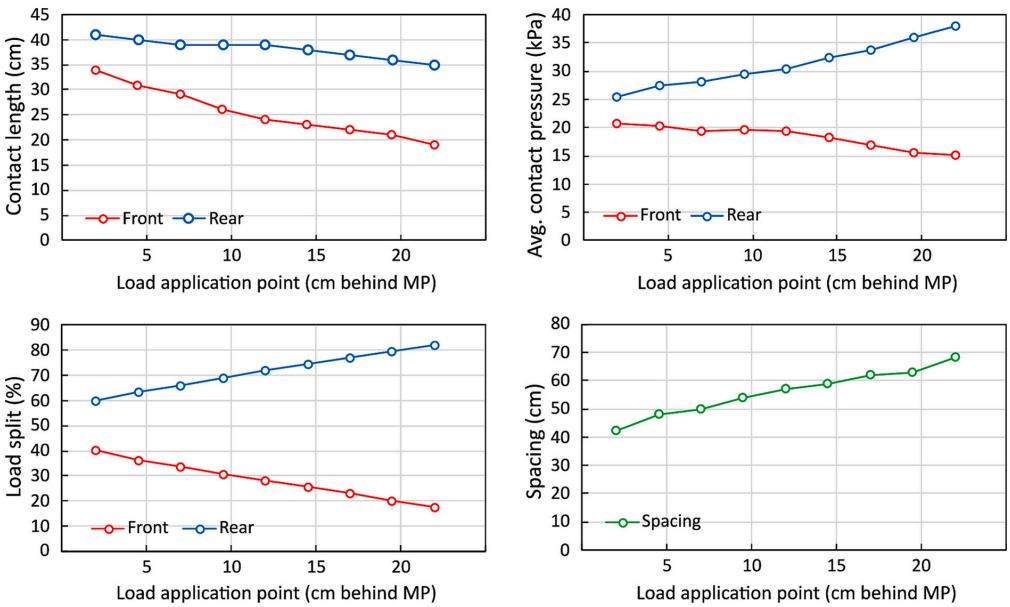


**Fig. 7.** Measured contact zone lengths, pressures, load split and spacing as a function of the load application point.

from MP. A more detailed view of the changing ski characteristics when moving the load application point is illustrated in Fig. 7.

### 3.3. The effect of normal load on the coefficient of friction

The effect of normal force on the friction, for three different temperatures, is shown in Fig. 8a. The general level for the friction coefficient was on average 0.0319, 0.0372 and 0.0396 at −2 °C, −10 °C and + 5 °C respectively. In terms of relative changes between different normal loads, the ΔCOF was calculated for three separate tests for each temperature, as shown in Fig. 8b. The most pronounced behavior is visible for the measurements at melting temperature ($T_{air}$ = +5 °C). At this temperature, the friction coefficient was highest at 500 N and decreased for normal loads above or below. A relative difference of 9.2% can be observed from the highest point at 500 N to the lowest at 800 N. The measurements at the coldest temperature (−10 °C) showed ΔCOF to vary around −2% to 2% with no clear trends. For intermediate temperatures (−2 °C), COF was observed to be independent of the normal load, with a difference of less than 0.5% between the three highest loads.

### 3.4. The effect of load application point on the coefficient of friction

The effect of the load application point on the friction, for three different temperatures, is shown in Fig. 9a. The general level for the friction coefficient was on average 0.0328, 0.0434 and 0.0377 for −2 °C, −10 °C and + 5 °C respectively. For comparison of the relative differences at each temperature, the ΔCOF is shown in Fig. 9b. The influence of LAP on the friction coefficient was most pronounced at the warmest

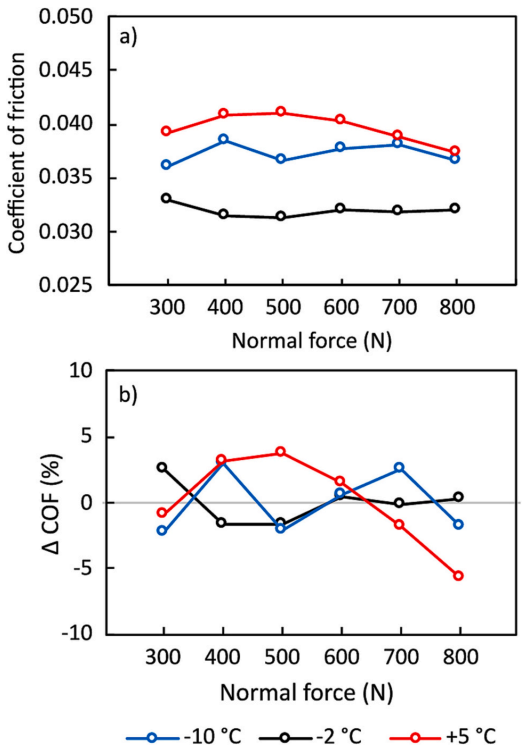


**Fig. 8.** The effect of normal force on the friction coefficient of a modern cross-country ski, at three different air temperatures. a) Average COF and b) the relative difference within each temperature. Testing speed of 6 m/s.

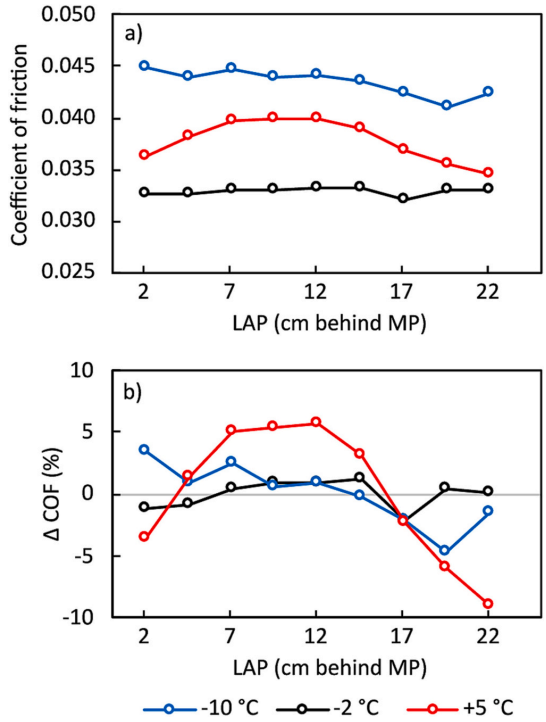


**Fig. 9.** The effect of load application point on the friction coefficient of a modern cross-country ski, at three different air temperatures. a) Average COF and b) the relative difference within each temperature. Testing speed of 6 m/s.

temperature. At this temperature, the friction coefficient was highest at the neutral position (12 cm behind MP) and fell when the load was shifted either forward or backward. This trend resembles that of the effect of normal load for the same temperature. A 15% difference in COF can be observed from the highest point at 12 cm to the lowest at 22 cm. The impact of LAP on the COF at intermediate temperature (−2 °C) was minimal, with differences of ±1%. The highest point was at 14.5 cm behind MP and the friction was reduced slightly by moving the load forward or backward. At the coldest temperature (−10 °C), a declining trend in the COF was observed as the LAP was moved backward, continuing until a minimum at around 19.5 cm behind the MP.

## 4. Discussion

### 4.1. Contact pressure measurements

Contact pressure distribution measurements were performed to understand how the apparent contact area and contact pressure between ski and snow changed with the loading. In short, the findings of this part of the study showed an increase in the apparent contact area and contact pressure for increased normal loads. For the particular ski tested in this study, the increase in contact area was non-linear and started to level off once the normal forces exceeded 600 N. The changing trend at 600 N can be explained by the contact zones moving towards the binding with increasing load, and the increased bending stiffness in this part of the ski limits further expansion of the contact area. Temperature changes have previously been shown to affect the bending stiffness of skis (Breitschädel et al., 2010). However, for the temperature range in this study, we believe this to be of minor influence.

Moving the load application point backward reduced the apparent

contact area, increased the apparent contact pressure, shifted the load split towards the rear contact zone and increased the spacing between the front and rear zones. The reduction in total apparent contact area surprised us at first but was confirmed by measurements of the same ski from the Madshus factory. Considering a modern cross-country ski is in essence a symmetric leaf spring with a non-uniform bending stiffness, movement of the LAP away from the highest point of the ski camber curve effectively reduced the total compression of the ski (Kalliorinne et al., 2023). Since the formation of the contact zones depends on the compression of the ski camber, this explains the observations. Our findings when moving the LAP can be compared to theoretical calculations by Mössner et al. (Mössner et al., 2023) who studied leaning. They did this by applying a transverse moment of 21 Nm at the binding, which translates to a movement of the LAP by 6 cm. For backward leaning, this increased the rear peak pressure by 8.6 kPa. From our findings, a similar shift in LAP resulted in an increased peak pressure of 5.8 kPa. Given that these are two different skis, these results appear a reasonable comparison.

Compared to the measurements from the Madshus factory, performed by scanning the distance to the sole when compressed on a hard surface, our results gave in general slightly longer contact zones. The length of the front contact zone was on average 14% longer and the rear zone 5% longer. The load split in the neutral position compared well to similar measurements carried out by Schindelwig et al. (Schindelwig et al., 2014) who reported a 20/80 front/rear load split with peaks at 54 cm and 141 cm from the ski tip. Nilsson et al. (Nilsson et al., 2013) showed that the peak force did not increase much between full and half body weight, but the contact lengths increased significantly. This contrasts our findings but may be a result of the use of soft rubber mats and Teflon sheets between the ski and pressure sensors, to distribute load and simulate snow contact.

The hardness of snow varies greatly and is influenced by a range of factors such as meteorological history and preparation such as grooming or compaction. Our measurements of contact pressures were performed directly onto load cells with a calculated surface hardness of approximately 0.45–0.9 $Nmm^{-3}$ which corresponds to a hard and well compacted snow surface (Mössner et al., 2023). On softer snow our contact pressure measurements may yield conservative estimates of apparent contact areas. In a study by Theile et al. (Theile et al., 2009) on repeatedly compacted snow with a hardness of around 7 $Nmm^{-3}$, an elastic deformation of only 20 μm in the snow matrix was reported. Elastic deformation on this scale is unlikely to have large effects on the contact pressures or apparent contact area. However, on softer snow Mössner et al. (Mössner et al., 2023) showed how the apparent contact area and pressure distribution of skis were affected by the snow hardness in the range of 0.04–0.32 $Nmm^{-3}$. The repeated compaction, high snow density, the compact base and the thin snow layer used in our friction measurements suggest the test track in this study is relatively hard and comparable to firm ski tracks and only small elastic deformations are expected.

### 4.2. Friction measurements

In the following sections, the effect of normal force and load application point on the friction coefficient are discussed together and grouped for each testing temperature, since different frictional mechanisms dominate at various temperatures.

#### 4.2.1. Cold temperatures

The measurements at the coldest temperature (−10 °C) showed small changes in ΔCOF of ±2% with different normal loads. Previous tribometer experiments of single sliders on snow or ice have reported decreasing COF for higher normal loads at similar cold temperatures (Buhl et al., 2001). Therefore, it was surprising to not see the friction coefficient drop for increased normal loads in our experiments. Buhl et al. (Buhl et al., 2001) explained this load dependency as an increase in frictional heat with higher loads. If we assume that the initial dry friction process conforms to classical friction laws (real contact area is proportional to the normal force), the frictional energy released per unit area is greater for a smaller apparent contact area or higher apparent contact pressure. Because of the increased heat generation, the transition from dry to lubricated friction will occur earlier along the slider length and lower the friction for the remaining contact area of the ski. In contrast to previous studies on rigid sliders with a constant area, for a modern ski, the apparent contact area also increases for higher normal loads which will increase the friction (Bäurle et al., 2006). We believe that for a modern ski at cold temperatures, higher apparent contact pressures contribute to reducing friction, while a larger apparent contact area increases friction. These two mechanisms cancel each other and can explain the independence of normal load on COF observed in Fig. 9b.

For the effect of the load application point on the friction coefficient, a steady drop was seen as the load was moved backward on the ski. This can be explained by both the reduction in the apparent contact area and the change in load split. A smaller total apparent contact area can result in less friction if the counter surface (snow) is hard enough to resist additional compaction and plowing contributions. Our testing was performed on a single snow track with multiple runs over it, which made the snow track well-compacted after some runs. Shifting the majority of the load onto one contact zone will concentrate the frictional heat and yield a thicker lubrication film and thus lower friction, compared to having two zones with sub-optimal lubrication. Again, this can only be done when the snow is sufficiently strong. For weaker snow, we expect increased load split to be unfavorable due to larger deformations in the snow. While in this study only the load split towards the rear contact zone was tested, we cannot see a reason why it should not be equally valid by shifting the same amount of load towards the front zone.

#### 4.2.2. Intermediate temperatures

The measurements at −2 °C had the lowest friction level and the COF was observed to be independent of the normal load and independent of the load application point. At this temperature, even though the coefficient of friction is low, it is not zero. This implies that there is frictional heat transferred to the snow contact points. Yet, by altering the normal load or the LAP the friction coefficient remained unchanged. This can either be an effect of a relatively constant water film or two mechanisms canceling each other.

The first can be explained by the snow grains at this intermediate temperature already having a thin liquid-like layer (Kietzig et al., 2010). The increase in apparent contact pressure of the ski will only lead to an increase in the number of contact points, where limited “conditioning work” is required from the ski to bring the contact points to a favorable friction regime. Therefore, a linear relationship between load and friction force is expected, resulting in the COF being independent of factors such as normal load and load application point. The second theory is explained by two opposing contributions, as proposed by Bäurle et al. (Bäurle et al., 2006). The reasoning is that reduction in friction by thicker lubrication films is balanced by the increase in real contact area with this film. The fact that two opposing mechanisms balance perfectly over the wide range of loads and load application points in this study is difficult to understand. Similarly, we acknowledge that the limited frictional heating at low COF values must lead to further melting or conditioning of the contact points.

#### 4.2.3. Melting temperatures

For the measurements at melting snow temperature ($T_{air} = +5$ °C), the friction coefficient was highest at 500 N and decreased for normal loads above and below. The decrease in friction towards the lowest normal loads can mainly be attributed to the decrease in apparent contact area for the ski. At air temperatures above zero, the snow will start to melt, and there will be liquid water present on the surface. This excess water causes an increase in contact area which causes increased friction due to capillary attachments and suction. With these snow

conditions, it is beneficial to reduce the contact area. In ski racing, this is done by choosing a ski base with rough surface topography. These structures allow air to interrupt the formation of a continuous water film.

The decrease in friction coefficient for the highest normal loads, in the range of 500–800 N, can be attributed to an increase in apparent contact pressure without a corresponding increase in the apparent contact area. For these soft and wet snow conditions, the real contact area starts to approach a maximum, dictated by the apparent contact area and porosity of the snow. As the normal load can be increased without affecting the contact area, the friction force is expected to be unchanged and a reduction in friction coefficient is the result.

The measurements for different load application points showed a point of maximum friction around 12 cm behind MP. The reduction in friction for LAP above 12 cm can be explained by the same reasoning: reduction in the apparent contact area, as explained in the previous paragraph. The decrease in friction from LAP 7 cm to 2 cm is more difficult to explain. Even though the apparent contact area increases, the overall friction is reduced. Looking at Fig. 7 there is no discontinuous trend for the contact zone measurements around the LAP 2 cm to 12 cm. This means the decrease in friction cannot be directly linked to either of these characteristics causing the maxima point.

### 4.3. Practical implications

Before a race, athletes typically evaluate their skis based on their gliding performance and how they feel in terms of stability, balance, and other factors. The findings from this study suggest that within the range of movement for a regular binding, there are possible gains. Especially for cold and warm temperatures, the friction can be reduced by moving the binding backward.

We also tested binding positions far outside the normal range, where even larger gains were achievable. For the largest effect observed in this study, an estimated time saving of 74 s could be achieved over a distance of 10 km according to the model of Moxnes et al. (Moxnes et al., 2014). More specifically, at cold/dry and warm/wet conditions, shifting the majority of the load to one of the contact zones appears to be advantageous. Reaching these load application points with a regular binding requires the skier to actively lean backward. This may be possible for short periods during a race, for example while sliding down a hill in the tucked position, but it is expected to affect the skier's balance negatively. While the current skis are not designed for such a large range of load application point movement, we believe that future ski designs may be able to incorporate these principles in a ski with adequate handling properties.

## 5. Conclusion

In conclusion, the study found that the effect of normal load and load application point on friction coefficient varied depending on the snow temperature. The results show that friction was reduced upon moving the binding towards the rear for air temperatures of +5 °C and − 10 °C, while no effect was seen at −2 °C. The trend at warm and cold conditions was explained by a decrease in the apparent contact area and a shift in the load split of the ski. At the cold temperature, this led to more frictional heat per area and thus a faster transition from dry to lubricated friction. At warm temperatures, this led to a smaller area in contact with water and less capillary drag.

For the effect of normal loads, no changes were observed for the friction coefficient at temperatures below zero. This may be explained by canceling contributions from two opposing mechanisms. Namely, a higher apparent contact pressure contributes to reducing friction, while a larger apparent contact area contributes to increased friction. At air temperatures of +5 °C and melting snow conditions, the friction coefficient was highest at 500 N and decreased for normal loads above and below.

Tests with an in-house developed contact zone pressure rig showed a non-linear relationship between the apparent contact area and average contact pressure for increased normal loads. Moving the load application point changed the apparent contact area, and the average contact pressure, and shifted the load split and the spacing between the front and rear zones. The presented results give new insight into how a modern ski responds to loading, and how these changes in contact pressure profiles affect the coefficient of friction. This information should be considered in ski construction and racing.

## Funding sources

This work is funded by the Norwegian Research Council (NFR) through the Nano2Glide consortium, project number 296540.

## Declaration of Competing Interest

The authors declare that they have no known competing financial interests or personal relationships that could have appeared to influence the work reported in this paper.

## Data availability

Data will be made available on request.

## Acknowledgments

The authors would like to thank the Nano2glide consortium (Brav, Madshus, IDT Sports, Olympiatoppen and SINTEF). We would also like to thank the mechanical workshop at IBM-NTNU and the technical staff at the Department of Civil and Environmental Engineering for helping with the experimental work.

## References

Auganæs, S.B., Buene, A.F., Klein-Paste, A., 2022. Laboratory testing of cross-country skis – investigating tribometer precision on laboratory-grown dendritic snow. Tribol. Int. 168, 107451 https://doi.org/10.1016/j.triboint.2022.107451.

Bäckström, M., Dahlen, L., Tinnsten, M., Estivalet, M., 2009. Essential Ski Characteristics for Cross-Country Skis Performance (P251), pp. 543–549.

Bäurle, L., Szabó, D., Fauve, M., Rhyner, H., Spencer, N.D., 2006. Sliding friction of polyethylene on ice: tribometer measurements. Tribol. Lett. 24, 77–84. https://doi.org/10.1007/s11249-006-9147-z.

Bäurle, L., Kaempfer, T.U., Szabó, D., Spencer, N.D., 2007. Sliding friction of polyethylene on snow and ice: contact area and modeling. Cold Reg. Sci. Technol. 47, 276–289. https://doi.org/10.1016/j.coldregions.2006.10.005.

Bowden, F.P., Hughes, T.P., 1939. The mechanism of sliding on ice and snow. Proc. R. Soc. Lond. 172.

Breitschädel, F., Klein-Paste, A., Løset, S., 2010. Effects of Temperature Change on Cross-Country Ski Characteristics. Procedia Eng. 2, 2913–2918. https://doi.org/10.1016/j.proeng.2010.04.087.

Buene, A.F., Auganæs, S.B., Klein-Paste, A., 2022. Effect of Polydimethylsiloxane Oil Lubrication on the Friction of Cross-Country UHMWPE Ski Bases on Snow. Front. Sports Active Living 4. https://doi.org/10.3389/fspor.2022.894250.

Buhl, D., Fauve, M., Rhyner, H., 2001. The kinetic friction of polyethylen on snow: the influence of the snow temperature and the load. Cold Reg. Sci. Technol. 33, 133–140. https://doi.org/10.1016/S0165-232X(01)00034-9.

Colbeck, S.C., 1992. A Review of the Processes that Control Snow Friction.

Eriksson, R., Nupen, W., 1955. Friction of runners on snow and ice.

Federolf, P., Scheiber, P., Rauscher, E., Schwameder, H., Lüthi, A., Rhyner, H.-U., Müller, E., 2008. Impact of skier actions on the gliding times in alpine skiing. Scand. J. Med. Sci. Sports 18, 790–797. https://doi.org/10.1111/j.1600-0838.2007.00745.x.

Hasler, M., J. W, W. Nachbauer., 2021. Snow Temperature behind Sliding Skis as an Indicator for Frictional Meltwater. Front. Mech. Eng. 7, 738266 https://doi.org/10.3389/fmech.2021.738266.

Hoset, M., Rognstad, A., Rolvag, T., Ettema, G., Sandbakk, O., 2013. Construction of an instrumented roller ski and validation of three-dimensional forces in the skating technique. Sports Eng. 17. https://doi.org/10.1007/s12283-013-0130-2.

I. o. f. standardization, 1985. ISO 7140:1985 Cross-country skis — Determination of dynamic performance — Laboratory measurement method.

Kalliorinne, K., Hindér, G., Sandberg, J., Larsson, R., Holmberg, H.-C., Almqvist, A., 2023. The impact of cross-country skiers' tucking position on ski-camber profile, apparent contact area and load partitioning. Proc. Instit. Mech. Eng. Part P: J. Sports

Eng. Technol. https://doi.org/10.1177/17543371221141748, 17543371221141748.
Kietzig, A.-M., Hatzikiriakos, S.G., Englezos, P., 2010. Physics of ice friction. J. Appl. Phys. 107, 081101 https://doi.org/10.1063/1.3340792.
Lintzén, N., 2016. Properties of Snow with Applications Related to Climate Change and Skiing.
Moldestad, D.A., 1999. Some Aspects of Ski Base Sliding Friction and Ski Base Structure: Norwegian University of Science and Technology.
Mössner, M., Hasler, M., Nachbauer, W., 2021. Calculation of the contact area between snow grains and ski base. Tribol. Int. 163, 107183 https://doi.org/10.1016/j.triboint.2021.107183.
Mössner, M., Schindelwig, K., Heinrich, D., Hasler, M., Nachbauer, W., 2023. Effect of load, ski and snow properties on apparent contact area and pressure distribution in straight gliding. Cold Reg. Sci. Technol. 208, 103799 https://doi.org/10.1016/j.coldregions.2023.103799.
Moxnes, J.F., Sandbakk, O., Hausken, K., 2014. Using the power balance model to simulate cross-country skiing on varying terrain. Open Access J. Sports Med. 5, 89–98. https://doi.org/10.2147/OAJSM.S53503.
Nachbauer, W., Kaps, P., Hasler, M., Mössner, M., 2016. Friction between ski and Snow. In: Braghin, F., Cheli, F., Maldifassi, S., Melzi, S., Sabbioni, E. (Eds.), The Engineering Approach to Winter Sports. Springer New York, New York, NY, pp. 17–32.
Nilsson, J., Karlöf, L., Jakobsen, V., 2013. A new device for measuring ski running surface force and pressure profiles. Sports Eng. 16, 55–59. https://doi.org/10.1007/s12283-012-0109-4.
Schindelwig, K., Hasler, M., van Putten, J., Rohm, S., Nachbauer, W., 2014. Temperature Below a Gliding Cross Country Ski. Procedia Eng. 72, 380–385. https://doi.org/10.1016/j.proeng.2014.06.065.
Theile, T., Szabo, D., Luthi, A., Rhyner, H., Schneebeli, M., 2009. Mechanics of the Ski–Snow Contact. Tribol. Lett. 36, 223–231. https://doi.org/10.1007/s11249-009-9476-9.

# Paper III

Cold Regions Science and Technology 225 (2024) 104264

Contents lists available at ScienceDirect

Cold Regions Science and Technology

journal homepage: www.elsevier.com/locate/coldregions

# Experimental investigation into the effect of macroscopic cross-country ski parameters on gliding friction

Sondre Bergtun Auganæs [a,*], Audun Formo Buene [a,b], Alex Klein-Paste [a]

[a] Department of Civil and Environmental Engineering, Norwegian University of Science and Technology, Høgskoleringen 7a, 7034 Trondheim, Norway
[b] Department of Material Science and Engineering, NTNU, Sverres gate 12, 7012 Trondheim, Norway

ARTICLE INFO

*Keywords:*
Cross-country skiing
Friction testing
Ski-snow friction
Contact pressure
Load response
Ski design optimization

ABSTRACT

The complexity of the load response on a modern cross-country ski makes it difficult to address the individual macroscopic parameters' influence on ski-snow friction. In this study, a custom adjustable ski was developed to isolate the effect of normal force, apparent contact area, spacing and load split on the coefficient of friction. These parameters were tested in a ski-snow tribometer at relevant sliding speeds, normal loads, slider sizes and snow conditions for cross-country skiing. At cold air temperatures (−10 °C) the friction was governed by the average contact pressure, whereas at warmer air temperatures (−2 °C and + 5 °C) the friction was governed by the apparent contact area. Additionally, the effect of load split between the front and rear slider showed different trends depending on the temperature. Smaller spacing between the two sliders led to reduced friction across all temperatures. These findings provide new insights for optimizing cross-country ski gliding performance in various snow conditions.

## 1. Introduction

Cross-country skiing is a sport characterized by the interplay between human physiology, equipment mechanics, and the natural environment. At the interplay between equipment and environment lies the interaction between the skis and the snow surface they glide upon. Due to the arched profile of cross-country skis the magnitude and placement of the load on the ski is a decisive factor of how the ski distributes the load over the snow (Mössner et al., 2023). Auganæs et al. (2023) demonstrated that several tribological parameters such as the average contact pressure, apparent contact area and load split changed when either the load or the load application point on a cross-country ski was altered.

Various friction mechanisms contribute to the overall resistance of a ski sliding on the snow. These include compaction, micro-plowing, adhesion, viscous shearing, and water-bridging (Almqvist et al., 2022). Which of these mechanisms dominates the total friction depends on the friction regime the system operates within. Depending on the thickness of a (liquid-like) water layer on the ice grains, the friction regime can be dry, boundary, mixed or hydrodynamic (Kietzig et al., 2010). In the dry friction regime, there is predominantly solid-to-solid interaction. The friction originates from shearing the adhesive bonds between the tips of the snow asperities and wax on the ski base. In practice, truly “dry friction” seldom occurs in skiing because a molecular thin liquid-like layer is still present at the sliding interface even at the lowest temperatures relevant for ski races (Petrenko and Whitworth, 1999). The boundary friction regime is characterized by a liquid-like layer thickness of a few molecular layers. In this regime, the temperature of the ice contact spots is below the melting temperature (Kietzig et al., 2010). The thickness of the liquid-like layer is strongly dependent on temperature (Dash et al., 2006), but also on the counter material forming the interface (air or waxed UHMWPE in this case) (Makkonen, 2012).

In most cases, there will be a mix between some lubricated contacts and boundary lubrication. Boundary contacts dominate the first part of the slider before a gradual transition to mixed lubrication further back on the slider due to repeated frictional heating of contact points (Colbeck, 1992). Because of this, the coefficient of friction will vary along the ski. To be able to model the overall friction, the ski needs to be divided into segments where the friction force needs to be calculated with the correct parameters of water film thickness, normal load and real contact area (Nachbauer et al., 2016). These parameters are very hard to measure dynamically under real conditions with long skis at high speeds and loads, and varying snow conditions. Therefore, there is still disagreement around the real contact area and film thickness. Reported

* Corresponding author.
*E-mail address:* sondre.auganaes@ntnu.no (S.B. Auganæs).

https://doi.org/10.1016/j.coldregions.2024.104264
Received 12 February 2024; Received in revised form 9 May 2024; Accepted 27 June 2024
Available online 29 June 2024

values for the relative real contact area range from 0.4 to 7% during static experiments (Bäurle et al., 2007; Mössner et al., 2021; Theile et al., 2009), up to almost 100% during dynamic sliding at high speed of 25 m/s or snow temperatures close to 0 °C (Bäurle, 2006; Hasler et al., 2021).

Several studies of sliders on ice have investigated the reduction in the coefficient of friction (μ) by increasing normal force (Bowden and Hughes, 1939; Buhl et al., 2001; Bäurle et al., 2006; Scherge et al., 2013). The effect is explained as increased frictional power per area, which leads to a faster transition to lubrication along the slider (Bäurle et al., 2006). Another way to increase the frictional power per area is to reduce the apparent area of contact. Bäurle et al. (2006) reported a decrease in the coefficient of friction as a result of this approach. Their results indicate that increasing the average contact pressure is beneficial for the reduction in friction, at least for temperatures below −5 °C. However, most of these measurements were conducted on ice, which is a harder material compared to snow. In the context of snow, an increase in contact pressure is only advantageous in the range where the bearing surface possesses sufficient strength to support the ski base without undergoing substantial deformations.

The question of whether compaction holds a significant relevance for cross-country skiing within groomed tracks is a subject open to debate. The study conducted by Theile et al. (2009) shed light on this aspect by revealing that the snow's compaction due to repeated loading amounted to merely 20 μm, and the energy expended in this compaction process contributed to only 0.1% of the overall friction. However, it's worth noting that the snow utilized in their study was very hard, exhibiting a Young's modulus of 1200 MPa. This significantly surpasses the 100–250 MPa range identified for machine-made snow in the uniaxial compression study by Lintzen and Edeskär (2014). Additionally, Hasler et al. (2022) conducted a study on snow wear, revealing that during the initial ski run, the snow experienced compaction of 0.5–1.0 mm, whereas subsequent runs showed minimal to no additional permanent compaction. This also points towards a lesser influence of compaction in the total frictional resistance of a ski.

Recent studies have shed light on how the load response on modern cross-country skis leads to simultaneous changes of several parameters on the macro level (Auganæs et al., 2023; Kalliorinne et al., 2023; Mössner et al., 2023). These parameters include apparent contact area, average contact pressure, peak pressure, distance from load application to center of pressure, load split or load partitioning, and the distance between the contact zones. In our previous work, we discussed some of these parameters in connection to friction results but acknowledged that it was difficult to explain the response of each parameter because of the interconnected response of these parameters.

To address this complexity, the present study investigates the impact of these ski parameters on the friction coefficient by individually isolating each parameter using an adjustable test ski. This is done at relevant speeds, loads, apparent contact areas and snow conditions for cross-country skiing. This approach aims to provide a better understanding of how the cross-country ski design affects friction.

## 2. Method

This section is divided into three parts. 1) Development of an adjustable test ski, 2) The protocol for friction measurements with the adjustable test ski, and 3) Preparation of ski and snow surface.

### 2.1. Development of an adjustable test ski

To gain insights into the friction response of the macroscopic parameters it was essential to isolate and control individual variables while keeping others constant. To accomplish this, we constructed a rigid ski using a 1.6-m Rexroth aluminum profile. This ski allowed us to attach 3D-printed sliders of various lengths (20 cm, 30 cm, or 40 cm) and a width of 4.5 cm underneath, as depicted in Fig. 1. The design allowed variation of the normal load and load application point, without affecting the contact area, load split, or spacing between the front and rear slider.

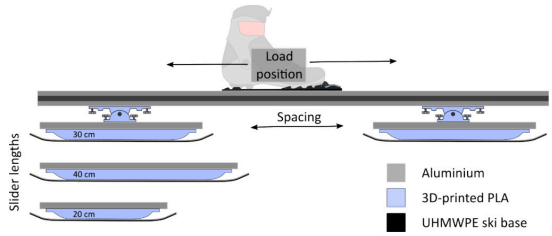


**Fig. 1.** Schematic of the fully adjustable test ski, enabling modifications to the length of contact zones, spacing and load application point.

To overcome the initial challenges posed by beam flexing and subsequent plowing, we implemented a design modification by establishing load transfer points at the center of each slider through hinged connections. To prevent a too abrupt buildup of pressure, we introduced 2 mm thick aluminum sheets beneath each slider, extending 5 cm beyond both the front and rear portions. This ensured a more gradual pressure increase, thereby contributing to more stable track conditions. Fig. 2 shows the measured pressure profiles across the various sliders, providing a visual representation of pressure profiles. As outlined in our previous paper the measured deformation of the load cells (counter surface) corresponds to a snow hardness of 0.45–0.9 $Nmm^{-3}$ (Auganæs et al., 2023).

Additionally, we applied an ultra-high molecular weight polyethylene (UHMWPE) ski sole material beneath the metal sheets and secured it with double-sided tape. The sole material was not stone-grinded or structured. The surface roughness of the sole material was assessed using a non-destructive elastomeric 3D imaging system (GelSight mobile, GelSight, USA), revealing an average surface roughness (Sa) value of 1.10 μm.

### 2.2. Friction measurement protocol for the adjustable test ski

Friction measurements were conducted using the full-scale linear tribometer, where the adjustable ski was driven across the 6.5 m long snow track. Detailed information regarding the configuration and accuracy of the tribometer can be found in the prior study by Auganæs

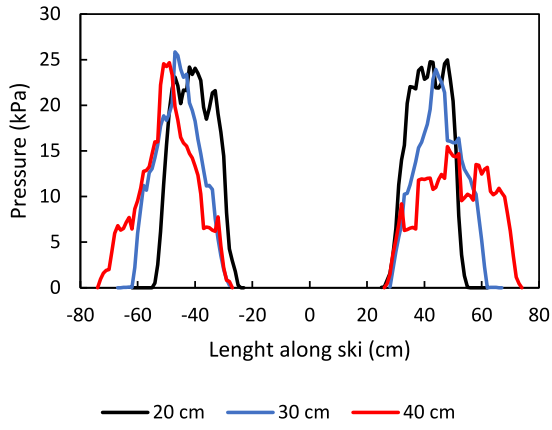


**Fig. 2.** Pressure profiles for the different slider configurations on the adjustable ski. The profiles were measured with a normal force of 370 N on the ski, with the load application point at 0 cm (midpoint). Note that negative values represent positions behind the midpoint of the ski.

et al. (2022), while the updated data acquisition system is elaborated upon in the work of Buene et al. (2022). The coefficient of friction is determined by averaging the force measurements obtained from a horizontal load cell (S2M 100 N, HBM, Germany) and dividing this value by the force measured using two vertical load cells (U9C 1 kN, HBM, Germany).

Before each test series, a run-in protocol was carried out using a skate cross-country ski. This protocol involved gradually increasing the normal load from 100 N to 400 N and subsequently ramping up the speed from 1 m/s to 5 m/s. Subsequently, the adjustable test ski was mounted in the rig, and run in by ramping the normal load up to 800 N, before the specific parameters such as normal force, apparent contact area, load split, or spacing were tested. Table 1 presents a detailed overview of the range of the test parameters along with the respective values of the isolated variables.

To reduce the differences in impact from the decreasing friction with run number (polishing trend) on our data, all test configurations (the various loads, areas, load splits, or spacings) were cycled/repeated three times to distribute the effects of polishing between the test configurations. During the tests, track polishing was observed by a decreasing coefficient of friction for each cycle. This was corrected for using a linear fit of the polishing for each series. More details on the post-processing procedure of friction data to correct track polishing can be found in the supporting information.

*2.2.1. Average contact pressure (normal force and apparent contact area)*

To investigate the effect of average contact pressure between ski and snow, either the normal force or the apparent contact area could be altered while keeping the other constant. To evaluate the effect of normal force, the slider area was kept constant while incrementally varying the applied force. This process involved incremental steps of 100 N, decreasing from 800 N to 300 N, with three runs on each load. This cycle was then repeated three times so that the number of runs on each load was nine.

The experiments focused on normal force were carried out separately for different contact areas. This resulted in distinct normal force curves for each of the three apparent contact areas, namely 180 $cm^2$, 270 $cm^2$, and 360 $cm^2$.

Since the test of the different contact areas was performed on separate snow tracks (0.018 $m^2$ in the inner track, 0.027 $m^2$ in the middle track and 0.036 $m^2$ in the outer track), a notable challenge arose due to the varying friction levels associated with these track changes. To address this issue, we used a cross-country ski as a reference before each test to determine the relative difference in the friction between the tracks. This relative difference was then utilized to adjust the friction coefficient either upwards or downwards for the subsequent measurements on the other tracks. The quantified differences are presented in Table 2.

We encountered a particular challenge at melting temperatures where the snow track experienced notable alterations over a 2-h testing period, leading to a 33% variance as indicated in Table 2. These major changes brought into question the reliability of using a reference ski under such fluctuating conditions. As a response, we initiated a new series of tests, adjusting both the normal load and the contact area on the same snow track. These modified tests produced distinct outcomes, which are detailed as the results for warm conditions. Our test sequence consisted of three runs each at normal loads of 900 N, 600 N, and 300 N using the 40 cm slider, followed by the 30 cm and 20 cm sliders. This cycle was repeated three times to ensure triplicate data for each configuration.

**Table 1**
Overview of experimental test variables and their selected values.

| Test variable | Normal force (N) | Area ($m^2$) | Load split (%) | Spacing (cm) |
|---|---|---|---|---|
| Normal force | **300–800** | 0.018–0.036 | 50 | 60 |
| Contact area | 300–800 | **0.018–0.036** | 50 | 60 |
| Load split | 400 | 0.027 | **5–95** | 60 |
| Spacing | 400 | 0.027 | 50 | **20–100** |

The tested range for each variable is highlighted, while the other variables were kept contestant.

**Table 2**
The initial difference in friction coefficient between the tracks measured with a reference ski.

| Snow track | Inner | Middle | Outer |
|---|---|---|---|
| Reference μ at −10 °C | 0.0567 | 0.0538 | 0.0482 |
| Difference (%) | +5.1 | – | −11.6 |
| Reference μ at −2 °C | 0.0439 | 0.0431 | 0.0423 |
| Difference (%) | +1.8 | – | −1.9 |
| Reference μ at +5 °C | 0.0439 | 0.0617 | 0.0636 |
| Difference (%)[a] | −33.4 | – | +2.9 |

The middle track was established as the baseline value (zero). A negative value indicates a 'slower' track, and the friction coefficient for the subsequent measurement series was reduced by the same amount. Conversely, a positive value signifies a 'faster' track, and the friction coefficient for the subsequent series was increased accordingly.

[a] Due to the large observed deviation between the track at this temperature, the friction data was removed from the analysis. Consequently, a different testing procedure was selected for this specific temperature condition.

*2.2.2. Load split*

The effect of load split was tested with 30 cm sliders (area = 270 $cm^2$) and a 60 cm spacing on the adjustable test ski. The load application point was moved in steps of 15 cm over the entire length of the ski. The load split corresponding to a given load application point was measured in the pressure profile rig and found to be symmetrical, as seen in Table 3. The measurements were performed in the following test order of load split (front/rear); 50%, 66%, 81%, 94%, 34%, 20%, 4%. This cycle was then repeated three times to get nine runs in each position.

*2.2.3. Spacing*

The distance between the end of the front zone and the start of the rear zone is referred to as the spacing parameter. The effect of spacing was tested with 30 cm sliders (area = 270 $cm^2$) and a normal load of 400 N. The spacing was altered in the range of 20 to 100 cm in the following testing order 60, 40, 20, 80, and 100 cm. This cycle was repeated three times to get nine runs in each position.

*2.3. Preparation of ski and snow surfaces and meteorological parameters*

To ensure consistent and lower glide friction of the adjustable test ski and the reference ski, they underwent a cleaning and waxing procedure before each test. Swix$^{tm}$ base cleaner was applied and allowed to dry for 5–10 min. Then, a dry Fiberlene cloth was used to wipe the ski's sole clean. A liquid wax spray was applied and allowed to dry for 15 min. The used wax was Swix$^{tm}$ HS6, HS7 or HS8, respectively for the cold, intermediate and warm test conditions. Finally, the ski soles were polished using a roto nylon brush, brushing at a rate of 1500 rpm and moving

**Table 3**
Measured load split for the different load application points, with an applied force of 370 N plus 22 N as the specific weight of the adjustable ski.

| Load application point (cm from midpoint) | Front slider force (N) | Back slider force (N) | Load split (%) |
|---|---|---|---|
| 45 | 380 | 12 | 94.1 |
| 30 | 319 | 73 | 81.3 |
| 15 | 257 | 135 | 65.5 |
| 0 | 197 | 195 | 50.2 |
| −15 | 133 | 259 | 33.9 |
| −30 | 76 | 316 | 19.5 |
| −45 | 16 | 376 | 4.1 |

back and forth at a speed of approximately 0.5 m/s.

Three different snow conditions were chosen based on temperature regimes where different responses on friction can be expected (Kietzig et al., 2010). The preparation of the dendritic snow track at a temperature of −10 °C (denoted "cold conditions") followed the methodology outlined in a prior study by Auganæs et al. (2022). In brief, dendritic snow was produced under −20 °C conditions. The freshly produced snow was then uniformly distributed in the testbed and compacted by passing a 30 cm wide compaction board over the snow at a speed of 0.5 m/s and a normal load of 800 N. This compacted snow was subsequently allowed to sinter for 16 h. Each snow bed consisted of four individual tracks. The same procedure was used for preparing the track for intermediate conditions ($T_{snow}$ = −2 °C). This left a 1 cm thick layer of new snow atop a 4 cm thick base layer of hard snow/ice.

Preparing the snow track for warm conditions ($T_{snow}$ = 0 °C, $T_{air}$ = +5 °C) involved removing the top layer of snow from prior testing for sieving. The sifted snow was then reintroduced into the track and leveled with a steel blade. Then the snow was allowed to sinter for 16 h at a temperature of −2 °C. Four hours before testing, the air temperature was adjusted from −2 °C to +5 °C, leading to increased humidity and water content in the upper layer of snow.

The snow's characteristics were evaluated by measuring the snow surface before starting a test. The snow temperature was measured at the midpoint of the track, as well as the snow density and humidity for 6 spots with 0.5 m intervals using SLF snow sensor (FPGA company GmbH, Switzerland) and Doser snow moisture meter 011 (GmbH, Germany). The characteristic values shown in Table 4 are the average for three separate tracks under cold and intermediate conditions, and two tracks under warm conditions.

To measure the hardness of the snow surface, we conducted tests using a 3D-printed hemisphere with a diameter of 20 mm. This hemisphere was dropped from a height (h) of 48 mm and a weight (m) of 76 g. The penetration distance into the snow ($S_{dyn}$) was read from a pipe connected to the hemisphere, with markings for each millimeter. Based on these measurements, we calculated the penetration resistance (PR) using the following formula:

$$PR = \frac{m^{*}g^{*}h}{S_{dyn}} + m^{*}g$$

The hardness of a material can be defined as the reaction force per penetration depth, per contact area or volume displaced (Mössner et al., 2013). The hardness was then calculated as:

$$H = \frac{PR}{A}$$

Where A is the surface area of the 3D-printed hemisphere in contact with the snow.

**Table 4**
Measured snow parameters at the different temperatures.

| | Cold | Intermediate | Warm |
|---|---|---|---|
| Snow temperature (°C) | −10.4 ± 0.2 | −2.5 ± 0.2 | 0 |
| Air temperature (°C) | −9.9 ± 0.3 | −2.1 ± 0.3 | 5.2 ± 0.4 |
| Density (kg/m$^3$) | 405 ± 43 | 438 ± 65 | 692 ± 80 |
| Doser snow humidity (%) | 18 ± 2 | 20 ± 2 | 67 ± 12 |
| Snow hardness (N/mm$^2$) | 0.464 ± 0.13 | 0.153 ± 0.027 | 0.085 ± 0.015 |

For each temperature, the average value is calculated from measurements in three separate tracks (tracks 1–3).

## 3. Results

### 3.1. The effect of apparent contact area (contact length)

Fig. 3 shows the experiments conducted for three different apparent contact areas. For all three snow conditions, the friction was significantly higher for the longest sliders (360 cm$^2$), compared to the shortest sliders (180 cm$^2$). Notably, a consistent and steady trend in friction was evident for both cold (−10 °C) and warm conditions (+5 °C). However, in the case of intermediate conditions (−2 °C), a slight decrease in friction was observed when transitioning from the 180 cm$^2$ contact area to the 270 cm$^2$ contact area. Subsequently, there was a substantial increase in friction when moving to the largest contact area of 360 cm$^2$. The relative difference in the coefficient of friction, achieved by doubling the apparent contact area, amounted to 14%, 20%, and 16% at temperatures of −10 °C, −2 °C, and + 5 °C, respectively.

### 3.2. The effect of normal load

Fig. 4 shows the effect of normal load on the friction coefficient. As anticipated, the highest friction occurs at the coldest temperature, while the lowest is found at the intermediate temperature. For the coldest condition, there was a clear decreasing trend as the load increased. Only at the highest load does the trend become discontinued. A relative difference in friction of 18% was found by increasing the load from 300 N to 700 N. At melting conditions, there is a friction minimum at 500 N, with increasing friction for higher and lower loads. At intermediate conditions, the trend shows little or no effect of normal load on the friction coefficient, except for the highest load of 800 N where the friction increased.

### 3.3. The effect of average contact pressure

The friction as a function of both load and area is plotted in Fig. 5. The corresponding contact pressures are indicated by the black isobar lines. At the coldest temperature, a notable observation is the correlation between contact pressure and friction. Here, the highest friction is associated with regions of low contact pressure, while the lowest friction is found at high contact pressures. The friction contour lines align closely with the contact pressure lines, particularly in areas of low contact pressure.

At intermediate temperatures, friction was more dependent on the

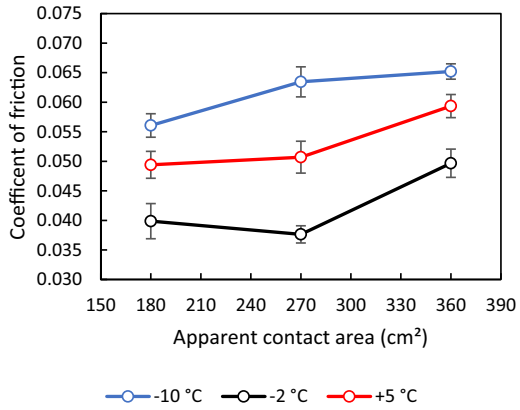


**Fig. 3.** The effect of apparent contact area on the coefficient of friction at three different temperatures. Each data point represents the average of the different tested loads and the error bars represent ±1 standard deviation from the mean. The testing speed was 5 m/s.

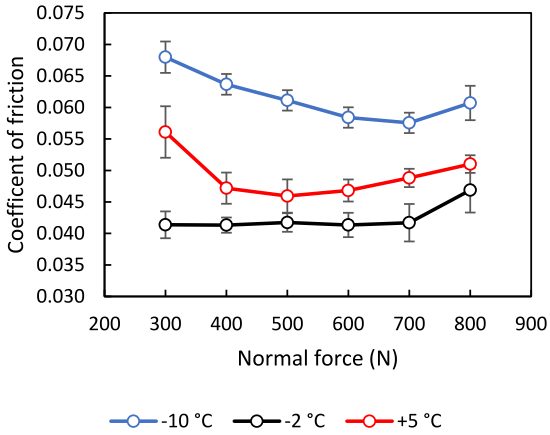


**Fig. 4.** The effect of normal force on the coefficient of friction at three different temperatures. Each data point is the average result calculated from three different apparent contact areas, totaling 27 runs per data point. Error bars indicate one standard deviation in both directions. The testing was conducted at a speed of 5 m/s.

contact area than the normal force. The friction was highest for the combination of high load on a large contact area and decreased towards a minimum for an area of 270 $cm^2$ and a normal load of 600 N.

Under melting conditions, there is a pronounced correlation between the apparent contact area and friction coefficient. As illustrated in Fig. 5, the highest friction corresponds to the largest area, and friction drops towards smaller areas. Again, the lowest friction is observed in the region between 180 $cm^2$ and 270 $cm^2$ with a normal force of 600 N.

### 3.4. The effect of load split

As the load application point is moved along the ski, the respective load split between the front and rear slider changes. Fig. 6 illustrates the impact of this load split on the coefficient of friction, analyzed for the three snow conditions. A load split of 95% indicates that the entire load is concentrated on the front slider and the weight of the test ski accounts for the rest.

Under cold conditions, the lowest friction occurs when the load is positioned over either the front or rear slider, as depicted in Fig. 6. This suggests that concentrating the load over one slider is beneficial. This observed benefit of higher contact pressure is consistent with the earlier shown dependence of contact pressure in Fig. 5. Additionally, the data indicate that having more of the load split towards the front from the midpoint reduces friction compared to having more of the load split towards the rear slider. A relative difference of around 7% is the result of changing the load split from 35% to 65%.

At intermediate temperatures, we noticed a trend where friction increases when the load is shifted from the rear towards the front slider, reaching its peak with the entire load over the front. This shift corresponds to a notable relative difference in friction of approximately 17%.

Under warm conditions, the friction exhibits a minimum value at a 50% load split. Intriguingly, as the load is moved either towards the front or the rear, friction increases, but there is a slight decrease again when the entire load is placed over one slider. This trend is relatively symmetric, indicating that there is no significant difference in whether the load is moved forward or backward from the midpoint.

### 3.5. The effect of spacing between contact zones

The effect of spacing shown in Fig. 7, reveals a slight but rather consistent upward trend in friction with increased spacing across all

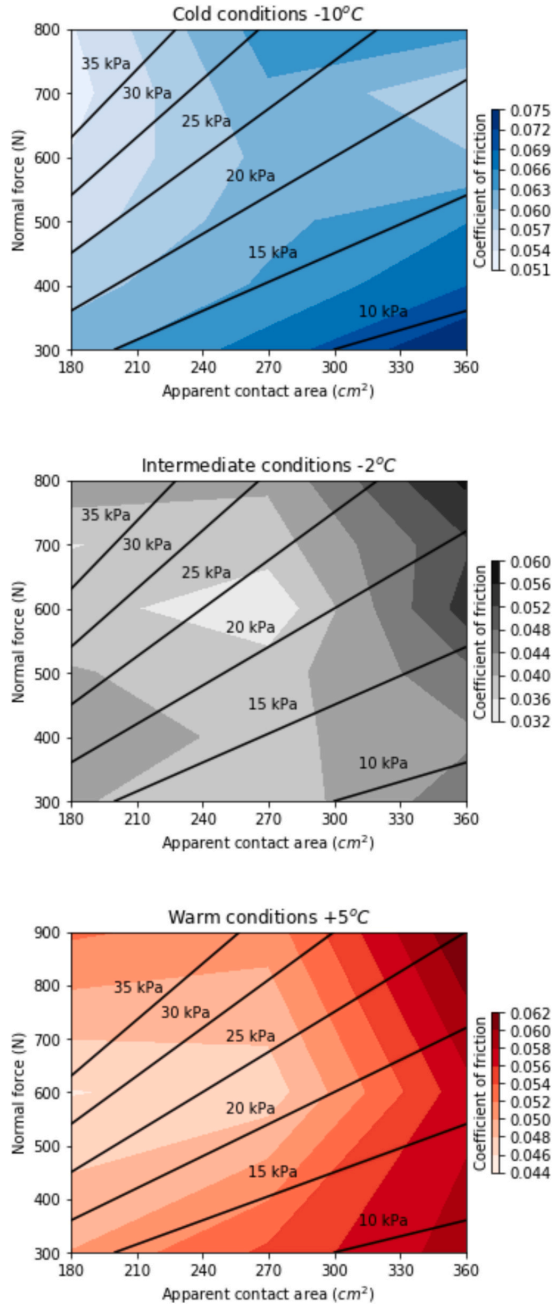


**Fig. 5.** These contour plots illustrate the relationship between the coefficient of friction, normal force, and apparent contact area. The isolines on the plot represent levels of average contact pressure. Each contour line connects points with the same friction coefficient value, providing a visual representation of how friction changes with variations in normal force and contact area. The testing for this data was conducted at a constant speed of 5 m/s.

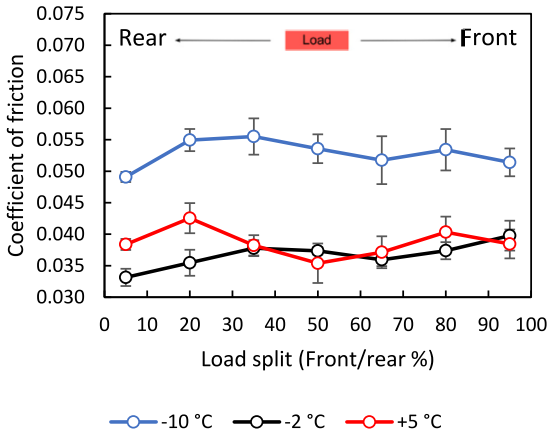


**Fig. 6.** The effect of load split between the front and rear slider (5% equals all the load over the rear slider). The tests were conducted using 30 cm sliders, a normal load of 400 N, and a speed of 5 m/s. Error bars represent one standard deviation in both directions.

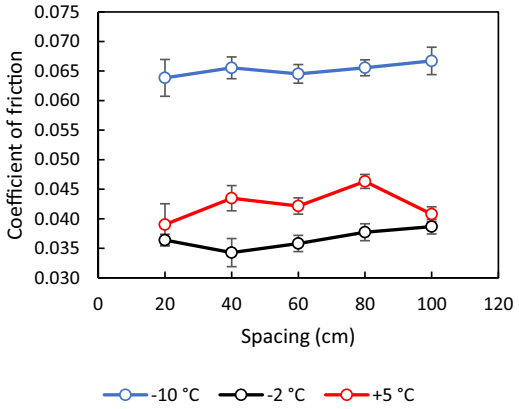


**Fig. 7.** The effect of spacing between the front and rear slider on the friction coefficient at a speed of 5 m/s and a normal load of 400 N. The error bars represent one standard deviation in each direction.

temperatures. This trend is notably consistent under cold and intermediate conditions. Specifically, under cold conditions, we observed a relative change in the coefficient of friction of approximately 5% when the spacing was increased from 20 cm to 100 cm. However, a trend at the warmest temperature is not as clear. This suggests the possibility of different factors influencing spacing under warmer conditions, or that there is less influence of spacing at this temperature.

## 4. Discussion

### 4.1. Method evaluation

Conducting multiple friction measurements with a ski sliding over the same snow surface poses a challenge due to gradual alterations in the snow caused by mechanisms like abrasion and friction-induced melting (Hasler et al., 2022). These changes typically lead to a reduction in the measured coefficient of friction with each successive pass of the ski. To address these changes, we implemented a sequential test order, aiming to evenly distribute the polishing effect across various skis while balancing this against the added uncertainty and additional time associated with manual changes. Additionally, we utilized the linear trend line of the series to correct the data based on the run number. This post-processing involved adjusting the original data by "lifting" it to the same level as the first run in the series. One of the primary advantages of this correction was to mitigate the impact of polishing on the averages and standard deviations between the skis. Without this correction, the effect of run order would influence the average, particularly for series with a high polishing effect.

The slope of the polishing curve depends on the friction level of the ski-snow system. A higher-friction ski-snow system exhibits a more pronounced decrease in the coefficient of friction with each subsequent run. For instance, in the load dependence test at −10 °C, the series with the most pronounced polishing had a relatively high coefficient of friction of around 0.06, which decreased by an average of 25% after 54 runs. In contrast, at −2 °C, the ski had a lower friction level of approximately 0.04 and experienced a 6% reduction over the same number of runs. The observed trend in polishing may be better characterized by an exponential rather than a linear function, as explained in Auganæs et al. (2022). Initially, the rate of change in friction due to polishing is rapid, but this rate gradually diminishes over time, suggesting that the system approaches a limit where further runs do not significantly change the surface, or the system reaches some sort of equilibrium. However, within a certain range, the polishing trend can still be approximated with linear behavior.

An action to mitigate the effect of polishing could thus be to run in the track until the coefficient of friction stabilized. However, we argue that this would reduce the transferability or accuracy of the results to a skiing competition, as it would be more equal to testing on an ice track. The run number at which the track best simulates race conditions will also depend on various factors such as the number of laps and athletes, snow type, and weather conditions during the race. Moreover, conducting more than 150 runs before starting each test would be time-consuming.

In the ski comparison example outlined in the supporting information a distinct pattern emerged: the relative differences between the skis diminished with each cycle. Notably, the variations between the skis in the final cycle were significantly less pronounced than those in the initial cycle. This observation suggests that conducting tests on excessively polished or icy surfaces may not accurately reflect a ski's performance. We propose that averaging trial one, two and three offer a reasonable compromise, which distributes the variance of the snow track over all the samples in the testing matrix. We argue that the main objective with laboratory testing is to reduce uncertainties in glide testing to find significant trends, rather than simulating the snow conditions of a race. In this regard, laboratory testing represents a balance between accuracy and precision.

The coefficient of friction observed in all tests was high compared to some findings in existing literature. We attribute this elevated friction level to several factors. Firstly, the sole material not being structured may have contributed to some degree. A comparison to our previous study, Auganæs et al. (2023), where a race-ground cross-country ski was utilized under similar snow conditions, revealed a lower friction coefficient of approximately 0.04 at −10 °C. Furthermore, the utilization of dendritic new snow likely raised friction levels beyond those typically observed in the literature. The increased friction of dendritic snow surfaces can be attributed to the additional work required for compression and/or fracture of large grains, contrasting with older snow that has undergone some degree of metamorphosis. However, the coefficient of friction level of 0.06 is in line with the results of Buhl et al. (2001) at the same temperature of −10 °C, and the friction level of 0.04 at −2 °C are in line with the by Hasler et al. (2016). This just underlines that the absolute level of friction coefficient is dependent on the system of snow and ski used (load, temperature, humidity, snow type, speed, slider configuration etc.), and this varies a lot in the literature.

### 4.2. Cold temperatures

The highest friction levels (up to μ = 0.07) were observed at the lowest temperature of −10 °C. This was expected because, at such low temperatures, the liquid-like layer on the snow surface is thinner, leading to the initial contact between the ski and snow that primarily consists of boundary contacts. In this friction regime, the contacts have higher friction force due to stronger surface adhesion bonds (Kietzig et al., 2010). As the ski slides over the snow, making repeated contact with ice asperities, frictional heat is generated. This heat, in turn, increases the thickness of the liquid-like layer, thereby reducing friction (Bowden and Hughes, 1939).

The amount of frictional power (J/s) generated by the ski is the product of the normal force, the speed of the ski and the coefficient of friction. A higher frictional power results in more energy being transferred to the snow per time unit. This is also the explanation for why studies have shown a lower coefficient of friction for higher sliding speeds or normal force at cold temperatures (Bäurle et al., 2006; Oksanen and Keinonen, 1982).

#### 4.2.1. The effect of normal load, apparent contact area and average contact pressure

The measurements at the coldest temperature (−10 °C) showed a clear relationship between the average contact pressure and the coefficient of friction. One way to alter the contact pressure is through the normal force, a relationship that has been previously established in cold conditions by studies such as Oksanen and Keinonen (1982) and Buhl et al. (2001).

Another way to alter contact pressure is by adjusting the apparent contact area of the ski or slider. Although early experimental results by Bowden and Hughes (1939) suggested that the apparent contact area had no impact on the coefficient of friction, later research by Bäurle et al. (2006) contradicted this by demonstrating that a smaller apparent contact area led to a lower coefficient of friction. They explained this phenomenon by noting that the frictional energy released per unit area is greater for a slider with a higher normal force or a smaller apparent contact area.

In other words, this means that a higher average contact pressure is beneficial for increased frictional power per area. Theoretically, an increase in the average contact pressure could result in the following scenarios regarding the contact spots:

1. The number of contact spots remains constant; therefore, existing contacts need to carry a higher load, which in turn leads to more heating of these contacts.
2. The number of contact spots increases and the load is divided equally among new and existing contacts. Therefore, each contact will carry the same load as before, which leads to the same degree of heating.

In practice, a real scenario is likely a combination of these two, influenced by the roughness and hardness of the interacting surfaces, as illustrated in Fig. 8. The elevated contacts on the snow surface will experience higher pressure as the ski compresses the snow matrix, while compression of the snow will also lead to the formation of additional contacts. The initial contacts subjected to higher pressure will consequently experience more heating, which can facilitate improved lubrication.

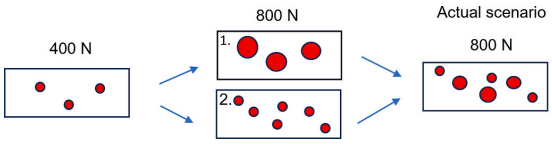


**Fig. 8.** Example of development of contact points on the snow surface when doubling the normal load. The same would apply for reducing the apparent contact area.

While numerous studies have manipulated either the load or the contact area (Bowden and Hughes, 1939; Buhl et al., 2001; Bäurle et al., 2006; Oksanen and Keinonen, 1982), less attention has been directed towards the combined effects (contact pressure) on friction. As per the explanation proposing increased frictional heat per unit area, it appears insignificant how the average pressure is modified. This holds when observing the lowest contact pressures in Fig. 5. In this study, we observed a relative decrease of 14% in the coefficient of friction when the contact area was reduced from 360 $cm^2$ to 180 $cm^2$, or when the normal force was increased from 300 N to 600 N. However, for the highest contact pressures, a more notable impact stems from the reduction of the apparent contact area. The same observation can be found in the study of Bäurle et al. (2006), where a 35% relative reduction in the coefficient of friction is evident when the contact area was reduced from 2 $cm^2$ to 0.8 $cm^2$. In contrast, when Bäurle et al. (2006) increased the load from 21 N to 52 N it resulted in a comparatively smaller 19% reduction in coefficent of friction. However, it should be noted that they changed the area by increasing the width of the slider and not the length. By changing the width of the slider the added area will not slide over the same snow contact points, as opposed to when the length is changed. When the area is increased by changing the length the added area might benefit from pre-heated contact points, and thus the friction would not increase as much. This might be the reason Bäurle et al. (2006) observed a larger drop in the coefficient of friction by changing the apparent contact area. They also operate with a pin-on-disc setup and higher pressures compared to the present study.

The results obtained from the load split measurements at cold temperatures further emphasize the advantage of higher contact pressure, as discussed earlier. We observed reduced friction when the majority of the load (80% or more) was concentrated on one of the two sliders. Additionally, a decreasing friction trend became evident as the load was shifted from 20% over the front slider progressively to 95% over the front slider. Our results provide some experimental evidence of the hypothesis proposed by Moldestad (1999). He suggested that in the case of cold temperatures or low snow humidity, it would be beneficial to induce higher pressure at the start of the contact area on the forebody (front zone). This approach decreases the contact area with boundary friction by promoting the development of a liquid-like layer. Consequently, the remaining part of the ski (rear slider) will experience reduced friction. This finding contributes to our understanding of optimal load split during skiing in cold weather conditions.

### 4.3. Intermediate temperatures

The measurements conducted at a temperature of −2 °C showed the lowest friction levels. Under these conditions, the friction is believed to be around a minimum due to the snow grains already having a thicker liquid-like layer (Kietzig et al., 2010). Given this understanding, one might expect that the influence of variations in the normal load or the apparent contact area on the friction coefficient would be less pronounced compared to colder conditions. Notably, it was observed that the coefficient of friction remained unchanged regardless of variations in the normal load. However, what was somewhat unexpected was the large influence of the apparent contact area on the friction coefficient under these conditions.

Comparing our findings to the research of Bäurle et al. (2006), conducted at intermediate temperatures of −5 °C, they also reported a dependence of the friction coefficient on the apparent contact area. Their study particularly highlighted that this influence was most significant for smaller areas with high contact pressure. Conversely, they observed that the influence of contact area on the friction coefficient diminished and eventually stabilized at larger contact areas, specifically when the contact pressure reached 100 kPa or lower. Following this line of reasoning, it can be inferred that the impact of the apparent contact

area should be relatively small when the contact pressure is below this value, which was not observed in the current study.

The findings on load split at intermediate temperatures revealed that shifting the load application point towards the rear slider led to reduced friction. Contrary to cold temperatures, the liquid-like layer at these milder conditions is presumed to be near optimal thickness. Consequently, when additional load is moved to the front slider, increased frictional work occurs in this region, potentially leading to a thicker liquid film. This increased film thickness could, in turn, raise the friction for the rest of the slider a situation that inversely mirrors the behavior noted in colder temperatures.

### 4.4. Warm temperatures

For the measurements conducted under warm temperatures, a noticeable correlation emerged between the friction coefficient and the apparent contact area. This correlation can be explained by viscous friction through excess water being present on the surface. Viscous shear is a frictional force that relies on several factors, including the real contact area ($A_r$), the velocity of relative motion ($v$), the viscosity of the fluid ($\eta$), and the separation distance between the surfaces ($h$, often described as the film thickness of the lubricating layer). The friction force can be expressed as:

$$F_{viscous\ shear} = \frac{A_r \acute{\eta} v}{h}$$

When excess water is present, we assume that the ski base structure is filled with water, and the relative real contact area is close to 100%. In this situation, friction is largely dependent on viscous shear, and the extent of the apparent contact area between the surfaces plays a pivotal role in determining the friction coefficient. This is particularly relevant in situations where there is a significant temperature fluctuation in the snow, such as transitioning from sub-zero temperatures during the night to above-freezing during the day. In such scenarios, the surface snow is likely to contain some free water while the temperature of the bulk snow still is cold and thus retains its strength.

By increasing the load with a constant area, the friction force should remain constant if the relative real contact area is close to 100%. If the friction force is constant while the normal force is increased, the result is a reduction in the coefficient of friction. This trend is seen for the lower normal forces of 300–500 N when looking at Fig. 4, where the friction coefficient drops to a minimum point around 500 N. Beyond this point, the coefficient of friction starts to increase again. A possible explanation for this could be the effect of squeezing out water between the contacts due to higher pressure (Bäurle, 2006). The squeeze-out will reduce the film thickness between the ice asperities and the ski base leading to a higher viscous shear force. The removal of water with low viscosity might increase the viscosity of the remaining lubrication layer, due to the higher viscosity of the liquid-like layer (Dash et al., 2006). Higher viscosity will also increase the shear friction.

Additionally, an interesting observation arises from the results of load split. There is a distinct advantage in maintaining a balanced load split of 50/50 between the two sliders. This can be explained by the load dependence graph shown in Fig. 4, which illustrates a minimum point in friction occurring at around 500 N. In the load split test, a total load of 400 N was used, equating to 200 N on each slider for a 50% load split. Deviating from this 50% split increases the coefficient of friction for the slider bearing less load, while only marginally decreasing it for the slider with more load. For instance, comparing the average friction coefficient at 300 N and 500 N (corresponding to 150 N and 250 N on each slider, respectively) with 400 N (200 N on each slider) demonstrates that the average friction coefficient for 300 N and 500 N is higher than that for 400 N.

### 4.5. The effect of spacing

The spacing between the contact zones determines the duration between the front and rear slider's contact with the surface on a gliding ski. Our measurements across three different temperatures showed an increase in friction with longer spacing. A possible explanation for this can be attributed to the snow having more time to cool between the passes of the front slider until the rear slider passes the same snow asperities. After the front slider passes, certain contact spots heat up, and before the rear slider follows, these spots have time to cool down. However, the time difference between the sliders' contact varies only from 0.04 s to 0.2 s, corresponding to spacings from 20 cm to 100 cm spacing (at a speed of 5 m/s). Whether this short variance in cooling time could result in an overall 5% increase in total friction is questionable.

Hasler et al. (2021) observed a rapid exponential decrease in snow temperature from −1.5 °C to −3.4 °C, within the first 4 s after a ski pass. Although this duration is considerably longer than the interval between the sliders in our study, it suggests that a short cooling duration affects the average snow temperature and might affect the friction to some degree. However, evidence challenging this explanation lies in the almost identical trend observed for both cold and intermediate conditions. Had the cooling effect been a predominant factor, a more pronounced increase in friction would likely have been observed in colder conditions.

An alternative explanation involves the energy dissipation during the compression work of the snow matrix. Snow exhibits a delayed elastic response, indicating that compressed snow requires time to restore its initial shape (Theile et al., 2009). Therefore, the duration between the front and rear slider could impact the extent of snow recovery. A longer duration allows for greater recovery, implying that the rear slider must perform repeated compression work. For instance, a complete recovery of the snow would necessitate the ski to compress the snow twice, implying that the rear slider performs the same compression work as the front slider. In the study by Theile et al. (2009), the measured delayed elastic recovery of snow after repeated loading was 20 μm, observed for a contact pressure of up to 150 kPa on very hard snow with a Young's modulus of 1200 MPa. The snow fully recovered its initial state after 1 min. They calculated the energy lost in the hysteresis loop due to repeated loading and unloading to be merely 1 J/s. Comparatively, they contrasted this energy loss with the theoretical total energy dissipation of a ski ($P = \mu v Fn$) sliding at a speed of $v = 20$ m/s, with $\mu = 0.1$ and $Fn = 400$ N, resulting in 800 J/s. Therefore, the energy lost to snow compaction was only 0.1% of the total energy dissipation.

Given the negligible energy loss calculated and the short recovery time of 0.2 s between the sliders in our study, it seems unlikely that the delayed elastic recovery of the snow can account for the observed differences in the coefficient of friction relative to spacing. However, Theile et al. (2009) used snow with 10 times higher Young's modulus than found in the compression test of artificial snow in a study by Lintzen and Edeskär (2014). This discrepancy might suggest that the compression work in their study is lower than what might be observed in our study or in field conditions.

### 4.6. Implications for ski design

In skate cross-country ski design, minimizing gliding friction is one of the most critical considerations. Due to the compression of the camber curve, a ski has a certain degree of self-regulating contact pressure with the snow. This is achieved through an increase of the apparent contact area with higher normal force or with softer snow. Such a design enables the ski to perform over a wide range of snow conditions. However, such a design complicates parameter adjustments due to their interconnection. By measuring the snow conditions before a race, there should be opportunities to reduce the coefficient of friction by adjusting the macroscopic ski properties for a ‘narrower’ and more specific set of snow conditions. For the tested ranges in our study, the following

recommendations are summarized in Table 5.

At cold temperatures, the key design parameter is to increase the average contact pressure. Given that the normal load exerted by the athletes is constant in the gliding position, the only method to increase the pressure is by reducing the apparent contact area. Additionally, it is favorable to have more of the load split onto the front zone of the ski. At intermediate temperatures, the findings suggest that friction can be reduced by decreasing the apparent contact area, shifting more of the load towards the rear, and reducing the spacing. At warmer temperatures, the results show that minimizing the apparent contact area is the parameter with the strongest influence across the tested range. Additionally, a balanced load split, with a 50/50 distribution, is beneficial.

These findings suggest that there is potential to reduce the friction by modifying the macroscopic parameters at different temperatures. However, translating the combination of macroscopic parameters to the current design of a cross-country ski is not straightforward. For instance, decreasing the apparent contact area on a modern ski can be achived by increasing the bending stiffness and/or the height of the camber profile. This adjustment results in shorter contact zones (apparent contact area), but also increases the spacing between them, unless the ski's length is also reduced. Altering the load split affects the apparent contact area as well. While this study does not delve into proposing novel ski designs, our findings indicate opportunities for enhancing the current state-of-the-art in ski design. The insights from this research could serve as a foundation for designing new skis that are more customizable to specific snow conditions.

At cold temperatures, the highest average contact pressure of 35 kPa performed best, suggesting that even higher pressures could reduce the friction even further. The apparent contact area of the shortest sliders on the adjustable ski is approximately 30% shorter than the apparent contact area of a cross-country ski with a normal force of 800 N. This implies that skate cross-country skis could reduce the apparent contact area for similar snow conditions when only considering minimizing the coefficient of friction. However, it's crucial to recognize that this pressure increase has its limits and must contextually be tied to the snow's strength. In other words, pressure cannot be increased excessively without considering the hardness of the snow.

The results from our study appear to contradict those of Breitschädel (2014), which found that the Norwegian national team generally preferred cold-condition skis with slightly longer contact zones (larger apparent contact area). However, the athletes' preference for skis with longer contact zones doesn't necessarily mean they had a lower coefficient of friction. Ski selection also involves factors like how the skis feel, with stability being a key criterion in choosing skating skis. Additionally, the wide variety of snow conditions encountered in the field may offer another possible explanation for the athletes' preferences.

An essential aspect of cross-country ski design development is its alignment with the athlete's experience and their subjective feeling of the ski's performance. Athletes, particularly at the elite level, have spent years honing their skills and developing a deep, intuitive understanding of how their skis should feel. This extensive training and experience enable them to discern minor changes in ski performance, making their feedback invaluable in the design process. However, this reliance on athlete perception also introduces certain limitations to how far ski design can be tuned from what is considered 'normal' or traditional. If certain modifications could theoretically reduce friction, they might not be readily accepted by athletes if these changes significantly alter the ski's familiar feel. Skiers might perceive these alterations as detrimental, impacting their skiing technique negatively, even if objective measures like reduced friction suggest otherwise.

The load split results at cold temperatures contrast the findings on the cross-country ski found in our previous paper (Auganæs et al., 2023), where a gradual reduction in the coefficient of friction was seen as the load split shifted from 40% to 18% (load application point moved towards the rear). Nevertheless, it's worth noting that this adjustment in load application point on a cross-country ski had an impact on the apparent contact area, introducing some ambiguity regarding the precise influence of load split on friction in the previous paper. Interestingly, our current study suggests that the typical placement of the binding or load application point on cross-country skis, resulting in a load split of around 30%, is not optimal for minimizing friction when solely considering the load split in cold conditions.

**Table 5**
Recommendations for macroscopic ski parameter at three different snow temperatures.

| Parameter | Parameter recommendations at each temperature (H = high, M = medium, L = low) | | |
|---|---|---|---|
| | Cold | Intermediate | Warm |
| Normal force (300–800 N)[a] | H | M | M |
| Area (180–360 $cm^2$) | L | L | L |
| Pressure (10–35 kPa) | H | M | M/H |
| Load split (5–95%) | H | L | L |
| Spacing (20–100 cm) | L | L | L |

[a] This parameter is not possible to alter in the design process for skis, which is why we also report contact area and contact pressure. However, this value is of interest when comparing gliding performance between skiers of different weight classes.

## 5. Conclusion

This study employed a custom-built adjustable ski designed specifically to isolate and examine macroscopic ski parameters at relevant speeds, slider sizes and contact pressures, at three different snow conditions. The study focused on understanding how factors such as apparent contact area, normal load, spacing, and load split influence the friction coefficient, revealing clear patterns that vary with snow temperature and humidity levels.

Notably, at cold snow temperatures, the study found that the average contact pressure is the primary factor affecting friction. Increasing this pressure, either through altering the apparent contact area or adjusting the normal load, consistently led to a decrease in the coefficient of friction. In contrast, under warmer and intermediate snow conditions, the apparent contact area consistently stood out as the most crucial element affecting the coefficient of friction. At cold temperatures, concentrating the load entirely on either the front or rear slider was beneficial. This is consistent with the beneficial effect of having a high contact pressure at this temperature. In the more typical load split range of 30–50% (front/rear), it was beneficial to move the load forward. At warmer temperatures, the trends are more ambiguous. The effect of spacing is not as strong, but in the typical range of 40–80 cm, there is a tendency that shorter spacing between the two sliders is beneficial.

These insights provide valuable guidance for ski design. By carefully considering these parameters, ski designers can effectively reduce ski-snow friction, optimizing performance in diverse snow conditions. This research advances the understanding of ski dynamics and provides practical guidance for tailoring ski designs to specific environmental conditions, potentially transforming the skiing experience.

## Funding sources

This work is funded by the Norwegian Research Council (NFR) through the Nano2Glide consortium, project number 296540.

## CRediT authorship contribution statement

**Sondre Bergtun Auganæs:** Writing – original draft, Visualization, Validation, Software, Methodology, Investigation, Data curation, Conceptualization. **Audun Formo Buene:** Writing – review & editing, Visualization, Supervision, Investigation, Conceptualization. **Alex Klein-Paste:** Writing – review & editing, Supervision, Funding acquisition, Conceptualization.

## Declaration of generative AI and AI-assisted technologies in the writing process

During the preparation of this work the authors used ChatGPT / OpenAi in order to correct the language and spelling in this article. After using this tool/service, the authors reviewed and edited the content as needed and takes full responsibility for the content of the publication.

## Declaration of competing interest

The authors declare that they have no known competing financial interests or personal relationships that could have appeared to influence the work reported in this paper.

## Data availability

Data will be made available on request.

## Acknowledgments

The authors would like to thank the Nano2glide consortium (Brav, Madshus, IDT Sports, Olympiatoppen and SINTEF). We would also like to thank the mechanical workshop at IBM-NTNU and the technical staff at the Department of Civil and Environmental Engineering for helping with the experimental work.

## References

Almqvist, A., Pellegrini, B., Lintzen, N., Emami, N., Holmberg, H.-C., Larsson, R., 2022. A scientific perspective on reducing Ski-snow friction to improve performance in olympic cross-country skiing, the Biathlon and Nordic combined. Front. Sports Active Liv. 4, 844883 https://doi.org/10.3389/fspor.2022.844883.

Auganæs, S.B., Buene, A.F., Klein-Paste, A., 2022. Laboratory testing of cross-country skis – investigating tribometer precision on laboratory-grown dendritic snow. Tribol. Int. 168, 107451 https://doi.org/10.1016/j.triboint.2022.107451.

Auganæs, S.B., Buene, A.F., Klein-Paste, A., 2023. The effect of load and binding position on the friction of cross-country skis. Cold Reg. Sci. Technol. 212, 103884 https://doi.org/10.1016/j.coldregions.2023.103884.

Bäurle, L., 2006. Sliding Friction of Polyethylene on Snow and Ice. Doctoral Dissertation. Swiss Federal Institute of Technology Zurich. https://doi.org/10.3929/ethz-a-005210667.

Bäurle, L., Szabó, D., Fauve, M., Rhyner, H., Spencer, N.D., 2006. Sliding friction of polyethylene on ice: tribometer measurements. Tribol. Lett. 24 (1), 77–84. https://doi.org/10.1007/s11249-006-9147-z.

Bäurle, L., Kaempfer, T.U., Szabó, D., Spencer, N.D., 2007. Sliding friction of polyethylene on snow and ice: contact area and modeling. Cold Reg. Sci. Technol. 47 (3), 276–289. https://doi.org/10.1016/j.coldregions.2006.10.005.

Bowden, F.P., Hughes, T.P., 1939. The mechanism of sliding on ice and snow. Proceed. Royal Soc. London Ser. A 172 (949).

Breitschädel, F., 2014. Technical Aspects to Improve Performance in Crosscountry Skiing. Doctoral dissertation,. Norwegian university of science and technology.

Buene, A.F., Auganæs, S.B., Klein-Paste, A., 2022. Effect of Polydimethylsiloxane Oil Lubrication on the Friction of Cross-Country UHMWPE Ski Bases on Snow. Front. Sports Active Liv. 4 https://doi.org/10.3389/fspor.2022.894250.

Buhl, D., Fauve, M., Rhyner, H., 2001. The kinetic friction of polyethylen on snow: the influence of the snow temperature and the load. Cold Reg. Sci. Technol. 33, 133–140. https://doi.org/10.1016/S0165-232X(01)00034-9.

Colbeck, S.C., 1992. A Review of the Processes that Control Snow Friction.

Dash, J.G., Rempel, A.W., Wettlaufer, J.S., 2006. The physics of premelted ice and its geophysical consequences. Rev. Mod. Phys. 78 (3), 695–741. https://doi.org/10.1103/RevModPhys.78.695.

Hasler, M., Schindelwig, K., Mayr, B., Knoflach, C., Rohm, S., van Putten, J., Nachbauer, W., 2016. A novel Ski–snow tribometer and its precision. Tribol. Lett. 63 (3) https://doi.org/10.1007/s11249-016-0719-2.

Hasler, M., Jud, W., Nachbauer, W., 2021. Snow temperature behind sliding skis as an indicator for frictional meltwater. Front. Mech. Eng. 7, 738266 https://doi.org/10.3389/fmech.2021.738266.

Hasler, M., Mössner, M., Jud, W., Schindelwig, K., Gufler, M., van Putten, J., Rohm, S., Nachbauer, W., 2022. Wear of snow due to sliding friction. Wear 510, 204499. https://doi.org/10.1016/j.wear.2022.204499.

Kalliorinne, K., Hindér, G., Sandberg, J., Larsson, R., Holmberg, H.-C., Almqvist, A., 2023. The impact of cross-country skiers' tucking position on ski-camber profile, apparent contact area and load partitioning. Proceed. Inst. Mech. Engineer. Part P. https://doi.org/10.1177/17543371221141748, 17543371221141748.

Kietzig, A.-M., Hatzikiriakos, S.G., Englezos, P., 2010. Physics of ice friction. J. Appl. Phys. 107 (8) https://doi.org/10.1063/1.3340792.

Lintzen, N., Edeskär, T., 2014. Uniaxial strength and deformation properties of machine-made snow. J. Cold Reg. Eng. 29, 04014020. https://doi.org/10.1061/(ASCE)CR.1943-5495.0000090.

Makkonen, L., 2012. Ice adhesion —theory, measurements and countermeasures. J. Adhes. Sci. Technol. 26 (4–5), 413–445. https://doi.org/10.1163/016942411X574583.

Moldestad, D.A., 1999. Some Aspects of Ski Base Sliding Friction and Ski Base Structure. Doctoral Dissertation. Norwegian University of Science and Technology.

Mössner, M., Innerhofer, G., Schindelwig, K., Kaps, P., Schretter, H., Nachbauer, W., 2013. Measurement of mechanical properties of snow for simulation of skiing. J. Glaciol. 59 (218), 1170–1178. https://doi.org/10.3189/2013JoG13J031.

Mössner, M., Hasler, M., Nachbauer, W., 2021. Calculation of the contact area between snow grains and ski base. Tribol. Int. 163, 107183 https://doi.org/10.1016/j.triboint.2021.107183.

Mössner, M., Schindelwig, K., Heinrich, D., Hasler, M., Nachbauer, W., 2023. Effect of load, ski and snow properties on apparent contact area and pressure distribution in straight gliding. Cold Reg. Sci. Technol. 208, 103799 https://doi.org/10.1016/j.coldregions.2023.103799.

Nachbauer, W., Kaps, P., Hasler, M., Mössner, M., 2016. Friction between ski and Snow. In: Braghin, F., Cheli, F., Maldifassi, S., Melzi, S., Sabbioni, E. (Eds.), The Engineering Approach to Winter Sports. Springer, New York, pp. 17–32. https://doi.org/10.1007/978-1-4939-3020-3_2.

Oksanen, P., Keinonen, J., 1982. The mechanism of friction of ice. Wear 78 (3), 315–324. https://doi.org/10.1016/0043-1648(82)90242-3.

Petrenko, V.F., Whitworth, R.W., 1999. Physics of Ice. OUP Oxford.

Scherge, M., Böttcher, R., Richter, M., Gurgel, U., 2013. High-speed ice friction experiments under lab conditions: on the influence of speed and normal force. ISRN Tribol. 2013, 703202 https://doi.org/10.5402/2013/703202.

Theile, T., Szabo, D., Luthi, A., Rhyner, H., Schneebeli, M., 2009. Mechanics of the Ski–snow contact. Tribol. Lett. 36 (3), 223–231. https://doi.org/10.1007/s11249-009-9476-9.

# Appendices

## Appendix A – Load cell set-up for the contact pressure profiles

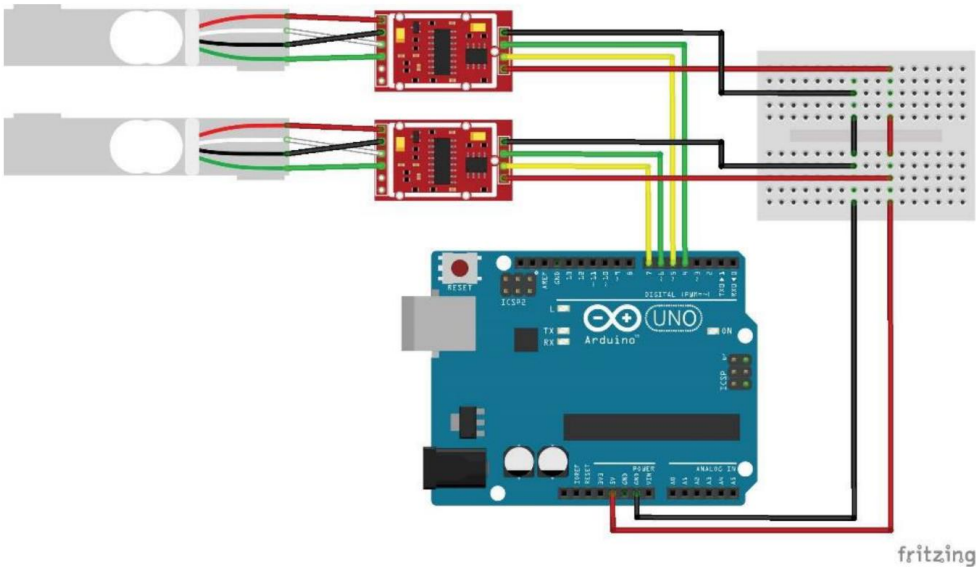


Example of the load cell set-up for the pressure profile rig. The loadcells is connected to an HX711 amplifier, which is wired to a breadboard for power and ground, and to the Arduino for the digital pins. The current set-up for the pressure rig uses 9 load cells.

**Arduino code for the load cells set-up**

```
#include "HX711.h"
//#include <Wire.h>
//#include <Adafruit_SSD1306.h>
//#include <Adafruit_GFX.h>

// OLED display TWI address
//#define OLED_ADDR   0x3C

HX711 scale1;
HX711 scale2;
HX711 scale3;
HX711 scale4;
HX711 scale5;
HX711 scale6;
HX711 scale7;
HX711 scale8;
HX711 scale9;
```

```
float val1, val2, val3, val4, val5, val6, val7, val8, val9,

//Adafruit_SSD1306 display(-1);

//#if (SSD1306_LCDHEIGHT != 64)
//#error("Height incorrect, please fix Adafruit_SSD1306.h!");
//#endif

void setup() {
  // initialize and clear display
/*  display.begin(SSD1306_SWITCHCAPVCC, OLED_ADDR);
  display.clearDisplay();
  display.display();

  // display a line of text
  display.setTextSize(2);
  display.setTextColor(WHITE);
  display.setCursor(0,0);
  display.print("YOUR LOGO");
  display.setTextSize(1);
  display.println("Load");
  display.println("Cell");
  display.println("Program");

  // update display with all of the above graphics
  display.display();

  delay(2000);

  display.clearDisplay();
  display.display();
*/
  Serial.begin(115200);
  Serial.println("HX711 Demo");

  Serial.println("Initializing the scale");
  // parameter "gain" is ommited; the default value 128 is used by the
library
  // HX711.DOUT  - pin #A1
  // HX711.PD_SCK - pin #A0
  // syntax: scale.begin(DOUT, CLK)
  scale1.begin(A1, A0);  Serial.println("Scale1 initialized");
  scale2.begin(A3, A2);  Serial.println("Scale2 initialized");
  scale3.begin(A5, A4);  Serial.println("Scale3 initialized");
  scale4.begin(A7, A6);  Serial.println("Scale4 initialized");
  scale5.begin(A9, A8);  Serial.println("Scale5 initialized");
  scale6.begin(A11, A10);  Serial.println("Scale6 initialized");
  scale7.begin(A13, A12);  Serial.println("Scale7 initialized");
  scale8.begin(3, 2);  Serial.println("Scale8 initialized");
  scale9.begin(5, 4);  Serial.println("Scale9 initialized");

  Serial.println("Before setting up the scale:");
  Serial.print("read: \t\t");
  Serial.println(scale1.read());      // print a raw reading from the ADC
  Serial.println(scale2.read());      // print a raw reading from the ADC
  Serial.println(scale3.read());      // print a raw reading from the ADC
  Serial.println(scale4.read());      // print a raw reading from the ADC
  Serial.println(scale5.read());      // print a raw reading from the ADC
  Serial.println(scale6.read());      // print a raw reading from the ADC
  Serial.println(scale7.read());      // print a raw reading from the ADC
  Serial.println(scale8.read());      // print a raw reading from the ADC
```

```
  Serial.println(scale9.read());      // print a raw reading from the ADC

  Serial.print("read average: \t\t");
  Serial.println(scale1.read_average(20));    // print the average of 20
readings from the ADC

  Serial.print("get value: \t\t");
  Serial.println(scale1.get_value(5));    // print the average of 5
readings from the ADC minus the tare weight (not set yet)

  Serial.print("get units: \t\t");
  Serial.println(scale1.get_units(5), 1); // print the average of 5
readings from the ADC minus tare weight (not set) divided
            // by the SCALE parameter (not set yet)

  scale1.set_scale(212000.f);    // -523000.f seems to give me 1:1 for mV
output testing with 5,10,15mV               // this value is obtained by
calibrating the scale with known weights; see the README for details
  scale2.set_scale(212000.f);    //(-1246.f);
  scale3.set_scale(202000.f);    //(-1246.f);
  scale4.set_scale(212000.f);    //(-1246.f);
  scale5.set_scale(210000.f);    //(-1246.f);
  scale6.set_scale(212000.f);    //(-1246.f);
  scale7.set_scale(208000.f);    //(-1246.f);
  scale8.set_scale(210000.f);    //(-1246.f);
  scale9.set_scale(212000.f);    //(-1246.f);

   scale1.tare();               // reset the scale to 0
   scale2.tare();
   scale3.tare();
   scale4.tare();
   scale5.tare();
   scale6.tare();
   scale7.tare();
   scale8.tare();
   scale9.tare();

  Serial.println("After setting up the scale:");

  Serial.print("read: \t\t");
  Serial.println(scale1.read());                 // print a raw reading
from the ADC

  Serial.print("read average: \t\t");
  Serial.println(scale1.read_average(20));       // print the average of 20
readings from the ADC

  Serial.print("get value: \t\t");
  Serial.println(scale1.get_value(5));    // print the average of 5
readings from the ADC minus the tare weight, set with tare()

  Serial.print("get units: \t\t");
  Serial.println(scale1.get_units(5), 1);        // print the average of 5
readings from the ADC minus tare weight, divided
            // by the SCALE parameter set with set_scale

  Serial.println("Readings:");
}

void loop() {
  Serial.print("one reading:\t");
```

```
  val1 = scale1.get_units(8);
  val2 = scale2.get_units(8);
  val3 = scale3.get_units(8);
  val4 = scale4.get_units(8);
  val5 = scale5.get_units(8);
  val6 = scale6.get_units(8);
  val7 = scale7.get_units(8);
  val8 = scale8.get_units(8);
  val9 = scale9.get_units(8);

   Serial.print(val9, 2); Serial.print(" ");  Serial.print(val8, 2);
Serial.print(" "); Serial.print(val7, 2); Serial.print(" ");
Serial.print(val6, 2); Serial.print(" "); Serial.print(val5, 2);
Serial.print(" "); Serial.print(val4, 2); Serial.print(" ");
Serial.print(val3, 2); Serial.print(" ");Serial.print(val2, 2);
Serial.print(" "); Serial.print(val1, 2); Serial.print(" ");
   Serial.println();
}
```

ISBN 978-82-326-8254-6 (printed ver.)
ISBN 978-82-326-8253-9 (electronic ver.)
ISSN 1503-8181 (printed ver.)
ISSN 2703-8084 (online ver.)





NTNU

Norwegian University of
Science and Technology